A Study on Transonic Tone Generation in Convergent-Divergent Nozzles

申, 昇永

https://doi.org/10.15017/1398550

A Study on Transonic Tone Generation in Convergent-Divergent Nozzles

Dissertation

Submitted to
Department of Energy and Environmental Engineering on
Graduate School of Kyushu University
in Partial Fulfillment of the Requirements for
the Degree of Doctor of Engineering

By
Seungyoung Shin

Kyushu University
October **2013**

Abstract

When a supersonic flow condition is non-isentropic condition that a shock wave occurs within the divergent section of convergent-divergent nozzle, transonic tone can occur at low nozzle pressure ratios. And the tone is distinct from other jet noise components. The main objectives of the present thesis were to get better understanding on the acoustic characteristics and generation mechanism of transonic tone in supersonic nozzle experimentally.

First, the effects of nozzle-lip thickness on the acoustic features of transonic tone have been investigated to check a location of the noise source. Far-field acoustic measurements are accomplished to obtain the noise spectra of the supersonic jets, which are issued from a supersonic nozzle with a design Mach number of 2.0. The acoustic characteristics of the supersonic jet, such as the transonic tone or screech tone frequency and amplitude will be discussed briefly in this thesis using the acoustic measurement results. The results obtained obviously show that the acoustic characteristics of transonic tone are differ from the screech tone and distinctly from the screech tone, it is found that the transonic tone has internal noise source.

To understand the transonic tone generation mechanism, the first shock wave the transonic tone had tried to correlate with flow oscillations. In particularly, the first shock wave oscillations and wall static fluctuations are considered with high speed video camera and simultaneous measurement system. And the results show that the frequencies of the shock wave and wall static pressure fluctuations correspond to the transonic tone and it is expect that a feedback loop between the shock wave and the nozzle exit.

In the present thesis, a tone reduction method is also considered by extension of the nozzle-lip length in 2-dimensional supersonic nozzle. And the transonic tone reduced at stage 1 about 5~10 dB when the nozzle-lip attached at the side of large separation zone in the nozzle and the extended nozzle-lip also affected the

shock wave oscillations, wall static pressure fluctuations and cross-correlations between the shock wave and the wall static pressure fluctuations.

Acknowledgement

I would like to my hearty thanks to my supervisor, Professor Toshiyuki Aoki for his guidance and encouragement to accomplish the present work both inside and outside the laboratory over the years. I also sincerely thank the committee members of my manuscript, Professor N.obuhiko Yamasaki and Professor Taro Handa for taking valuable time out their busy schedules to provide advice and suggestions to my work.

I want to express my special thanks to Dr. Makiko Yonamine and Dr. Sungjae Jung for their technical advice and encouragement during my first year for a doctorate. I also wish to express my gratitude to Mr. Nobuaki Kondoh who made a more complete work by providing much technical assistance. In addition, special thanks to graduate students, Mr. Akira Tokumoto, Mr. Yuya Yamasita, Mr. Hiroki Kuguyama, Mr. Akira Matunaga and Mr. Hiroyuki Marubayashi for their assistance, cooperation and kindness over the course of my graduate study.

I am also thankful to my special friends Youngjin Lee, Yongbaek Kang, Choongsik Kim and Fukuoka Central Church families for their constant encouragement, prayer and help with material and emotional support for life in Fukuoka.

I would like to express my gratitude toward my parents and parents-in-laws their un-failing love, patience, support and prayer through a long educational process. Finally, I am deeply thankful to my lovely wife and baby inside her for being my great delight, comfort and encouragement.

October, 2013

Contents

List of Figures

List of Tables

Nomenclature

a	sound speed
D	downward or down-side
D	nozzle exit diameter or diameter
f	frequency
L	length of nozzle-divergent section
M	Mach number
N	normal
NPR	nozzle pressure ratio
P	pressure
PSD	power spectral density
R	cross-correlation coefficient
SPL	sound pressure level
t	thickness
U	upward or upper side
r	radius from nozzle exit
X	distance along the jet axis from nozzle exit
γ	specific heat ratio
θ	angle of acoustic measurement installed or half angle of nozzle-divergence section
τ	time delay

Subscripts

0	stagnation state in the plenum chamber
a	ambient state
b	baffle
h	half
i	inside or sampling step

j	fully expanded condition of the jet
m	microphone
m	odd harmonics number
o	outside
p	pressure sensor
p	peak
s	shock wave

Chapter 1

Introduction

1.1 Background

1.1.1 Supersonic Jet Noise

Supersonic jets have long been used in many diverse fields of engineering applications such as supersonic aircrafts (Ennix et al., 1993), jet propulsion thrust vectoring (Strykowski, 1996), fuel injectors for supersonic combustion (Ramesh et al., 2000), soot blower devices (Jameel et al., 1994), coating technology for structural materials (Postel & Heberlein, 1998), supersonic ejectors (Bartosiewicz et al., 2005), jet pumps (Eames, 2002), etc. Until now, a great deal of studies has been experimentally and theoretically carried out to obtain detailed features of supersonic jet. It has been well known that the time-mean structure of supersonic jet is determined by nozzle pressure ratio and nozzle configuration (Love et al., 1959 ; Addy, 1981 ; Bülent Yüceil & Volkan Ötügen, 2002).

When a supersonic jet is issued from a nozzle exit, the high frequency noise problems occur. Many research have been conducted to understand the noise characteristics and generation mechanism including the appropriate noise control methods in suppressing the supersonic jet noise. Recently, the supersonic jet noise is being a very important issue to be resolved from the practical point of view of performance of fluidic device (Li & Halliwell, 1985 ; Krothapalli et al., 1986 ; Meier et al., 1990) as well as environmental noise problem (Thomas et al., 2002). However, it is not simple to understand and to control the jet noise generation because the understanding of jet noise is tied to the understanding of turbulence in jet flows.

Since Lighthill (1952, 1954) first introduced his acoustic analogy theory in

1952 and 1954, jet noise has been a topic of interest for many researchers. The idea that the sound radiated from aerodynamics flows can be modeled as a distribution of quadrupole sources has led to many different models and theories in order to predict the noise from jet flows. He established that the acoustic power radiated from a jet should scale as the eighth power of the jet velocity. While Lighthill's original theory is valid only for subsonic jet, other researchers have extended the previous theoretical studies of Lighthill into the range of supersonic jet velocities. In particular, Ffowcs Williams (1963) showed how turbulence convected downstream at a relatively high speed can be very strong source of noise in the far-field, and found that for very high speed jets, the acoustic power of the radiated noise should scale as the third power of the jet velocity.

It is now well known that the supersonic jet noise consists of three major components (Tam, 1995) : the turbulent mixing noise, the broadband shock-associated noise, and the screech tones. A typical far-field noise spectrum of an imperfectly-expanded supersonic jet in the upstream direction is described in Fig.1.1. The turbulent mixing noise is usually observed over a broad spectral hump centered around a Strouhal number (fD/u_j) of 0.1-0.2. The broadband shock -associated noise appears at a higher frequency than that of the turbulent mixing noise. The screech tone is observed between the mixing noise and the broadband shock noise. The mixing noise is generated in subsonic jet as well as supersonic jet, but other two noise components appear only in an imperfectly expanded supersonic jet which has a quasi-periodic shock cell structure in the jet plume.

The turbulent mixing noise of supersonic jet is produced by the fine-scale turbulence and the large-scale turbulence propagating downstream at supersonic Mach number relative to the ambient sound speed. The large-scale turbulent structures are capable of producing intense Mach wave radiation. Surprisingly, the existence of large-scale structures was not known until the early 1970s with works such as Crow & Champagne (1971), Brown & Roshko (1974), Winant & Browand (1974), and Browand & Weidman (1976). Depending on the references, researchers refer to the largest coherent scales within a jet flow as : large-scale

turbulent structures, large vortices, large eddies, coherent structures, etc.

For supersonic jets, the intensity as well as both the directional and spectral characteristics of the turbulent mixing noise strongly depend on the jet Mach number and the jet temperature (Fisher et al., 1973 ; Tanna, 1977a). The turbulent mixing noise increases as the jet Mach number increases. As the jet temperature is increased, the mixing noise also increases due to the increase in jet velocity with heating. Furthermore, Ffowcs Williams et al. (1975) and Krothapalli et al. (2000a) studied a particular turbulent mixing noise, referred to as crackle, which is generated due to the micro explosions of the cold ambient fluid entrained into the hot jet flow.

On the other hand, when a convergent nozzle is operated at supercritical pressure ratio (under-expanded), or when a convergent-divergent (C-D) nozzle is operated at off-design Mach number (over-expanded or under-expanded), a shock cell structure is formed in the jet flow. This causes the shock-associated noise, in addition to the basic turbulent mixing noise. Figure 1.2 shows the noise intensity of a supersonic jet from a convergent-divergent nozzle (Seiner & Yu, 1984). Since there is no shock-associated noise when a jet is correctly-expanded, the solid line and black circles represents the minimum noise level (consisting of only the turbulent mixing noise) of the jet at a given fully expanded jet Mach number. When the jet is imperfectly-expanded, the total jet noise consists of both the mixing and shock-associated noise components, as shown in Fig.1.2.

The shock-associated noise can be divided into two distinct components. The first component is broadband in nature, and is usually known as the broadband shock-associated noise. The broadband shock-associated noise is generated by the weak interaction between the downstream propagating large-scale turbulence structure of the jet flow and the quasi-periodic shock cell structure. The second component is discrete in nature, usually with several harmonics, and commonly referred to as the screech tone. The generation of screech tone is due to the acoustic feedback phenomenon, as shown in Fig.1.3.

The broadband shock-associated noise was first identified by Harper Bourne

& Fisher (1974). Since then, it has been studied experimentally by a number of researchers, such as Tanna (1977b), Tam & Tanna (1982), Norum & Seiner (1979, 1982a), and Seiner & Yu (1984). These researches have provided much detailed information on the acoustic characteristics of the broadband shock-associated noise. Harper Bourne & Fisher (1974) developed the theoretical model for the prediction of the characteristics of shock noise, by regarding each shock cell end as a compact source of acoustic radiation. They also showed that the intensity of the broadband shock-associated noise is proportional to the fourth power of the shock strength. Its noise spectrum is distinct from that of the turbulent mixing noise, as shown in Fig.1.1, and is characterized by a peak. The frequency of this peak varies with angle in the manner of a Doppler shift, and is proportional to the jet velocity and inversely proportional to the shock spacing.

The screech tone phenomenon was first described by Powell (1953a, b) as arising through an acoustic feedback mechanism. Figure 1.3 shows the generation mechanism of screech acoustic feedback loop : (1) A disturbance in the jet shear layer is convected downstream and is amplified in passing downstream. (2) The amplified large-scale turbulence structure interacts with the shock cell structure, scattering intense sound waves at that point. (3) These acoustic waves propagate through the ambient fluid in the upstream direction and interact with the jet shear layer close to the nozzle exit. (4) This interaction gives rise to a new downstream traveling disturbance that continues the cycle (receptivity processes).

Independently of the general noise components, the transonic tone can occur at low nozzle pressure ratios when a shock wave occurs within the divergent section of convergent-divergent nozzle without any abrupt area change. Such transonic tone through `whistler nozzles' has been studied by Hill & Greene (1977) and by Hussain & Hasan (1983). Resonance of similar flows discharging through a duct or `ejector', involving choked and supersonic conditions, have been studied by Witczak (1977) and by Krothapalli & Hsia (1996). The resonance in many cases could be traced to a coupling between the duct acoustic modes and the instability of the shear layer originating from the sudden expansion.

1.1.2 Motivation

Transonic tone can occur at low nozzle pressure ratios when a shock wave occurs within the divergent section of convergent-divergent nozzle without any abrupt area change. In the present study, the transonic tone also observed in convergent-divergent nozzles designed by characteristic method with a smooth convergence to the throat and then a smooth divergence up to the exit without any abrupt area change when a shock exists within the diverging section of the nozzle. In this range of operating conditions the flow often locks on to a resonance accompanied by very loud tones.

The ‘transonic tone’ or ‘transonic resonance’ was named by Zaman et al.(Zaman & Dahl 2002) at the first. Prior to that, of course, acoustic tones which occur at intermediate range of pressures when a shock exists within the diverging section of a nozzle have been noted, for example, in convergent-divergent nozzles as ‘a precursor to screech’ (Seiner J. M. 1998) as well as in subsonic diffusers (Zaman & Dahl 1990). Especially, a self-excited flow oscillation was observed from a series of experiments with two-dimensional diffuser at transonic conditions (Chen, Sajben & Kroutil 1979; Sajben, Bogar & Kroutil 1980; Bogar, Sajben & Kroutil 1983; Hsieh & Coakley 1987).

A few experimental and numerical researches on the diffusion of the transonic tone have been carried out (Bogar, Sajben & Kroutil 1983; Loh & Zaman 2002). In particular, Zaman et al. investigated the characteristics of the transonic tone in various nozzle conditions, and provided correlation equations to predict the frequency from a collection of data for single round nozzles (Zaman, Dahl, Bencic & Loh 2002). Moreover, they showed that transonic tone takes place similarly to the (no-flow) longitudinal acoustic resonance of a conical section with one end closed and the other end open. However, it remains unclear under what process the transonic tone can occur in actual flow complicated by shock oscillation and shock wave/boundary layer interaction phenomenon.

1.2 Objectives of Research

The primary objectives of this thesis are to investigate the characteristics and generation mechanism of transonic tone at low nozzle pressure ratios when shock wave occurs within the supersonic nozzle. These objectives are accomplished by experimental works. Three major objectives of the present work are listed as follows:

- **Acoustic characteristics of transonic tone and effect of nozzle-lip thickness on transonic tone in axisymmetric nozzle** – It may be helpful to consider some important characteristics of transonic tone. One of them, for example, is which region the transonic tone source exist. The objective of this part is to understand the acoustic characteristics of transonic tone and its variation according to nozzle pressure ratio and to examine which region has the transonic tone source by comparing the nozzle-lip thickness effects on the transonic tone frequency and amplitude with screech tone's one.
- **Transonic tone in 2-dimensional supersonic nozzle** – This objective is to investigate the relationship between the transonic tone and the first shock wave oscillation or wall static pressure fluctuation when the transonic tone occurs. There are some attempts to correlate the transonic tone and flow oscillation in 2-dimensional supersonic nozzle.
- **Effect of nozzle-lip length on transonic tone in 2-dimensional supersonic nozzle** – A new control technique of transonic tone is experimentally studied by changing the nozzle lip length. This objective is to examine the effect of nozzle-lip length on transonic tone as a supplement the validity of feedback mechanism of transonic tone. The variation of the first shock wave oscillation and wall static pressure fluctuation according to nozzle-lip length will also be discussed.

1.3 Overview of Thesis

The background and research progress of general supersonic jet noise and

transonic tone have been briefly explained in **Chapter 1**. The motivation and major objectives of the present thesis are also described in this chapter. Some brief reviews of transonic tone in supersonic jet are followed in **Chapter 2**. The fundamental acoustic characteristics of transonic tone and its control techniques are explained in this chapter. Chapter 2 will be helpful in getting the insight into the present situation of researches related to transonic tone, and understanding the needs for the present study.

Chapter 3 gives a full description of the facility and experimental apparatus used for the present work. This includes a description of high pressure air supply system, anechoic chamber, nozzle configuration, high-quality spark schlieren optical system and high speed video camera. The data acquisition devices such as a microphone and a pressure transducer are also described.

The results and discussion of the actual experimental works begin in **Chapter 4**. In this chapter, acoustic characteristics of transonic tone and the effect of nozzle-lip thickness on the transonic tone in axisymmetric convergent-divergent nozzle are discussed with comparing the acoustic characteristics of transonic tone to screech tone according to the nozzle-lip thickness variation.

Chapter 5 describes an experimental work to investigate characteristics and generation mechanism of the transonic tone in 2-dimensional supersonic nozzle. In particular, the frequency of the first shock wave oscillation and wall static pressure fluctuation are analyzed and tried to correlate to the transonic tone and a feedback mechanism for generation of transonic tone is proposed.

Chapter 6 describes an experimental work to investigate the effect of nozzle-lip length on transonic tone in 2-demensional supersonic nozzle. Especially, with considering the large separation zone location from which the feedback loop development is expected, the effect of nozzle-lip length on the transonic tone, the first shock wave oscillation, wall static fluctuation and variation of the cross-correlations will be reported.

Finally, **Chapter 7** summarizes the important findings obtained from Chapter 4, 5 and 6. Some recommended directions for future research are also suggested.

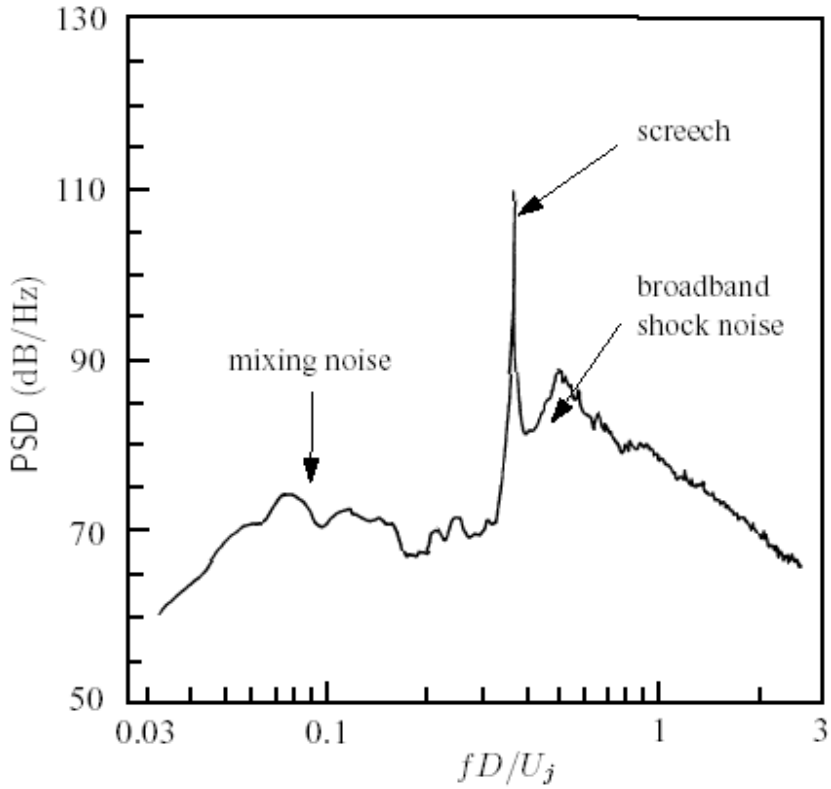

Figure 1.1 Far-field narrow-band noise spectrum of an imperfectly-expanded supersonic jet measured by Seiner & Yu (1984). Microphone is located at 150° from the jet axis

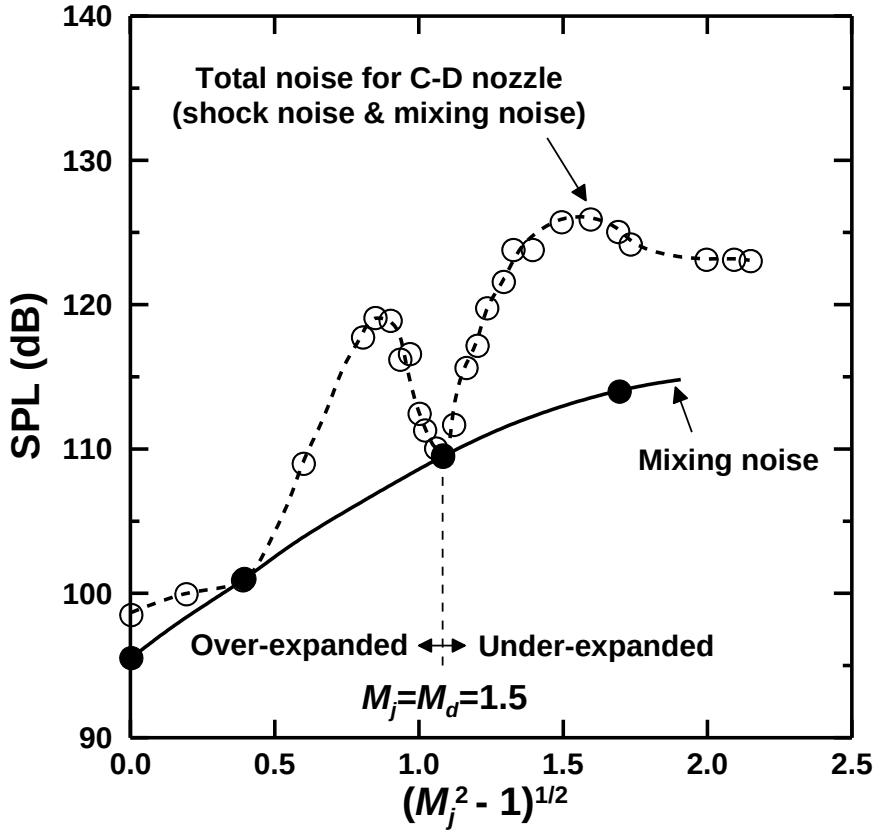

Figure 1.2 Overall sound pressure levels of unheated jet from a convergent-divergent nozzle (C-D) with a design Mach number M_d=1.5 at 150° to the jet axis (Seiner & Yu, 1984) : ○, imperfectly-expanded case ; ●, perfectly-expanded case

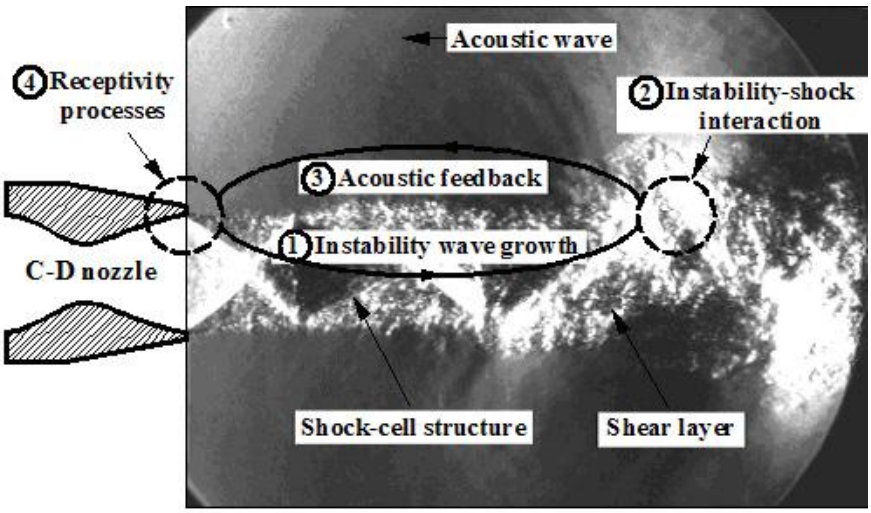

Figure 1.3 Fundamental mechanism of screech tone feedback loop. This is the flow visualization picture for imperfectly-expanded jet (M_j=1.51) obtained from the present work

Chapter 2

Survey of Previous Work

2.1 Introduction

The resonance phenomenon in nozzle flows has been studied in the past by many researchers not only because of academic interest, but also for its significance in many engineering applications ranging from mixing (Hill & Greene 1977) and jet noise control (Krothapalli & Hsia 1996) to buffeting in external flows (Mabey 1989) and rocket engine instability (Schwane, Wong & Torngren 2002). The occurrence of resonance can be self-excited or driven by external unsteady loads, or combination of these mechanisms. For instance, in the case of convergent-divergent nozzles without any abrupt area change, the nozzles are under a transonic flow condition at a pressure ratio much lower than the design value, and flow separation takes place just downstream of the shock wave. Consequently, self-exited resonance and tones are encountered with such a nozzle condition. These kind of phenomenon has been studied experimentally (Zaman, Dahl, Bencic & Loh 2002, Hunter 2004, Sajben & Kroutil 1980), as well as numerically (Hunter 2004, Loh & Zaman 2002). Zaman et al.(Zaman, Dahl, Bencic & Loh 2002) provide a complete overview of this activity.

2.2 Staging Phenomenon and Tone Generation Condition

According to Zaman(Zaman , Dahl, Bencic & Loh 2002), the resonant frequencies appears in multiple modes, with the fundamental order mode corresponding to a standing wave of a quarter-wavelength and higher order modes exist only in odd harmonics at a low nozzle pressure ratio. The Fig.2.1

shows the tone frequency *f* as the increasing and stage-jumping resonance with increasing nozzle pressure ratio. The vertical lines demarcate flow regimes determined from one-dimensional nozzle flow analysis, based simply on the throat-to-exit area ratio. From the left, first (dashed line), the second (dotted line) and the third (chain-dashed line) represents respectively the choking condition, exit shock condition and design condition when the flow is perfectly expanded. It seems from the boundaries in Fig.2.1 that the resonance could take place when a shock existed within the divergent section or when the flow was in the early stage of overexpansion. However, it turned out that one-dimensional analysis grossly under-predicts the location of the 'dotted' boundary, and the resonance always involves a shock within the divergent section.

2.3 Prediction of Transonic Tone Frequency

Zaman et al. (Zaman, Dahl, Bencic & Loh 2002) also suggested the empirical equations for the prediction of transonic tone frequency. It comes out that the resonant frequency f_N is strongly dependent on the divergent angle of the nozzle for θ smaller than 2 degree, as shown Fig.2.3. The curves in Fig.2.3 are least-squares-fits through the data for the round nozzle cases(open symbols). From the fitted curves the following equation is obtained, with θ expressed in degrees:

$$\frac{f_N l}{m a_0} = C_1(\theta_h) + C_2(\theta_h)(M_j - 1), m = 1,3,5$$

where $C_1(\theta)=0.2980\theta^{-0.370}$, $C_2(\theta)=0.9520\theta^{-1.029}$ for stage 1, and $C_1(\theta)=0.2210\theta^{-0.325}$, $C_2(\theta)=0.3630\theta^{-0.875}$ for stage 2. This equation was provided for the prediction the resonance frequency from a collection of data for axisymmetric nozzles. The throat-to-exit axial length (l) and the half angle of divergence (θ_h) are used to characterize the overall geometry of the divergent section.

2.1 Reduction of Transonic Tone

Zaman et al. showed that the acoustic resonance phenomenon was suppressed significantly by a disruption of the azimuthal coherence of unsteadiness in the boundary layer upstream or downstream of the shock induced separation (Zaman, Dahl, Bencic & Loh 2002). It was found that the transonic tone sufficiently reduced with only installing some trip around the throat or installing some tabs in the boundary layer of the exit but the latter resulted in changing the flow state, directly. Sound pressure level spectra, with and without boundary layer trips are shown in Fig. 2.4. The trip was composed of 4.5 in. wide pieces of adhesive tape (approximately 0.003 in. thick) placed close to but sufficiently upstream of the throat so that there was no change in the minimum area. These were spaced equally around the periphery. It can be seen that, at the highest M_j, there is no effect on screech. This is expected because screech occurs due to a feedback loop external to the nozzle. However, the trip essentially eliminates the transonic tones in this case, at the lower values of M_j.

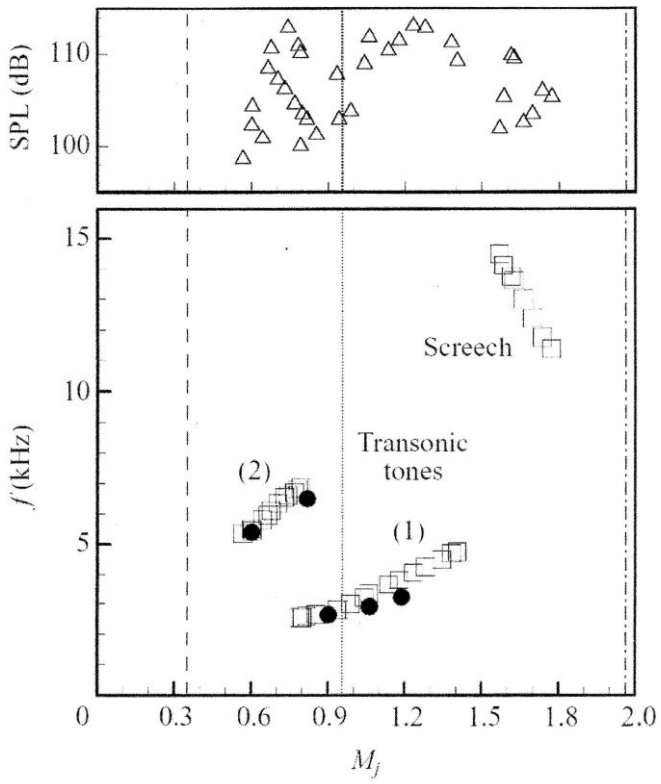

Figure 2.1 Variation of frequency and amplitude of acoustic tones with M_j (Zaman, Dahl, Bencic & Loh 2002)

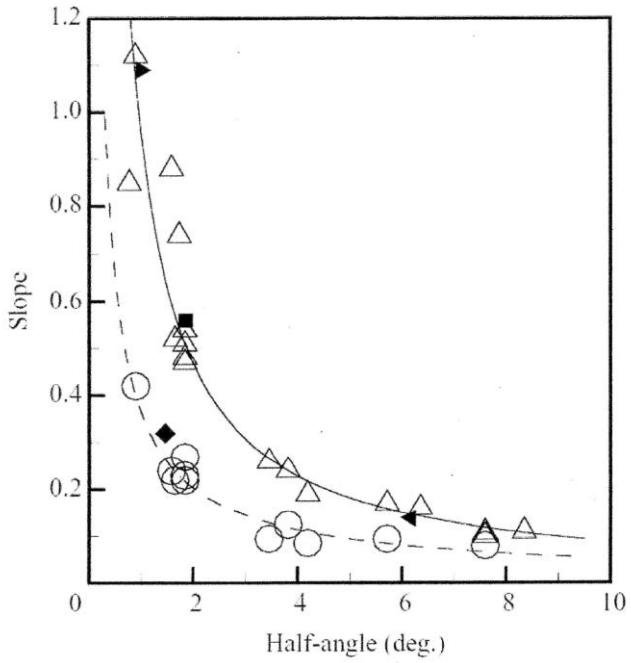

Figure 2.2 Slope variation of $f_N l/a_0$ versus M_j for various nozzles, as a function of the half-angle of divergence(θ); △-stage1,○-stage2
(Zaman, Dahl, Bencic & Loh 2002)

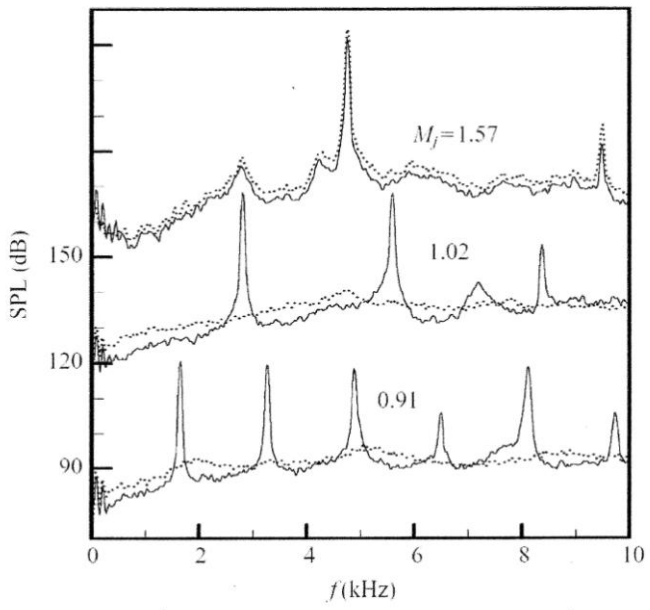

Figure 2.3 Tripped boundary-layer effect on resonance in sound pressure level; dotted line-tripped case, solid line-normal case (Zaman, Dahl, Bencic & Loh 2002)

Chapter 3

Experimental Apparatus

This chapter describes the experimental apparatus used in order to investigate the flow and acoustic characteristics of supersonic jets, including an anechoic test room, high pressure air supply, a supersonic nozzle, a schlieren optical system and a microphone. While the supersonic jet is exhausting into the anechoic test room from the nozzle exit, the flow visualization, wall static pressure and acoustic measurements are accomplished.

3.1 Anechoic Test Room

The present experimental works are conducted in an anechoic test room that is schematically shown in Fig.3.1. The anechoic test room has a dimension of 5.3m×4.9m×4.9m and is covered with sound absorption material (glass-wool foam) of a 325mm thickness. The acoustical foam is designed to absorb 95% of the incident noise for frequencies over 500Hz. According to some preliminary acoustic tests, the present test room is anechoic for all frequency components above approximately 120Hz and has the back ground noise of about 10dB.

At the end of the test room, the jet flow enters the exit of the test room which is used to control the ambient pressure in the test room to atmospheric condition. The ambient pressure and temperature in the test room are measured at p_a=101.3kPa and T_a=293K. All experimental devices have been set up to make simultaneous measurement and to control by personal computer installed externally.

3.2 High Pressure Air Supply

A piston-type air compressor is capable of supplying air at a maximum storage pressure of 3MPa. A high pressure storage tank provides a total capacity of $5m^3$. After leaving the high pressure storage tank, compressed dry air enter the plenum chamber, in which a honeycomb system reduces flow turbulence. A circular convergent-divergent nozzle and two-dimensional convergent-divergent nozzle are installed on the end of the straight pipe. For the circular nozzle, the end wall of the blowdown plenum chamber is connected with a circular straight pipe which has a length of 100mm and an inner diameter of 28mm, as shown in Fig.3.1. And the two-dimensional nozzle is connected with a rectangular straight pipe which has a length of 120mm, an inner height of 16.2mm and an inner width of 30mm. The pressure inside the plenum chamber is controlled by a pressure regulator valve which is located upstream of the plenum chamber.

The temperature in the plenum chamber is measured by using a thermocouple, and it maintains constant at room temperature (approximately 293K) during test. The pressure is measured by flush mounted pressure transducer (Toyoda PMS-5-200K) on the top wall of the plenum chamber. The pressure transducer is calibrated prior to each test. The uncertainty in pressure and temperature measurements is estimated to be less than ±2 per cent. These estimations are based on the maximum observed fluctuations in the measurements.

3.3 Convergent-Divergent (C-D) Nozzle

Figure 3.2 shows schematically two convergent-divergent nozzles used in the present study. The interior contour lines of these nozzles are manufactured based upon the method of characteristics (Puckett 1946, Foelsch, 1949) for a design Mach number of 2.0. For the circular convergent-divergent nozzle in Fig 3.2(a), has a throat diameter of 20mm, an exit diameter (D) of 26mm and a nozzle-lip thickness of 2mm at the exit of the nozzle, and has a straight section near the exit of the nozzle. For the two-dimensional convergent-divergent nozzle, the nozzle

has a throat height of 9.6mm, an exit height (*D*) 16.2mm, and a width 30mm (see Fig. 3.2(b)). And the divergent angles of the nozzles are not constant but total angle in divergent part of circular and 2-dimensional nozzle are about 3.48° and 4.1°, respectively. In the present study, the nozzle pressure ratio *NPR* (=p_0/p_a) is defined as the ratio of the pressure (p_0) inside the plenum chamber to atmospheric pressure (p_a). For the present convergent-divergent nozzles with a design Mach number of 2.0, the correct expansion at the exit of the nozzle is obtained at *NPR*=7.8.

In the present work, the fully expanded jet Mach number (M_j) will be used to describe the jet expansion condition because the jet Mach number rather than the nozzle pressure ratio has a physical meaning to characterize the supersonic jet. The jet Mach number is related to the pressure ratio, and is given as follows,

$$M_j = \sqrt{\frac{2}{\gamma - 1}\left[\left(\frac{p_0}{p_a}\right)^{(\gamma-1)/\gamma} - 1\right]} \tag{3.1}$$

where γ is the specific heat ratio of the gas (γ=1.4).

3.4 Schlieren Optical System

A high quality spark schlieren optical system is employed to visualize the supersonic jet flow, as illustrated in Fig.3.3. The system includes a light source, a collecting lense, pinhole, two concave mirrors and a vertical knife edge. And two types of light sources have been used in the experimental work. The one is nano-spark with a light intensity 10kJ and a duration time of 20ns. And the other one is continuum light source for capturing the shock wave oscillations by high speed video camera. The high speed video camera [Photron FASTCAM SA5] recorded the shock wave movements as the frame rate of 10,000fps for about 1.6 seconds with photo quality of 256×512pixel. The concave mirror has a diameter of 150mm and a focal length of 1000mm.

As shown in Fig.3.4, the output signal from the pressure transducer installed on the plenum chamber is transmitted to a personal computer (PC) through DC

amplifier, oscilloscope and a signal controller, and triggers a nano-spark light source. The remotely triggered light source provides a single spark, and then the light is passed across the test section between two concave mirrors. The schlieren images are recorded on a Nikon D100 digital camera or high speed video camera. (When the high speed video camera captured the test section, no trigger signal needs to light source.) An open shutter camera obtains the instantaneous images enough to freeze turbulent structures in the supersonic jets.

3.5 Pressure Transducer and Microphone

Calibrated pressure transducers (Kulite XCS-190, XCQ-062) mounted on the nozzle wall at several locations were used to measure and characterize the pressure fluctuation inside the nozzle.

Far-field acoustic measurements are carried out using microphones (Ono Sokki MI-6420) with a diameter of 1/4 inch. It has a sound pressure sensitivity of -24dB±3dB (0dB=1V/Pa), and measures the maximum sound pressure level up to 140dB. The microphones are calibrated using a sound pressure calibrator (Ono Sokki Model). The uncertainty in acoustic measurements is estimated to be less than ±1dB.

The acoustic signals are analyzed by using a 4-channel FFT analyzer (Ono Sokki Model DS0221), as shown in Fig.3.4. A FFT analysis is performed to obtain the power spectra and sound pressure level, providing the spectral data in the range from 0 to 40 kHz. The power spectra are averages of 20 samples, each of which contains 4096 data points.

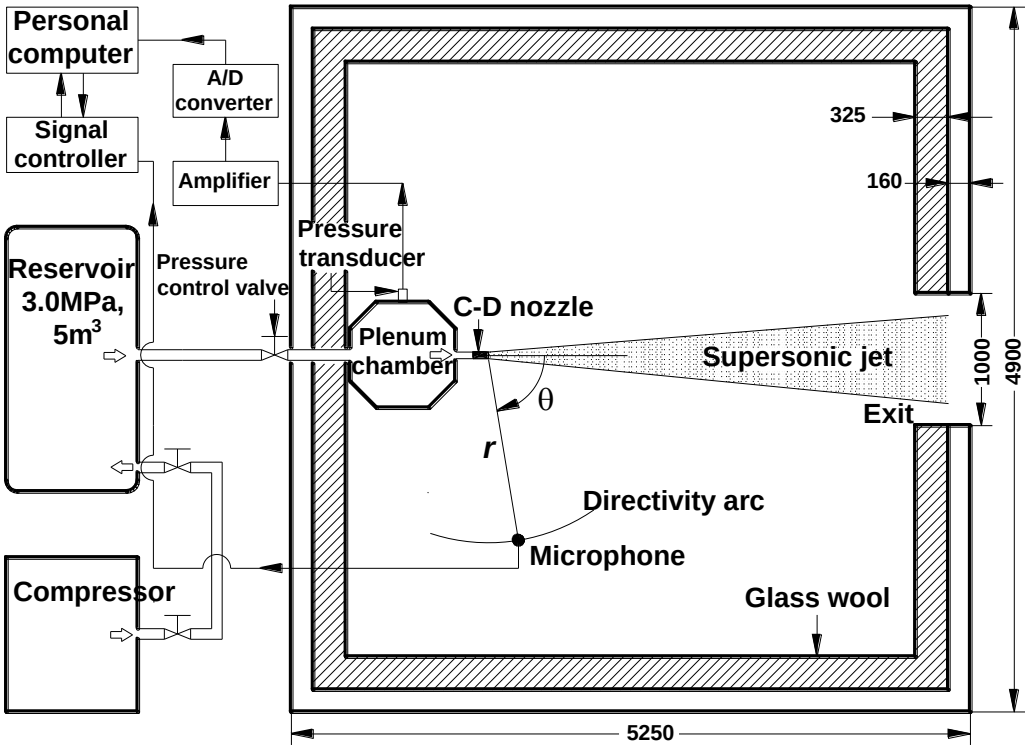

Figure 3.1 Schematic diagram of experimental facility (unit : mm)

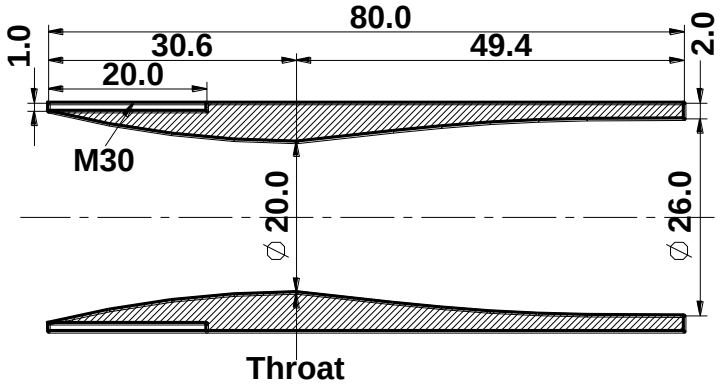

(a) Circular convergent-divergent nozzle

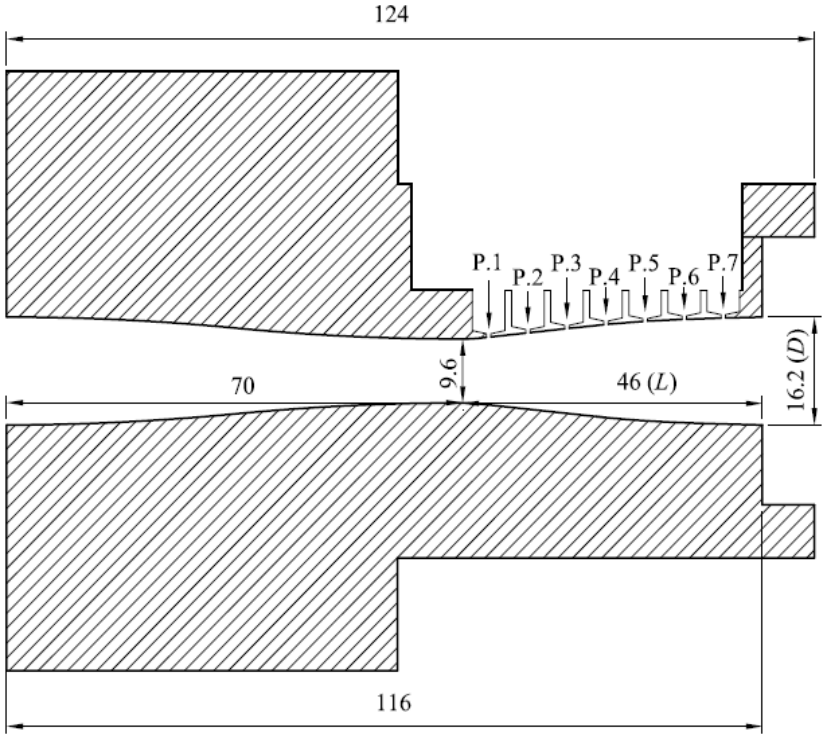

(b) Two-dimensional convergent-divergent nozzle

Figure 3.2 Details of a convergent-divergent nozzle (unit : mm)

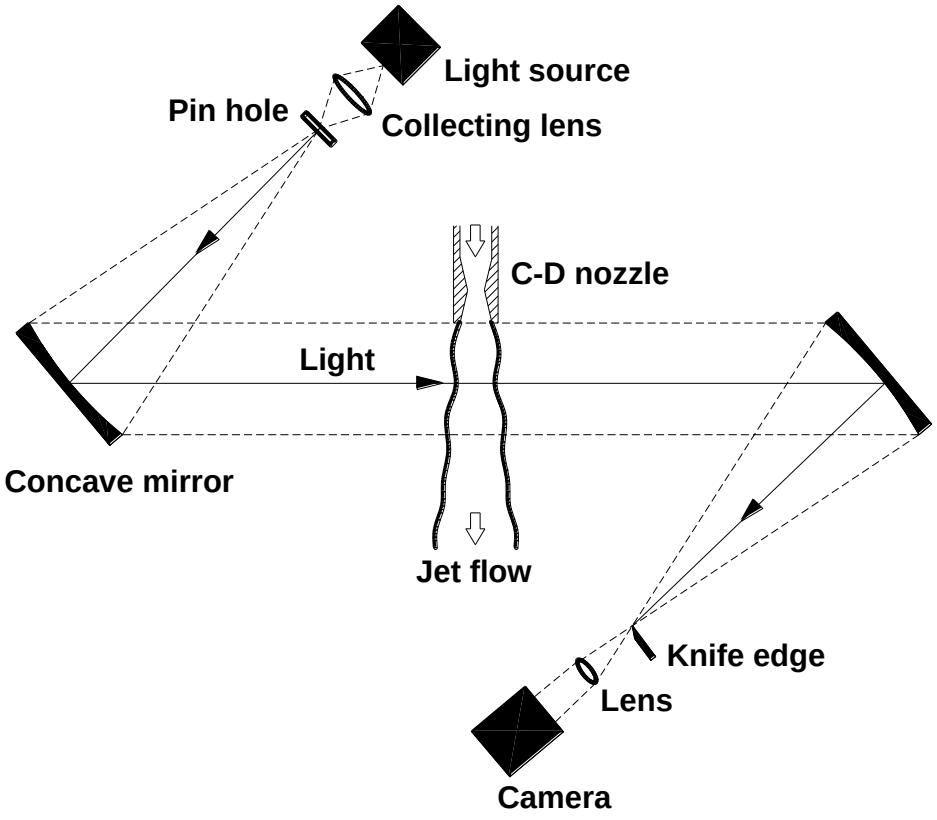

Figure 3.3 Spark schlieren optical system

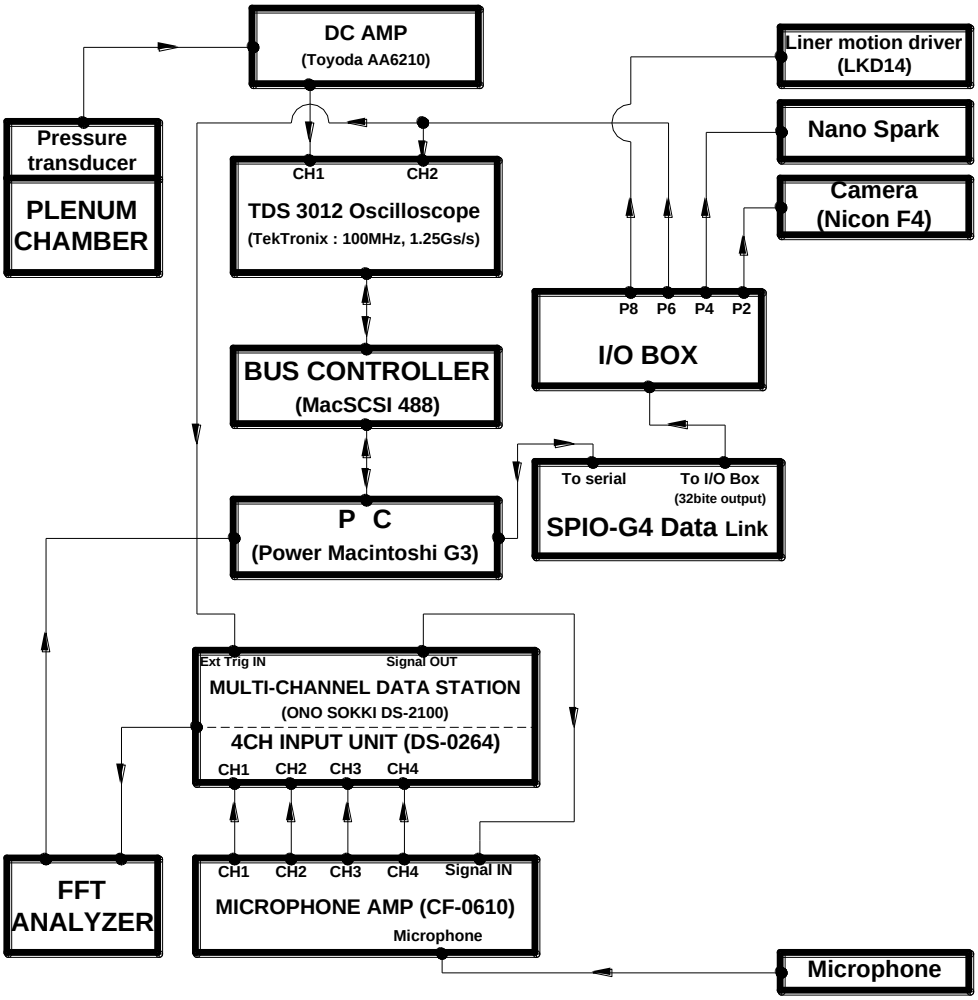

Figure 3.4 Schematic diagram of experimental procedure

Chapter 4

Acoustic Characteristics of Transonic Tone and Effect of Nozzle-Lip Thickness on Transonic Tone in Axisymmetric Nozzle

This chapter discusses the effect of nozzle-lip thickness on the transonic tone in axisymmetric convergent-divergent nozzle and describes a comparison the acoustic characteristics of transonic tone with screech tone according to the nozzle-lip thickness variation. A baffle plate made of an annular metal plate was installed at the nozzle exit to change the nozzle-lip thickness and its diameter was varied. Far-field acoustic measurements are accomplished to obtain the noise spectra of the supersonic jets, which are issued from an axisymmetric supersonic nozzle with a design Mach number of 2.0. The acoustic characteristics of the supersonic jet, such as the transonic tone frequency and amplitude will also be discussed in this chapter using the acoustic measurement results.

4.1 Experimental Conditions

In order to investigate the nozzle-lip thickness effect on the transonic tone, far-field acoustic measurements were made by using a condenser microphone which has 1/4 inch of diameter. The sound pressure measuring locations are schematically shown in Fig. 4.1. Four condenser microphones were located at 12°

interval between 60° and 96°angles from the jet direction along a circular arc of radius 1300mm(r/D=50) away from the exit of the nozzle. The nozzle pressure ratio (NPR) was varied between 1.2 and 2.8, isentropic corresponding to the jet Mach numbers of M_j=0.52 to 1.31. The nozzle pressure ratio applied in this study covers the supersonic jets ranging from choking condition to non-isentropic condition which means shock wave occurs within divergent section in the convergent-divergent nozzle.

An annular baffle plate was installed at the exit of the nozzle to change the nozzle-lip thickness. Details of a baffle plate are shown in Fig. 4.2 and Table 4.1. The width t_b of the baffle plate was varied in the range from 24mm to 76mm. As the simple nozzle has a thickness of 2mm between inner and outer wall at the nozzle exit plane as shown in Fig. 4.1(a), the nozzle lip-thickness (t) is given as $t=t_b$+2mm. In the present study, the nozzle-lip thickness is described as t/D non-dimensionalized by the exit diameter of nozzle (D=26mm). Note that t/D=0.1 indicates the basic case without a baffle plate at the nozzle exit.

4.2 Acoustic Characteristics of Transonic Tone

Fig. 4.3 shows a typical noise spectrum of a supersonic jet at low nozzle pressure ratios when a shock wave occurs within the divergent section of convergent-divergent nozzle where r/D=50, θ=96° and NPR=1.8. The spectrum is characterized by three noise components, the turbulent mixing noise, the transonic tones and its harmonics. At first, the detailed acoustic characteristics for the transonic tones will be explained in this chapter.

Fig. 4.4 shows the sound pressure spectra of the jet with NPR=1.2 to 2.8 measured at point of θ=96°, 84°, 72° and 60° degrees. At NPR=1.6 to 2.4, the peak value is observed at about 1kHz and 3kHz. These peak values show the transonic tones and stage1(shown in dotted blue line) and stage2(shown in dotted red line), respectively. It is not exact that the transonic tone exist at NPR1.2 or 1.4 but the case 1.6 of NPR, the transonic tone appear conspicuous and becoming

more and more apparent according to increase of NPR and then the stage 2 of the transonic tone level decreases more sharply than stage1's level. After all, no transonic tone can found at more than 2.6 NPR. What's interesting here is that the stage1 of transonic tone level gradually increased at NPR=1.6 to 2.2, and then fell rapidly at NPR=2.4 to 2.6. One more interesting fact is that the transonic tone frequency increased correspond to the increases of NPR. This characteristic is differ from screech tone which, as mentioned earlier, is arising through an acoustic feedback loop between nozzle exit and external shock cell structure. Fig. 4.5 obviously shows the transonic tone in distinction from the screech tone. The frequency data of screech tone had been measured as prior work at same condition with this work(Miyazato, Y. Kweon, Y. H. et al, 2004). In the Fig. 4.5, while the screech tone frequency decrease with NPR increasing, the transonic tone frequency is increased corresponding to NPR. And the result of transonic tone frequency is almost corresponding to the value of the empirical equation proposed by Zaman(Zaman, Dahl, Bencic & Loh 2002) as shown in Fig. 4.5.

The relationships between noise amplitude and Mach number is shown in Fig. 4.6 and Fig. 4.7. The increase or decrease tendency of two noise amplitude with Mach number are similar but the transonic tone has more gradual variation of amplitude with Mach number.

4.3 Effect of nozzle-lip length on Transonic Tone

Fig. 4.8 shows the variation of transonic tone amplitude with nozzle-lip thickness. In Fig. 4.8, it is clearly found that there is little variation, as less than 2 dB, of transonic tone amplitude with the variation of nozzle-lip length. The variation of screech tone amplitude, On the other hand, up to 15dB in Fig. 4.9. This fact is also easily found in Fig. 4.6 and Fig. 4.7. which shows the amplitude variation with Mach number. Overall, the transonic tone emitted at low nozzle pressure ratio relatively. And the transonic tone amplitude and amplitude variation is small compare to screech tone' one. Additionally, the frequency variations are plotted according to nozzle-lip length in Fig. 4.9. At stage 2 of transonic tone, the

frequencies are slightly varied but mostly uniform with nozzle-lip length changing.

Until now acoustic characteristics of transonic tone are discussed by examine the effect of nozzle-lip length on transonic tone with comparing screech tone. The tendency examined earlier, can be interpreted by discussing noise source location. For example, screech tone occur through feedback loop between nozzle exit and externally located shock cell structure. Therefore the effect of nozzle-lip length is much more than transonic tone which occur in divergent part of convergent-divergent nozzle. The fact that the transonic tone source exist at the inside of nozzle gives a good account for variation of transonic tone frequency according to NPR(or Mach number). That is, as Mach number increase, shock waves moves down stream and then, it is shorter and shorter the noise vibrating region between shock and nozzle exit. Actually, there is close connection between the characteristics of transonic tone and separation shock position in supersonic nozzle. Also it may be explained that the reason why the stage1 decreased rapidly between NPR2.4 and 2.6 in Fig. 4.4 is due to the small angle of half divergence which means expansion angle of divergent part of the nozzle geometry. If the half angle of divergence is sufficiently large, the shock wave moves gradually by NPR increase but the half angle is small, the shock wave moves to downstream rapidly by NPR increase, then, the transonic tone level fall rapidly. The convergent-divergent nozzle used for this chapter, has small of half divergence at nozzle exit.

4.4 Summary

This chapter described the acoustic characteristics and the effect of nozzle-lip length on transonic tone in axisymmetric supersonic nozzle. An annular baffle plate was installed at the nozzle exit to change the nozzle-lip thickness and its diameter was varied. Far-field acoustic measurements were made by using a

condenser microphone. Experiments were accomplished to obtain the noise spectrum of a supersonic jet at low nozzle pressure ratios when a shock wave occurs within the divergent section of convergent-divergent nozzle.

The results obtained clearly show that the transonic tone differently occurs from screech tone in nozzle systems as a source of internal noise. The frequency of transonic tone obtained by experimental work corresponds to Zaman's empirical formula approximately. Considering the results of acoustic characteristics and source location of transonic tone, it is worthy to investigate carefully into relationship between transonic tone and shock wave or flow fluctuation in divergent part of nozzle.

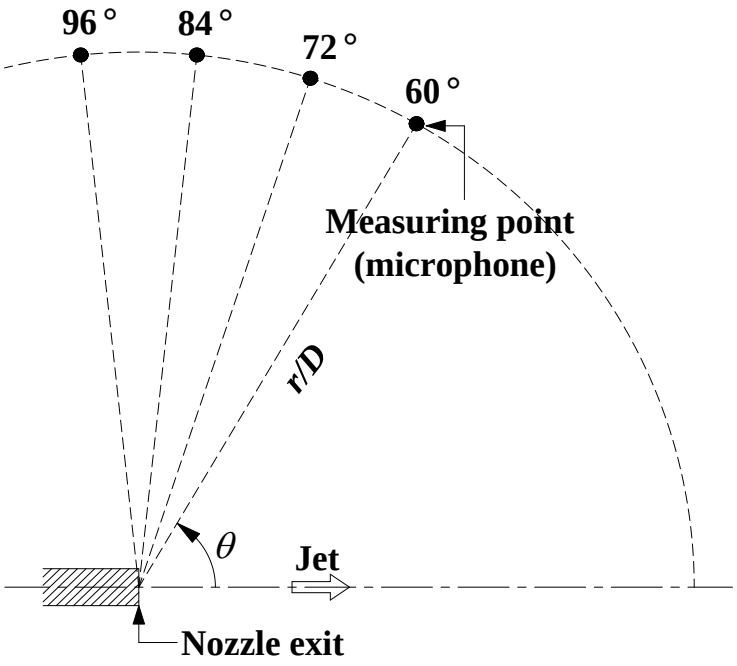

Figure 4.1 Microphone locations

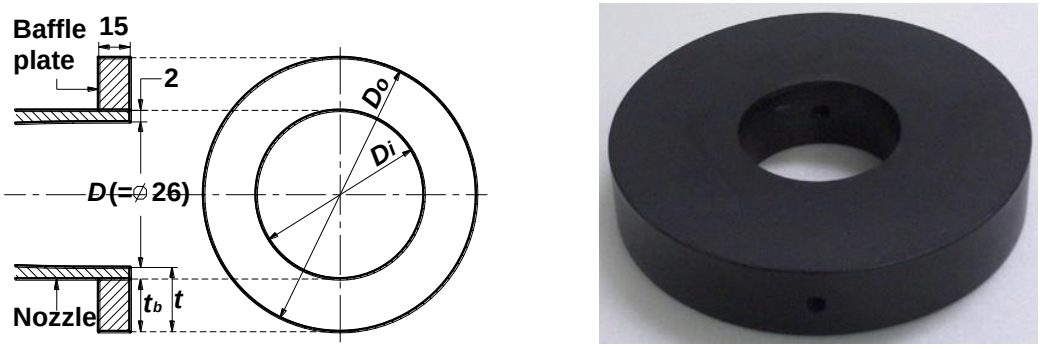

(a) Arrangement of a baffle plate (b) Picture

Figure 4.2 Arrangement and picture of a baffle plate (unit : mm)

Table 4.1 Detailed dimensions of baffle plates (unit : mm)

t/D	D_o	D_i	t_b	t (=t_b+2)
0.1	Simple nozzle (without a baffle plate)			2
1.0	78	30	24	26
2.0	130		50	52
3.0	182		76	78

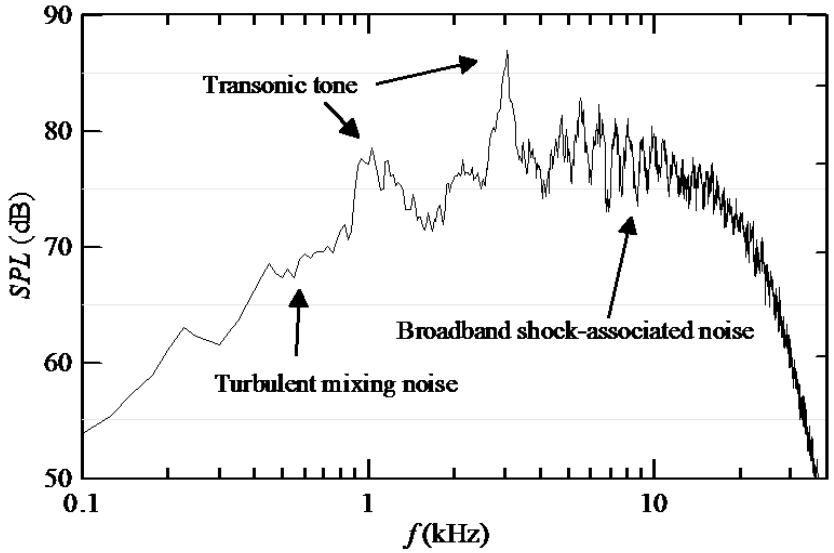

Figure 4.3 Typical far-field noise spectrum measured at r/D=50 and θ=96° (NPR= 1.8)

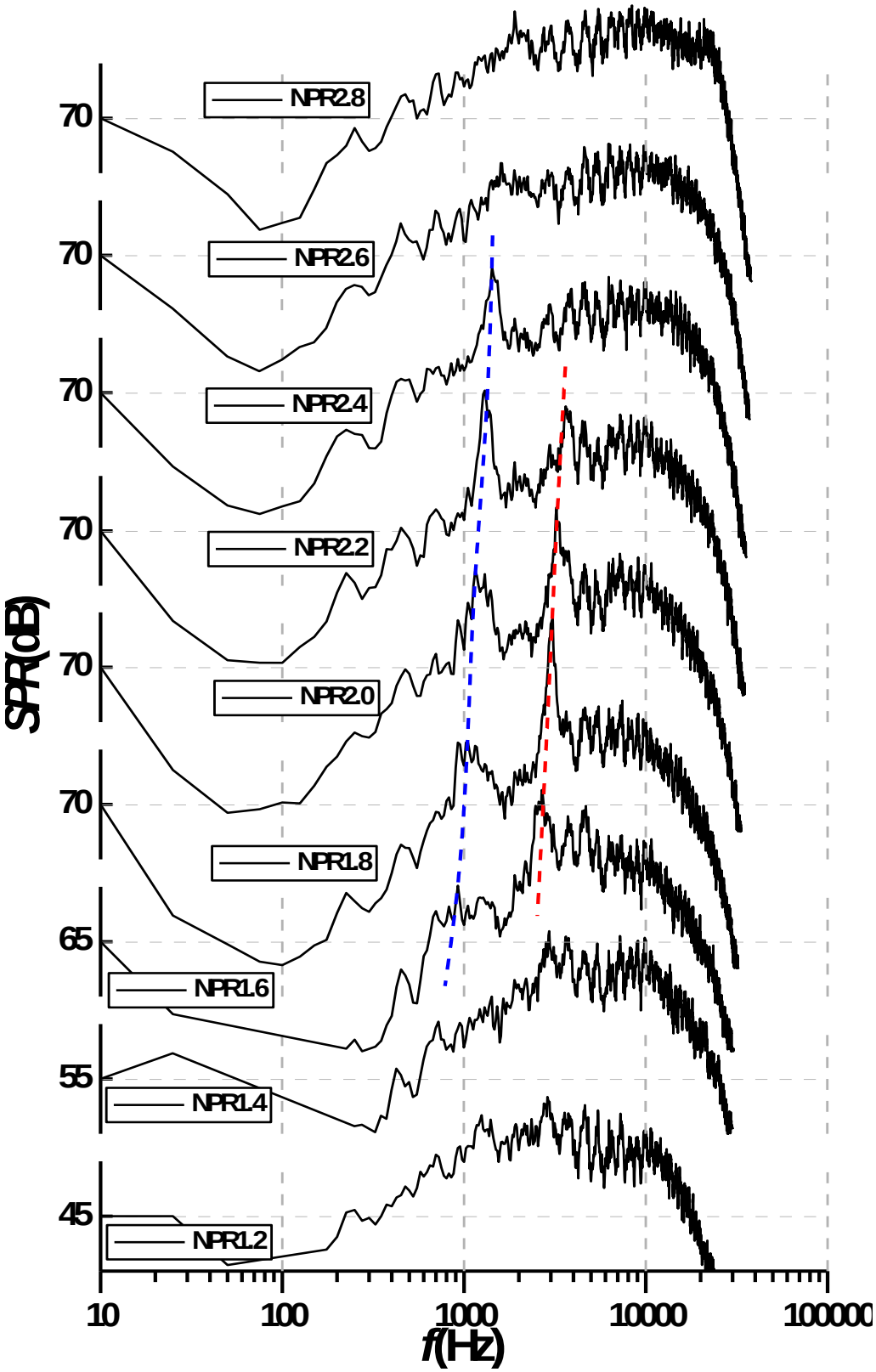

Figure 4.4 (a) Far-field noise spectrum variation with NPR(r/D=50 and θ=96°)

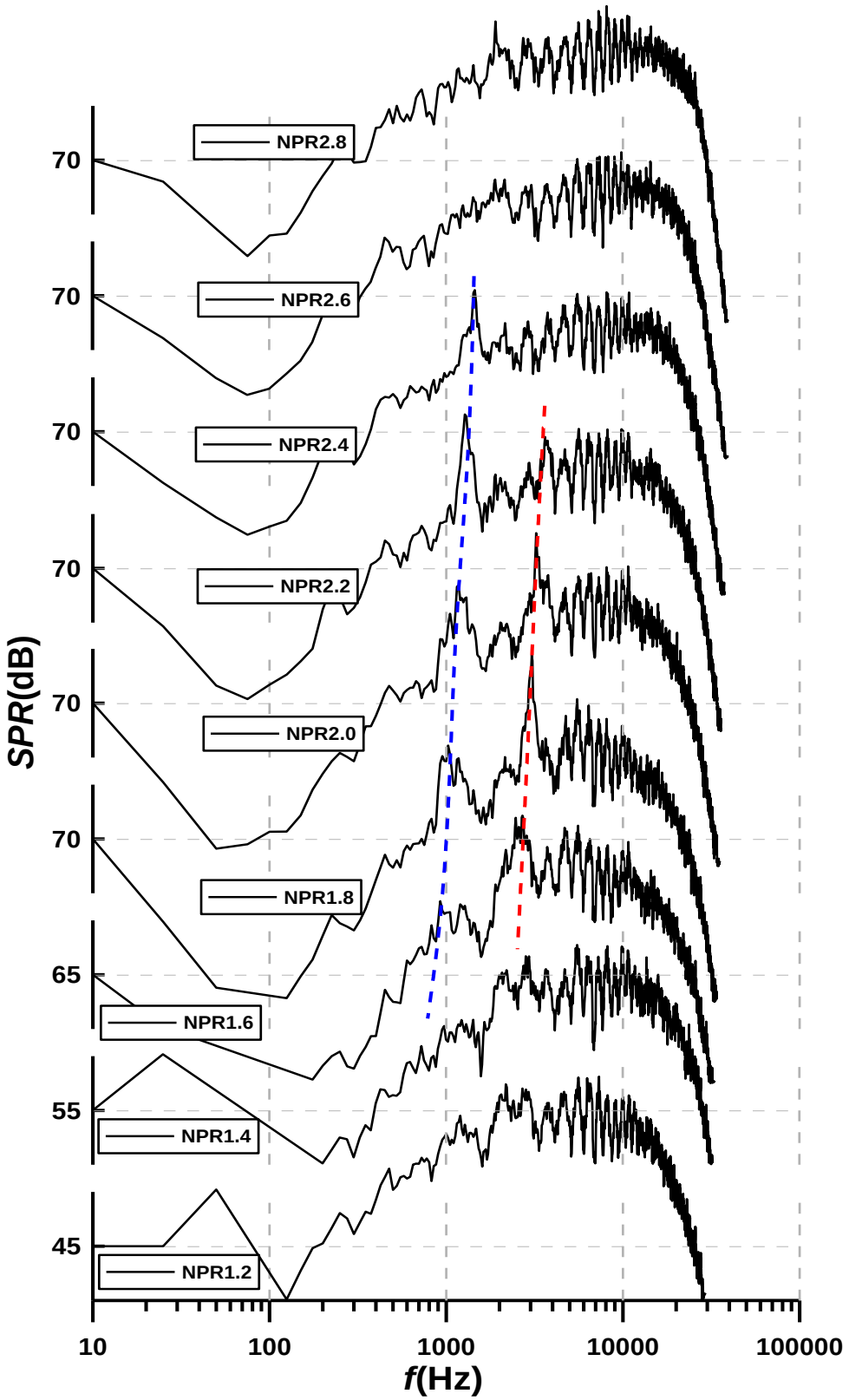

Figure 4.4 (b) Far-field noise spectrum variation with NPR(r/D=50 and θ=84°)

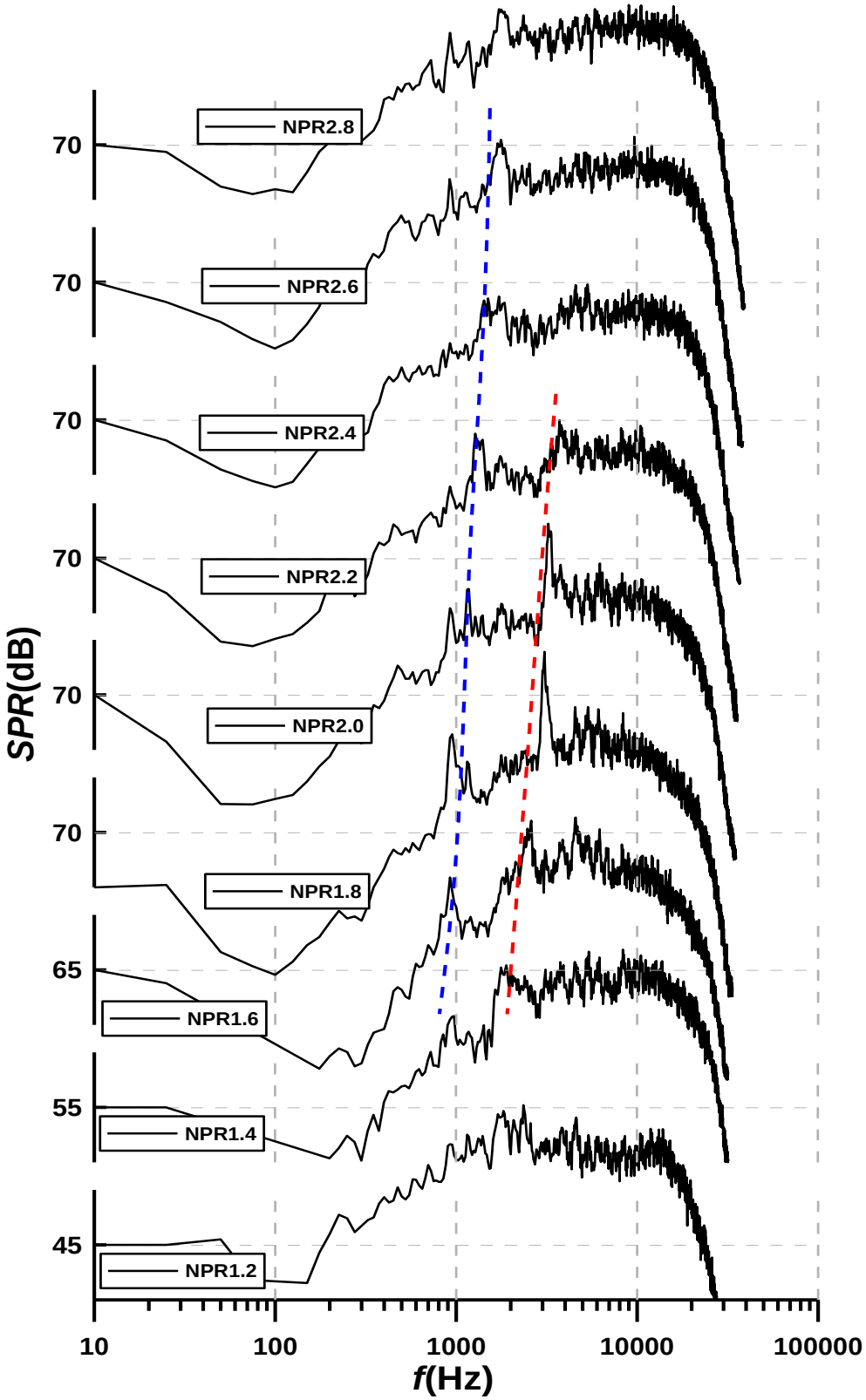

Figure 4.4 (c) Far-field noise spectrum variation with NPR(r/D=50 and θ=72°)

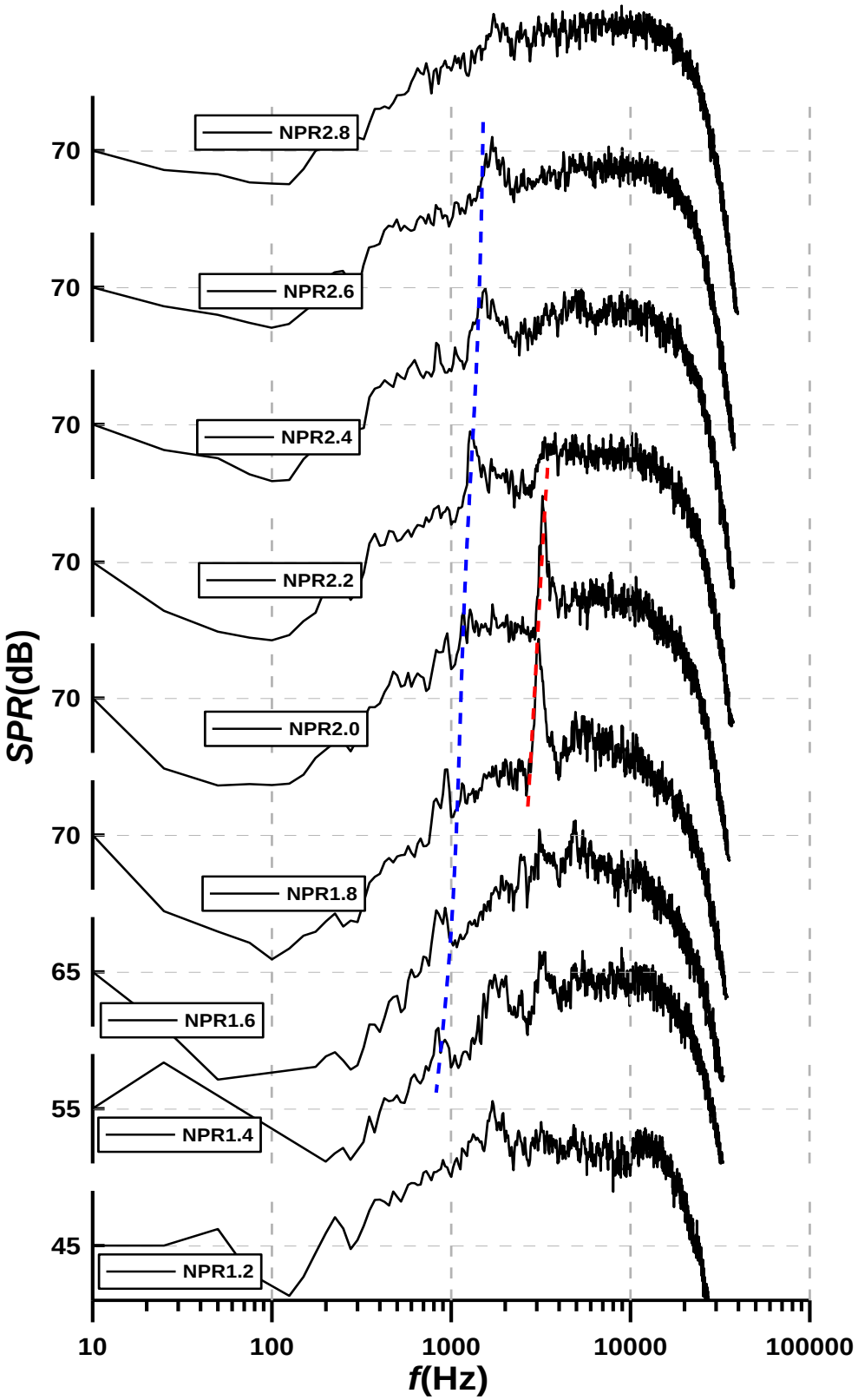

Figure 4.4 (d) Far-field noise spectrum variation with NPR(r/D=50 and θ=60°)

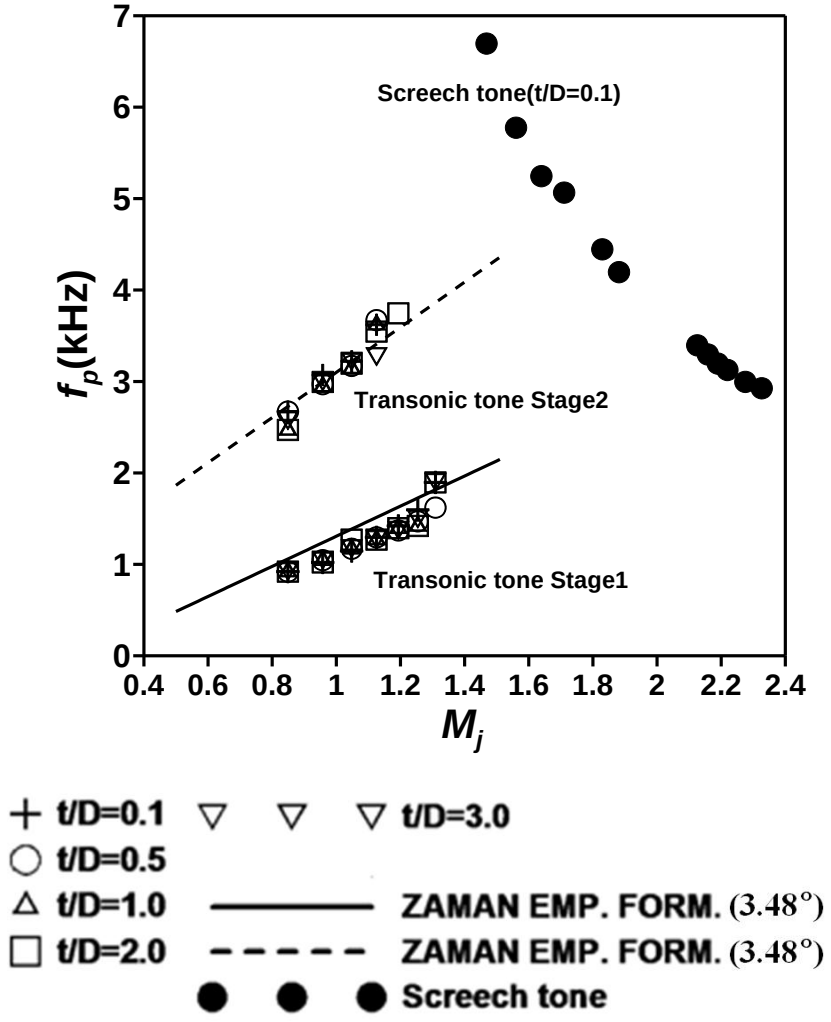

Figure 4.5 Peak frequency distribution of transonic tone and screech tone (*r/D*=50 and θ=96°)

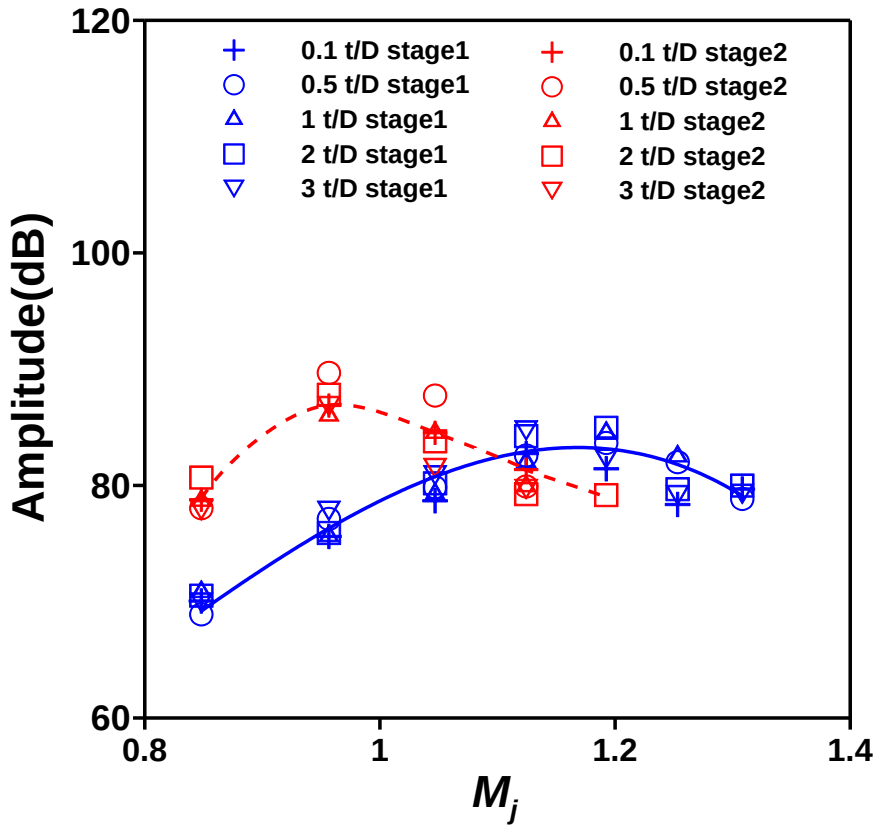

Figure 4.6 Relationship between transonic tone amplitude and M_j

(r/D=50 and θ=96°)

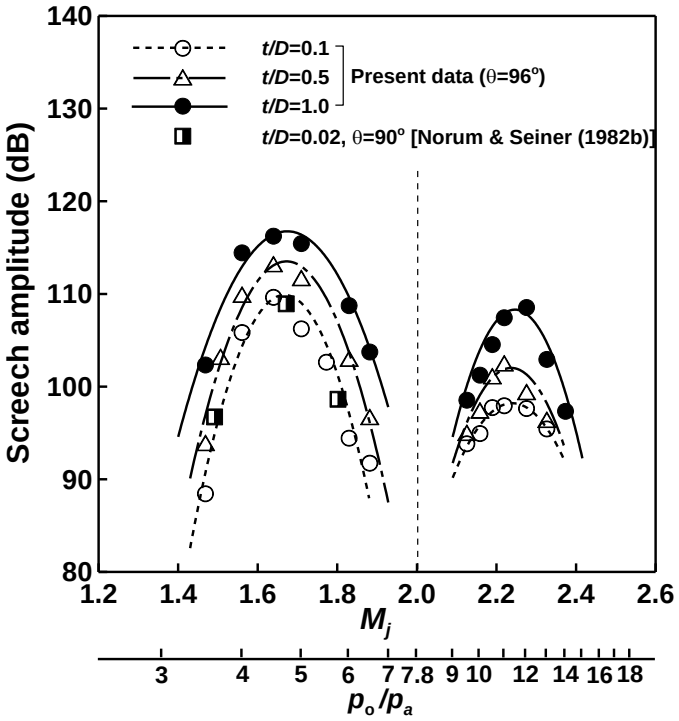

(a) *t/D*=0.1 ~ 1.0

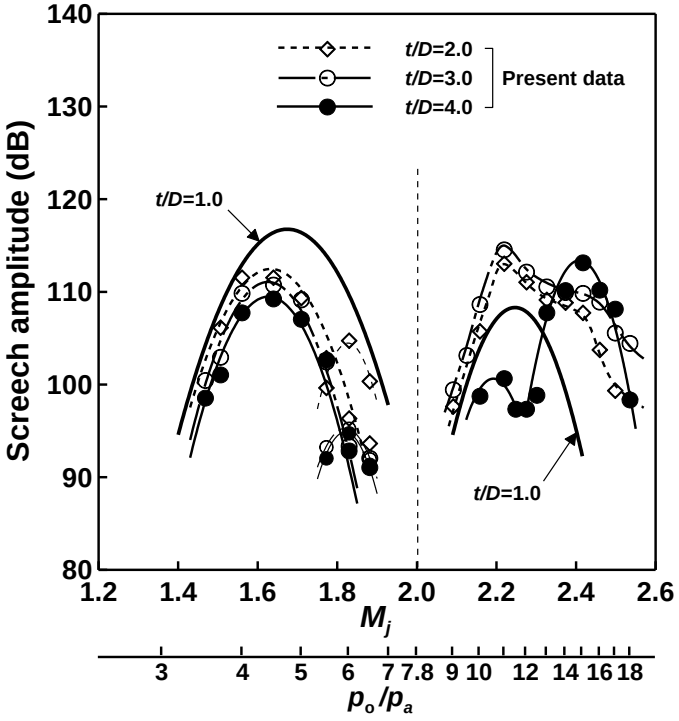

(b) *t/D*=2.0 ~ 4.0

Figure 4.7 Relationship between screech tone amplitude and M_j

(Miyazato, Y. Kweon, Y. H. et al, 2004)

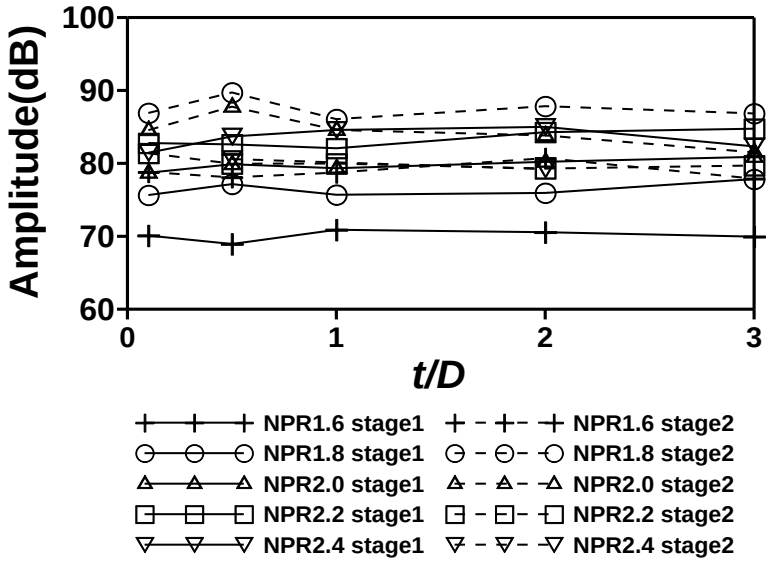

Figure 4.8 Variation of transonic tone amplitude with *t/D*

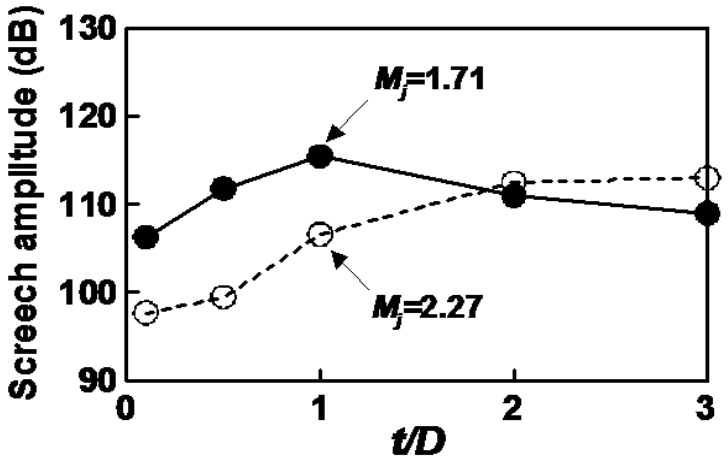

Figure 4.9 Variation of screech tone amplitude with *t/D* for over-expanded and under-expanded jets(Miyazato, Y. Kweon, Y. H. et al, 2004)

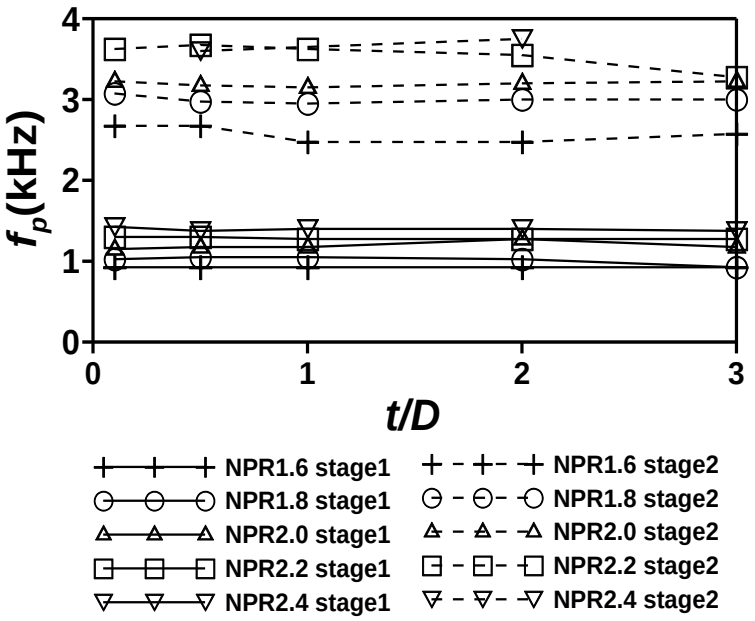

Figure 4.10 Variation of transonic tone frequency with *t/D*

Chapter 5

Transonic tone in 2-Dimensional Supersonic Nozzle

In the previous chapter, the acoustic characteristics of the transonic tone and the effect of nozzle-lip thickness on transonic tone were discussed to understand the transonic tone occurs inside of supersonic nozzle. As previously mentioned, it is worthy to examine the relationship between transonic tone and flow fluctuation. This chapter focuses on the frequency of first shock wave oscillation and wall static pressure fluctuation by using 2-dimensional supersonic nozzle which make possible to visualize the shock wave and attempts to correlate the transonic tone with shock wave oscillation or wall static pressure fluctuation. To analyze the shock wave frequency, a high speed video camera was employed for schlieren optical system and all measurements had been set up to capture output data simultaneously.

5.1 Experimental Conditions

Fig. 5.1 and Fig. 5.2 shows the 2-dimensional convergent-divergent nozzle made from brass as prefabricated type with a design Mach number of 2.0, which is installed in the end wall of plenum chamber. The nozzle has a throat height of 9.6mm, an exit height(H) 16.2mm, and a width 30mm and the length of divergent section was 46mm(L). For the present nozzle, the correct expansion state at the exit of the nozzle is obtained at NPR=7.82. Experiments are carried out for different nozzle pressure ratios from 1.2 to 3.0.

Acoustic measurements were made using a condenser microphone that has a

diameter of 1/4 inch. The microphone was located at angles of 60° from the jet direction, and a radial distance of 520mm(r/D=32) from the nozzle exit. The acoustic signals are analyzed by using a FFT analyzer. A FFT analysis provides the noise spectra, and providing the spectral data in the range from 0 to 40 kHz, with a frequency band width of 25 Hz.

A pressure transducer (Kulite XCS-190, XCQ-062) mounted on the nozzle pressure hole which stand at 6mm distance from nozzle exit. And sampling frequency was set-up as 50kHz at external computer.

The sidewalls of the supersonic nozzle have optical grasses to allow flow visualization by a schlieren optical system. To measure a frequency of the shock wave oscillations in the divergent section of the nozzle, visualization was performed by schlieren method with high-speed digital video camera (Photron FASTCAM SA5). The movie was recorded at 10,000fps for 1.6 second, and the frame has 256x512 pixels.

5.2 Acoustic Characteristics

Fig. 5.3 shows the noise spectra of two-dimensional supersonic nozzle flow with NPR 1.2 to 3.0 where the shock wave occurs in convergent part of the nozzle. The transonic tones have several dominant peaks with the fundamental frequency and its odd harmonics. For instance, the acoustic resonance for *NPR*=1.6 have the fundamental frequency at about 0.8 kHz(stage1) and the odd harmonics is at about 2.4 kHz(stage2). As previously mentioned, the frequency of the transonic tone increases with increasing *NPR* and the tone frequency is clearly observed at NPR 1.6 to 2.1. The present results are similar to the characteristics of general transonic tones of the axisymmetric nozzle. Fig. 5.4 shows the transonic tone frequency variation with NPR. In Fig. 5.4, Zaman's empirical formula(θ=4.1°) (Zaman, Dahl, Bencic & Loh 2002) estimates higher than experimental results but the stage 2 is agreeable to Zaman's equation(θ=6°) which the angle is recalculated by considering the shock position. Overall, there

are some gaps, at stage1, between experimental results and calculated value of Zaman's empirical formula which based on the data for single round nozzles but the tendency is obviously agreeable.

5.3 Flow Visualization

Schlieren photos of supersonic jets with a shock wave within the nozzle are shown in Fig. 5.5. In Fig. 5.5, each pair of photos respectively show the shock wave location when the first shock wave locates at minimum and maximum distance from nozzle exit. Under this experimental condition of NPR 1.4 to 3.0, the shock wave becomes λ-type pseudo-shock wave due to the boundary layer on the nozzle wall and oscillates in flow direction. It is found that the distance between the first shock wave and second shock wave is different with each other at some pair because the shock wave vibrates while expanding and contracting like a spring. The separation is asymmetric wherein one lambda foot is larger than the other, and large eddies are occurred in the shear layer of the large separation zone. Papamoschou et al. suggested that the instability mechanism in the nozzle flow separation is due to an interaction between the expansion fan reflected from the smaller lambda foot with the shear layer of the larger separation zone(Papamoschou & Johnson 2006). It can be expected that this interaction is related to the transonic tone feedback mechanism.

5.4 Shock wave oscillation

The movement of the first shock wave that obtained from the movies are shown in Fig. 5.6. And Fig. 5.6 (b) shows the movements of the first shock wave for *NPR*= 2.6 which is the condition for no emission of transonic tone. Abscissa represents the distance from the nozzle exit in millimeter and ordinate represents the recording time. When *NPR* reaches 1.8, as shown in Fig. 5.6 (a), the amplitude of the first shock wave oscillations is almost doubled compared with that of *NPR* 2.6. This means the flow field downstream of the first shock wave is excited when the transonic tone occurs, and the oscillations of the shock wave

becomes large.

Fig. 5.7 shows power spectral density(PSD) of the first shock wave oscillation. Overall, predominant frequencies at 1kHz and 2.5kHz are clearly shown even when transonic tone frequency is not conspicuous except for NPR2.8 and 3.0 but the PSD values are relatively larger when the transonic tone occur. The peak frequency of PSD is corresponding to the transonic tone frequency. It is reasonable to suppose that the transonic tone links to the first shock wave oscillation.

5.5 Wall Static Pressure Fluctuation

Fig. 5.8 shows PSD of the wall static pressure fluctuation at 6mm upstream from the nozzle exit for *NPR*1.2 to 3.0. For 10 times averaged FFT(Fast Fourier Transform) analyzing, sampling frequency of wall static pressure was set at 50kHz. At NPR1.2 which case has no shock wave occur in the nozzle, predominant frequency is not found. For the PSD of wall static pressure oscillations, two dominant peaks are observed at about 0.8~1 kHz and 2.5~3 kHz in almost case when the transonic tone occur in the nozzle but dominant peaks gradually disappeared with increase of NPR. These dominant peaks are occurred at nearly the same with frequency of the first shock wave oscillation and, of course, the transonic tone (stage1 and stage2). In particular, the case of NPR 1.8~2.1 that has stronger transonic tone in stage1, both frequency of shock wave and wall static pressure fluctuation also have been increased. In Fig. 5.9, transonic tone and each frequency of analyzed results are totally plotted with NPR and x_s. x_s define as the distance between shock wave and the nozzle exit. In Fig. 5.9, we can recognize obviously that the frequencies of shock wave and wall static pressure oscillation correspond to transonic tone frequency and at some condition, the intensity of flow oscillation becomes strong with the transonic tone amplitude increase. These results which show that each predominant frequency and its intensity are respectively corresponding to transonic tone frequency and amplitude suggest that the transonic tone has close correlation in frequency of

shock wave or wall static pressure oscillation.

5.6 Cross-correlation

To investigate the correlation between the transonic tone and the first shock wave oscillation or wall static pressure fluctuation, the cross-correlation coefficient(*R*) was evaluated and the cross-correlation coefficient(*R*) presented as

$$R = \frac{s_{xy}}{s_x s_y}$$

where

$$s_{xy} = \frac{1}{n}\sum_{i=1}^{n}(x_i - \bar{x})(y_i - \bar{y}),$$

$$s_x{}^2 = \frac{1}{n}\sum_{i=1}^{n}(x_i - \bar{x})^2$$

$$s_y{}^2 = \frac{1}{n}\sum_{i=1}^{n}(y_i - \bar{y})^2$$

and $\tilde{x}, \tilde{y}$ mean average of samples. Fig. 5.10 shows cross-correlations with time shift at typical NPR. The solid arrow marked in these charts mean a peak value of the cross-correlation corresponding to positive delay. Overall, the peak of the cross-correlation is larger or smaller at the case of NPR1.7 or 2.0 which has transonic tone occurrence and decaying-sinusoidal distributions of the cross-correlation are found at NPR 1.7 and 2.8. Positive delay time means an order of sequences between two of compared data and the plus and minus value of cross correlation mean that two of data has a proportional and inverse relationship, respectively. For example, the cross-correlation value marked as solid arrows in Fig. 5.10 (a) indicate that there are reverse relationships between shock wave oscillations and wall static pressure fluctuations. Precisely, that means wall static

pressure increase or decrease after some positive delay time from shock wave moves downstream or upstream, respectively. On the other hand, at negative delay time peak, the charts indicate that the shock wave respectively moves upstream or downstream after increase or decrease of wall static pressure. In this case, however, there is no validity physically because the shock wave should be moved downstream or upstream after increase or decrease of wall static pressure. But it seems that there can be feedback loop between shock wave oscillation and wall static pressure fluctuation when the transonic tone is emitted from the nozzle.(T.Handa et al.,2002) At Fig. 5.11 to Fig. 5.13, each peak value of cross-correlation was plotted totally and the shading part indicates occurrence conditions of the transonic tone. At shaded part where means the transonic tone occurring, most of the cross-correlation coefficients are noticeable than the other experimental case of NPR. Overall, the cross correlation values *R* at Fig. 5.12 and Fig. 5.13 is smaller than the values of Fig. 5.11. It can be explained that the reason why the low value of correlation is due to the sound pressure which includes not only transonic tone but also the other components of jet noise. However, it is obvious that there is closer correlation between transonic tone and flow oscillation or shock wave and wall static fluctuation when the transonic tone occur in the nozzle.

Table 5.1 shows that delay time of each oscillation data at maximum correlation and using this delay time, also velocities is represented. The subscript ‘s’, ‘p’ and ‘m’ indicate first shock oscillation, wall static pressure oscillation and sound pressure, respectively. Particularly, it is interesting that the delay time from shock oscillation to sound pressure(T_{s-m}) equal to the delay-time sum of the shock-wall pressure oscillation(T_{s-p}) and wall pressure oscillation-sound pressure(T_{p-m}) when the transonic tone occur(1.6~2.1NPR). And the velocities ‘V_{p-m}’ in Table 5.1, is come out to equal to almost sound speed. And it seems that the ‘V_{s-p}’ is the velocity of downstream-convected disturvance in large separation zone. But it calls for further investigation to find the upstream-propagating disturbanace between the shock wave and wall static pressure.

5.7 Summary

In this chapter, to understand the characteristics and generation mechanism of the transonic tone, the correlation between the transonic tone and flow oscillation were investigated from a shock-containing flow in divergent part of 2-demensional supersonic nozzle. To measure the frequencies of the first shock wave oscillations, a high-speed video camera was employed for Schlieren system. And for each experimental run, all measurements were sampled simultaneously at sampling rate 10kHz for high speed video camera and 50kHz for pressure transducers or microphone.

In the 2-dimensional nozzle, the present acoustic results are similar to the characteristics of general transonic tones of the axisymmetric nozzle. When the transonic tone occurs, the amplitude of the shock wave oscillations is double compared with that when the tone has not been generated. The results of each PSD shows that when the transonic tone is diffusing from the nozzles, the dominant frequencies of the shock wave oscillation and wall static pressure fluctuation correspond to transonic tone frequency. Moreover, amplitude of each dominant frequency of shock wave and wall static pressure also corresponds to transonic tone amplitude mostly. There are close correlations between shock oscillation, wall static pressure oscillation and transonic tone peak frequency when the transonic tone occurs.

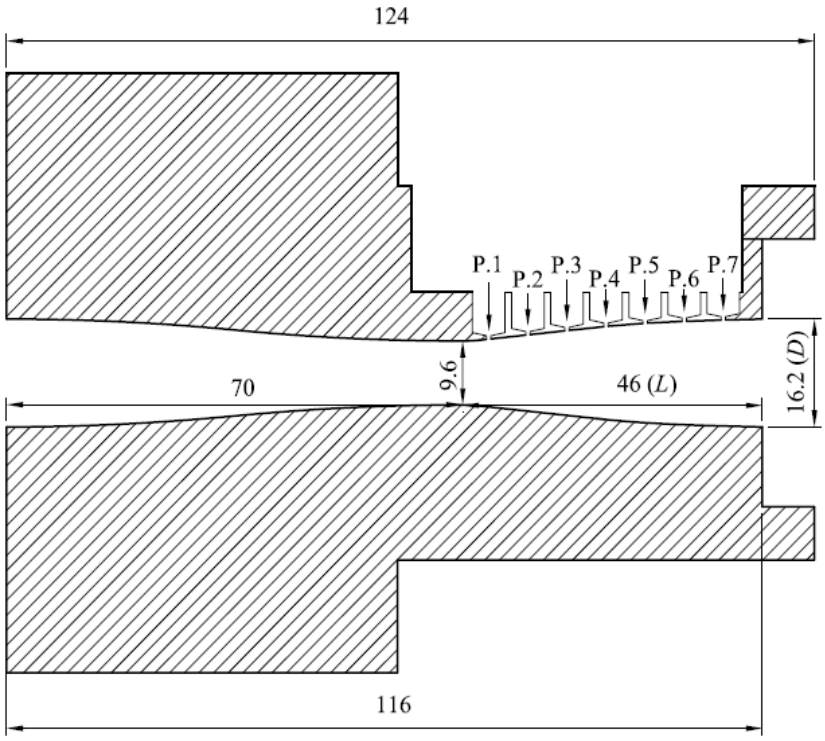

Figure 5.1 Schematic diagram of 2-dimensional convergent-divergent nozzle

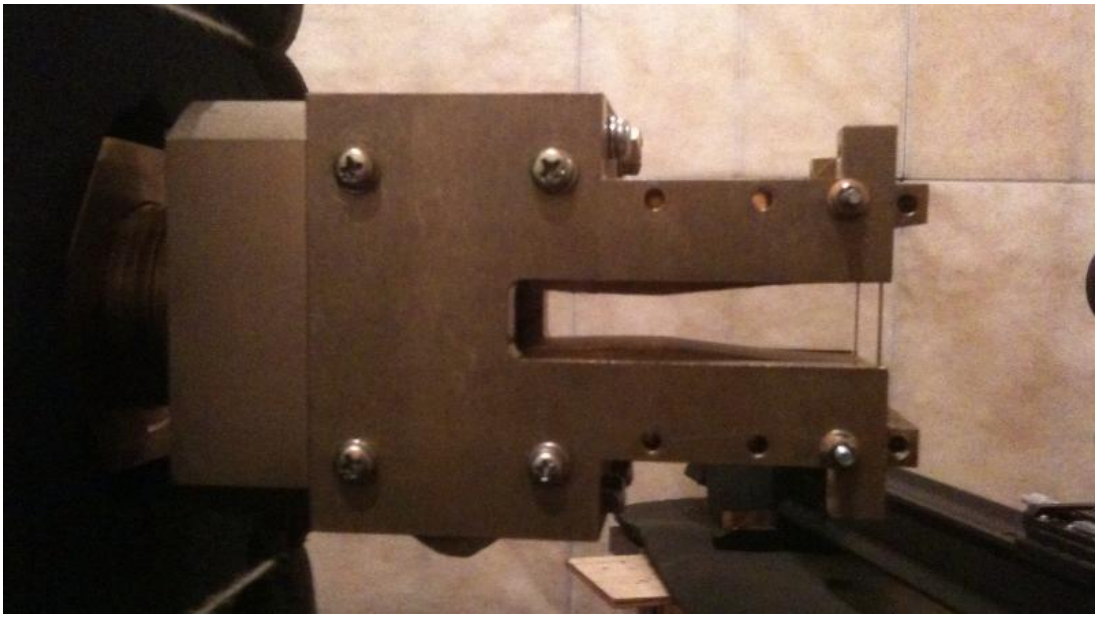

Figure 5.2 A photo of the 2-dimensional convergent-divergent nozzle

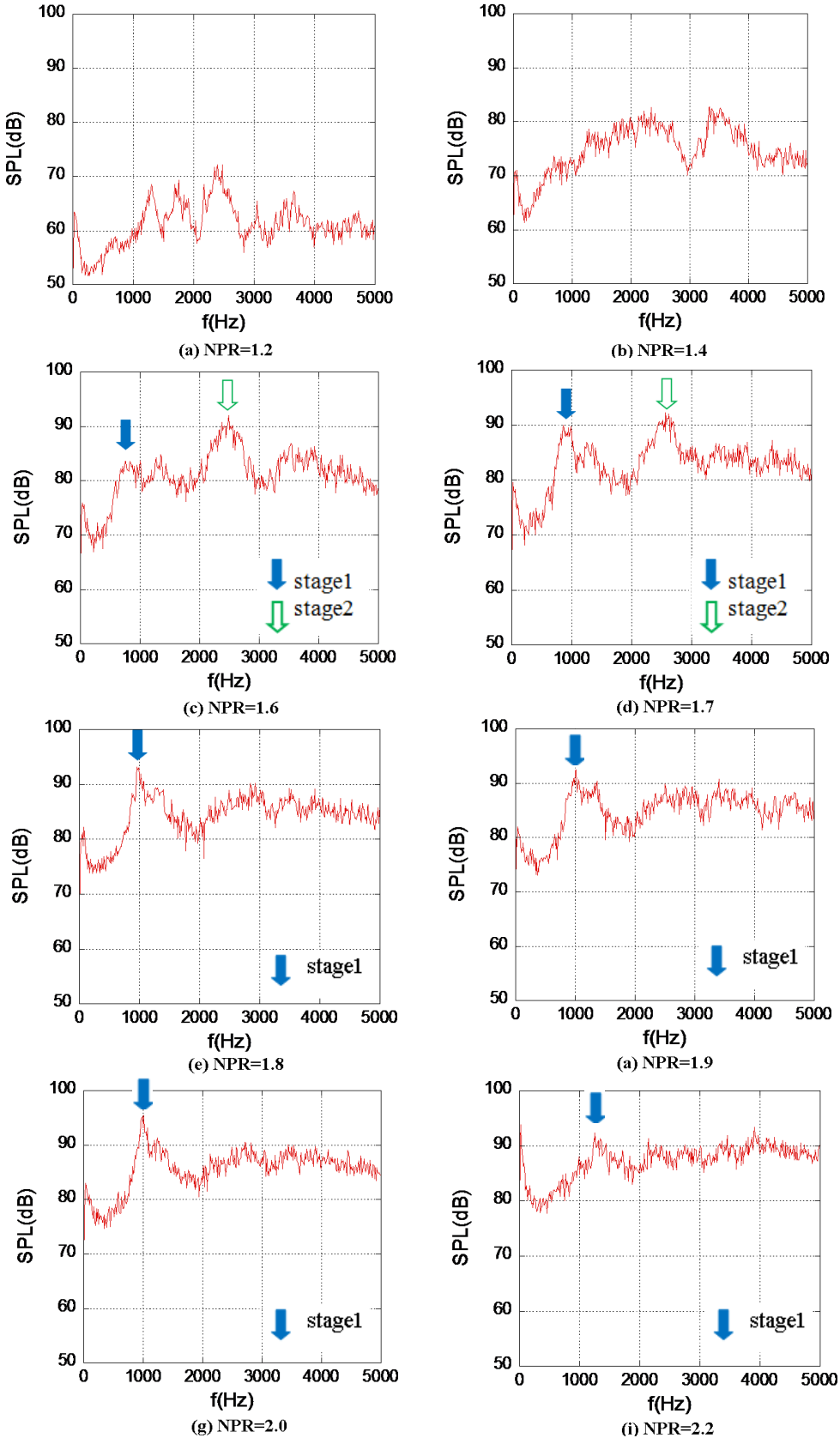

Figure 5.3 Sound pressure level spectrum(2-D nozzle, θ=60°)

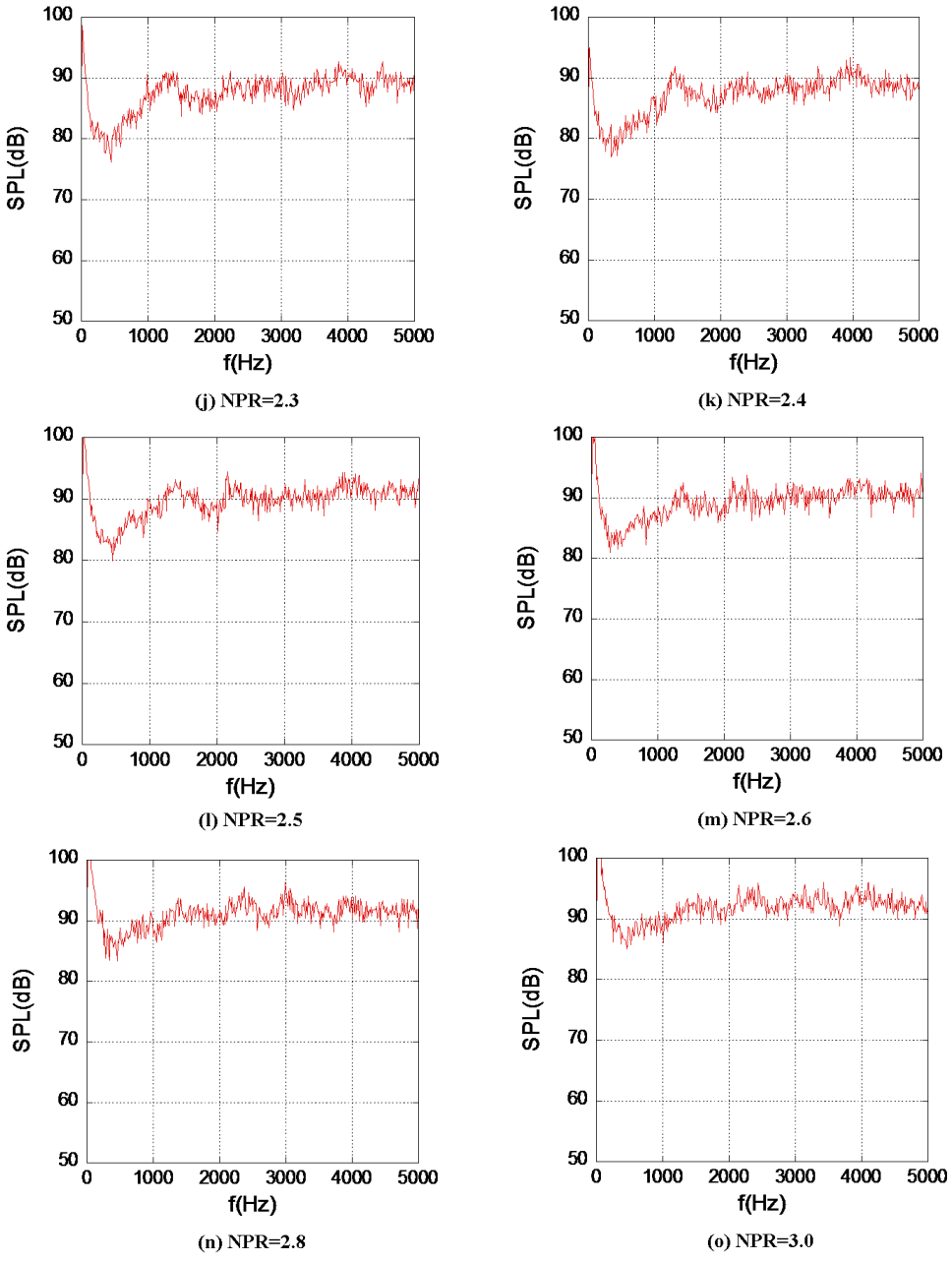

(j) NPR=2.3 (k) NPR=2.4

(l) NPR=2.5 (m) NPR=2.6

(n) NPR=2.8 (o) NPR=3.0

Figure 5.3 Continued

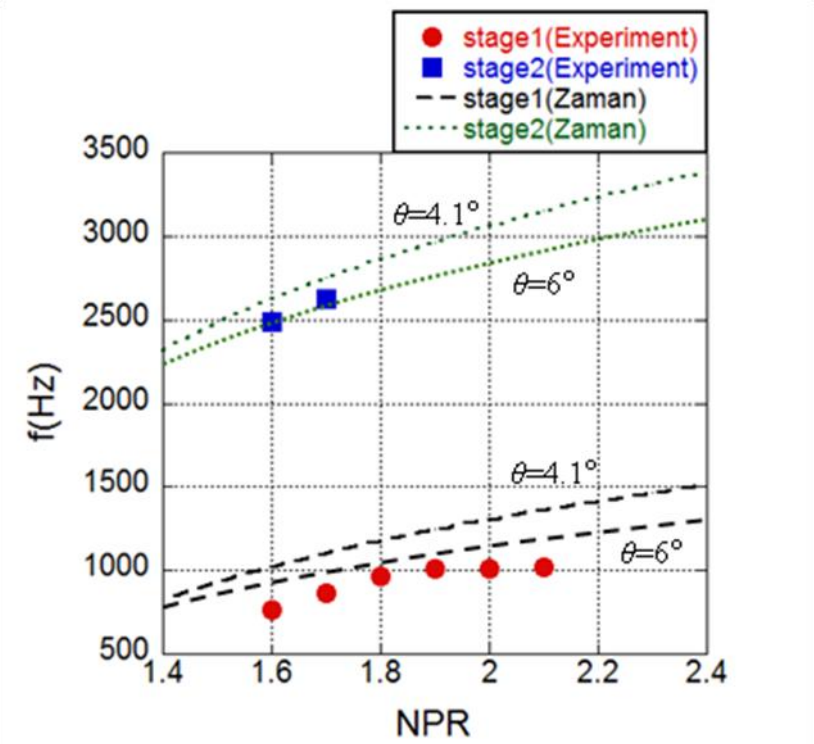

Figure 5.4 Transonic tone frequency variation with NPR

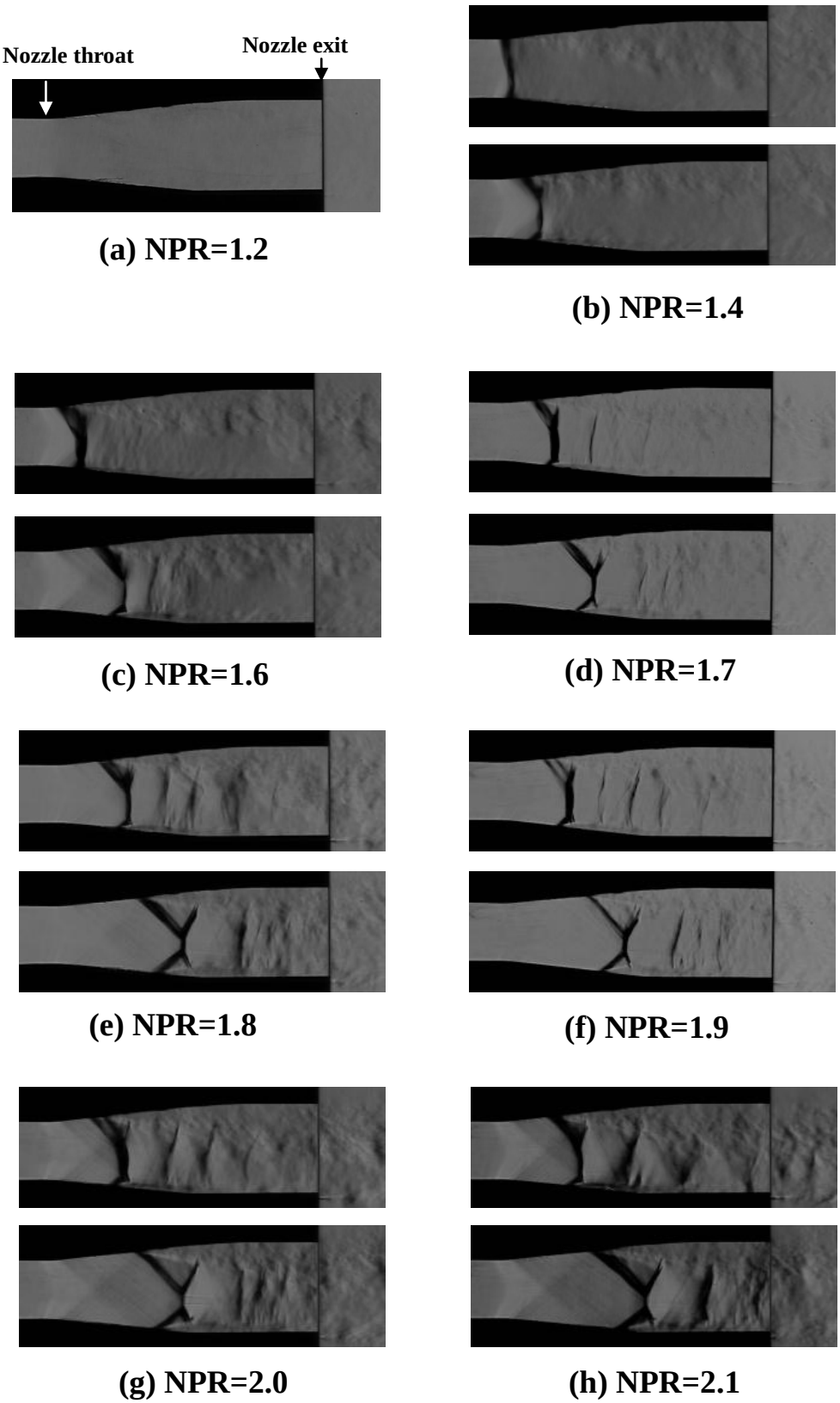

Figure 5.5 Schlieren images showing limit position of shock waves

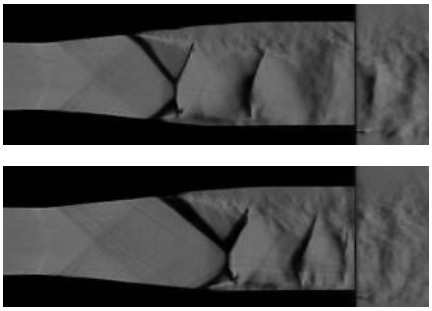

(i) NPR=2.2

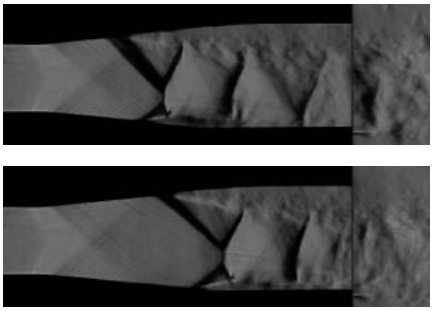

(j) NPR=2.3

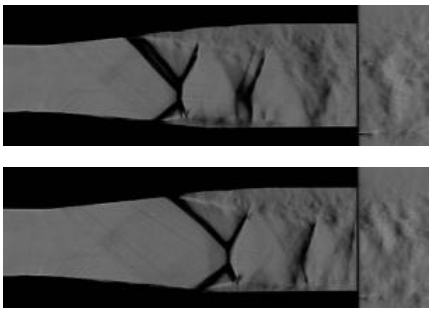

(k) NPR=2.4

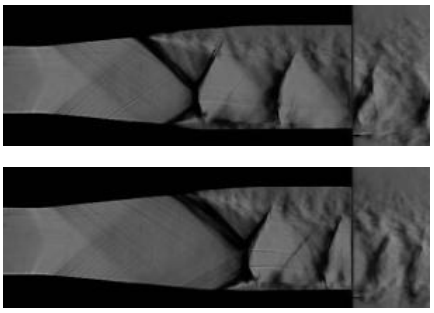

(l) NPR=2.5

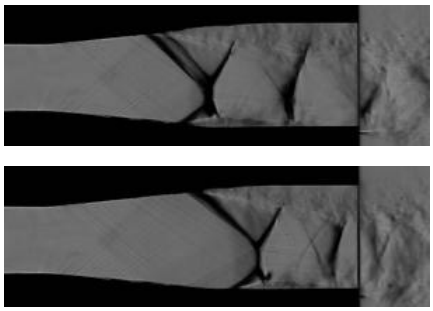

(m) NPR=2.6

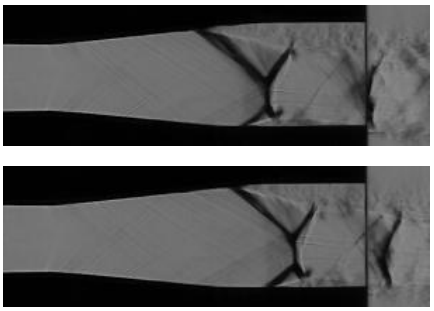

(n) NPR=2.8

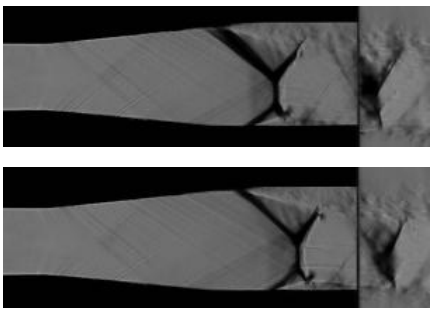

(o) NPR=3.0

Figure 5.5 Continued

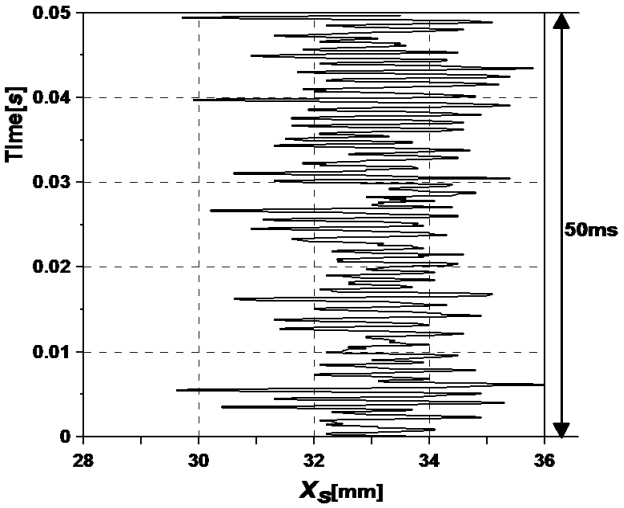

(a) *NPR*=1.8

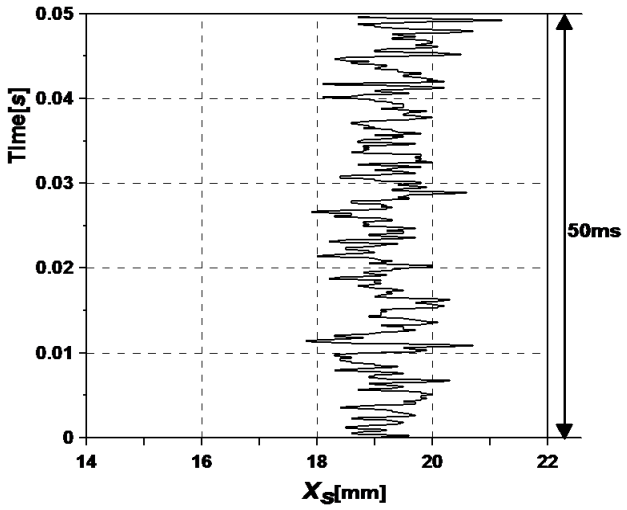

(b) *NPR*=2.6

Figure 5.6 Oscillations of the first shock wave

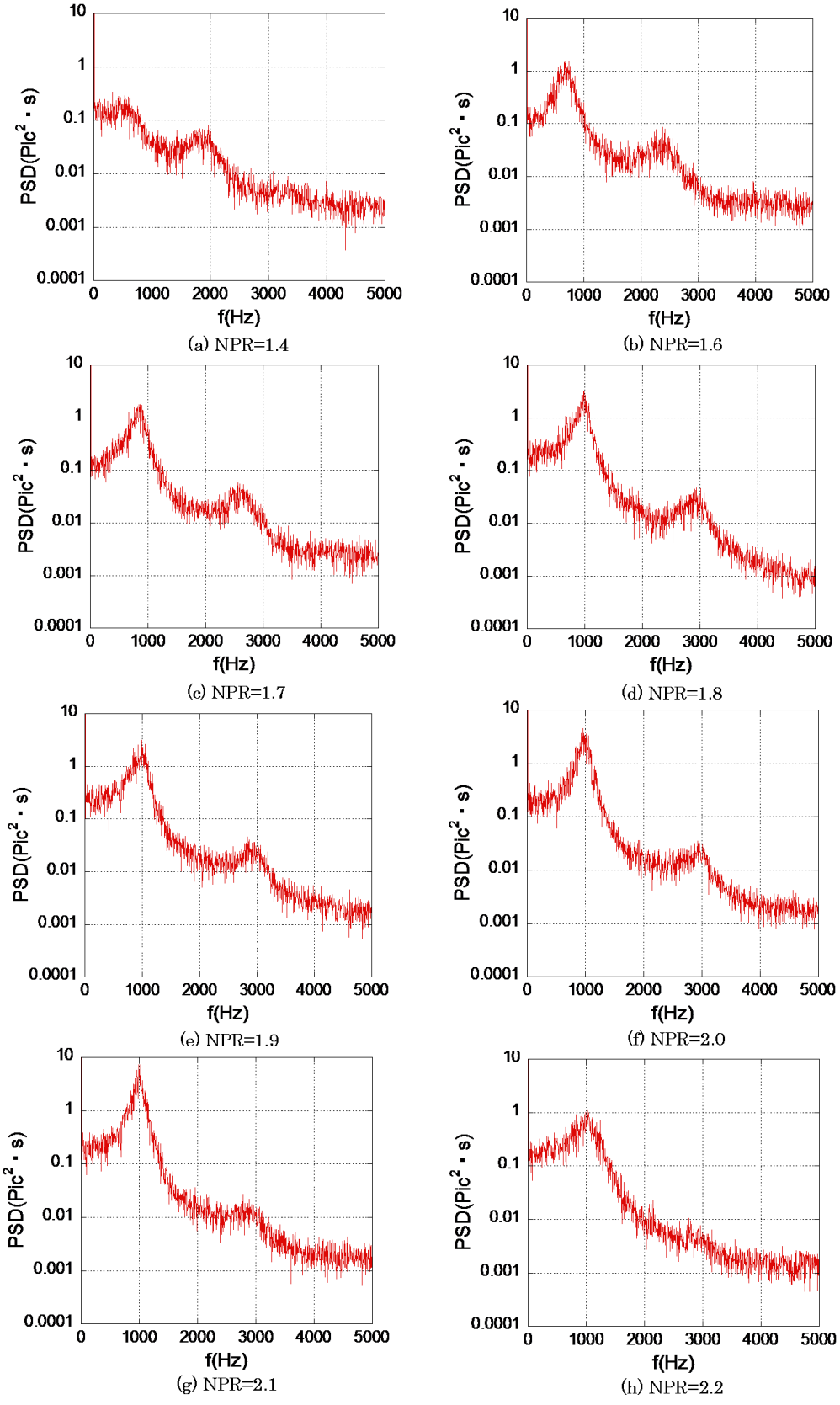

Figure 5.7 Power spectral density of the first shock wave oscillations

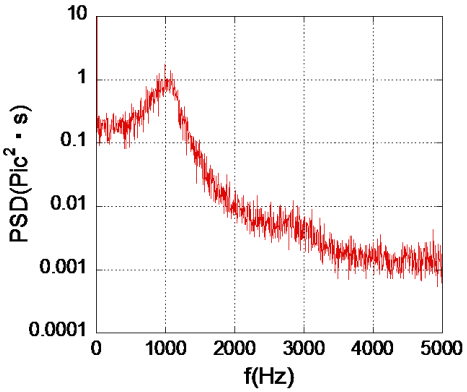

(i) NPR=2.3

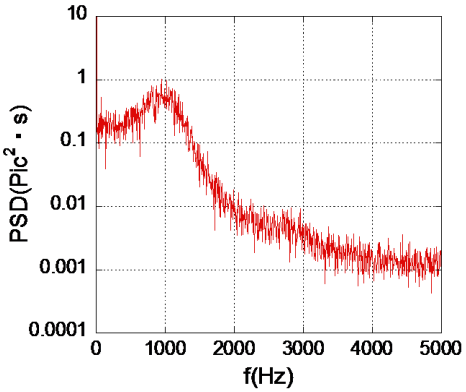

(j) NPR=2.4

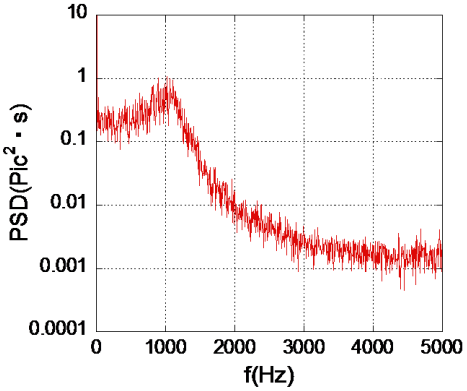

(k) NPR=2.5

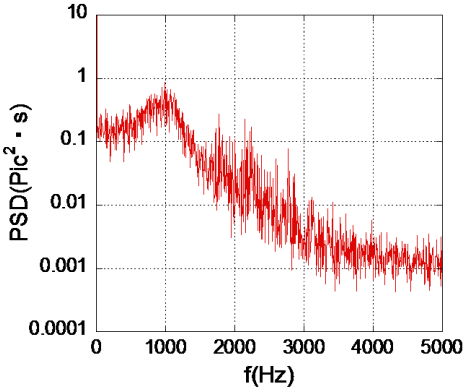

(l) NPR=2.6

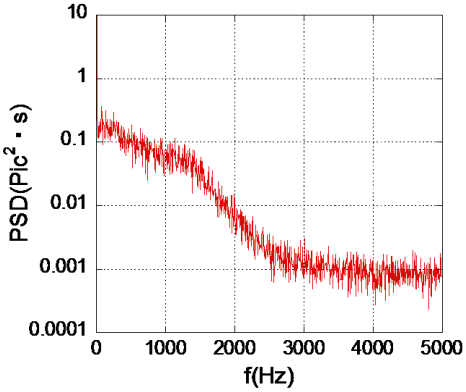

(m) NPR=2.8

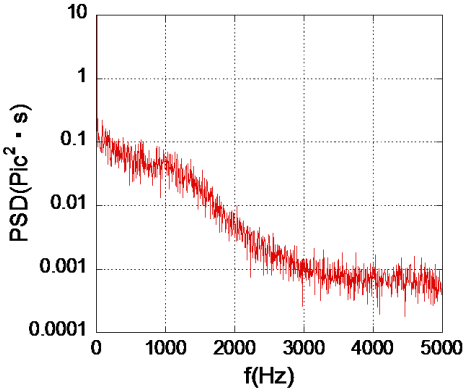

(n) NPR=3.0

Figure 5.7 Continued

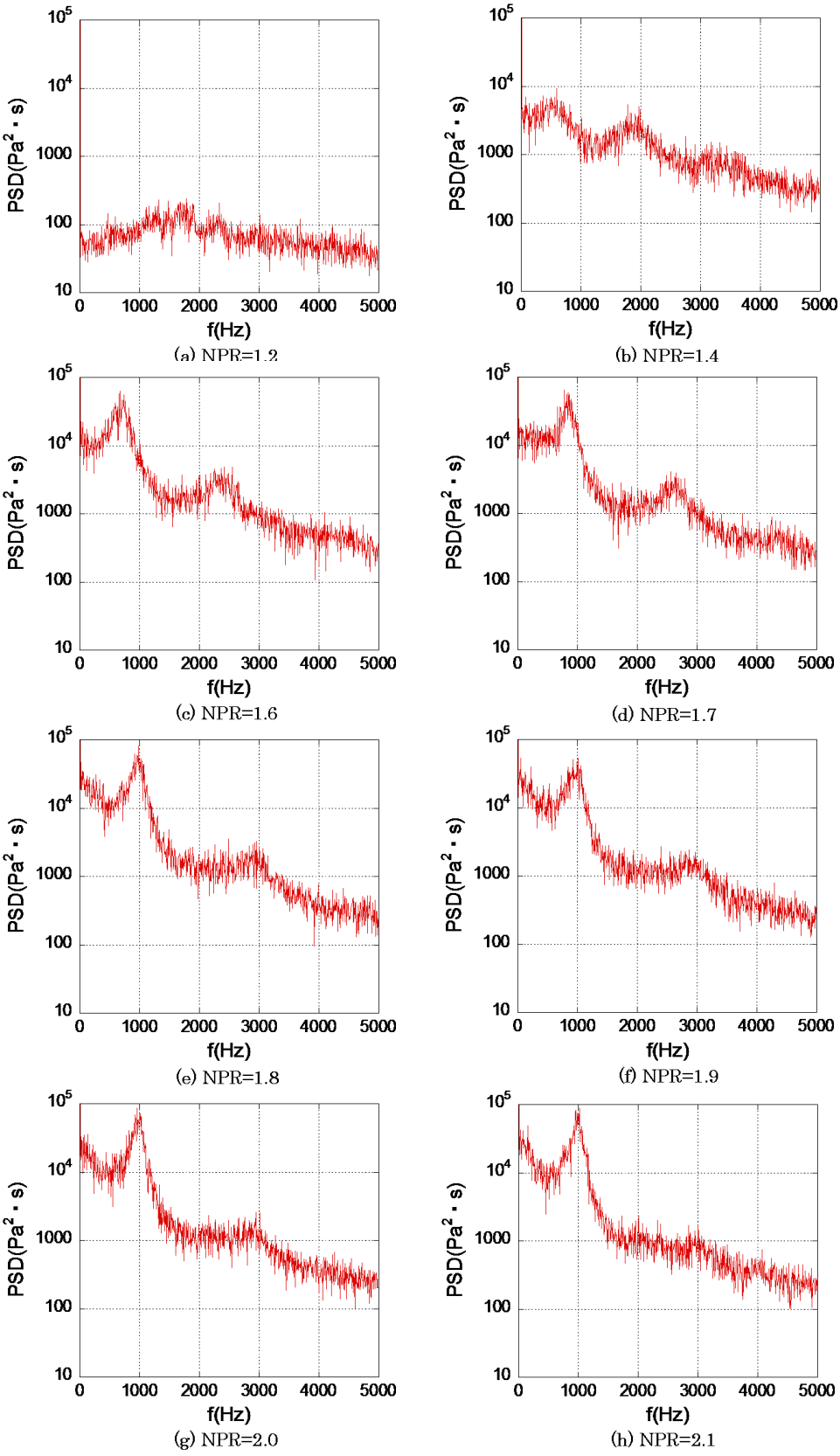

Figure 5.8 Power spectral density of wall static pressure fluctuation

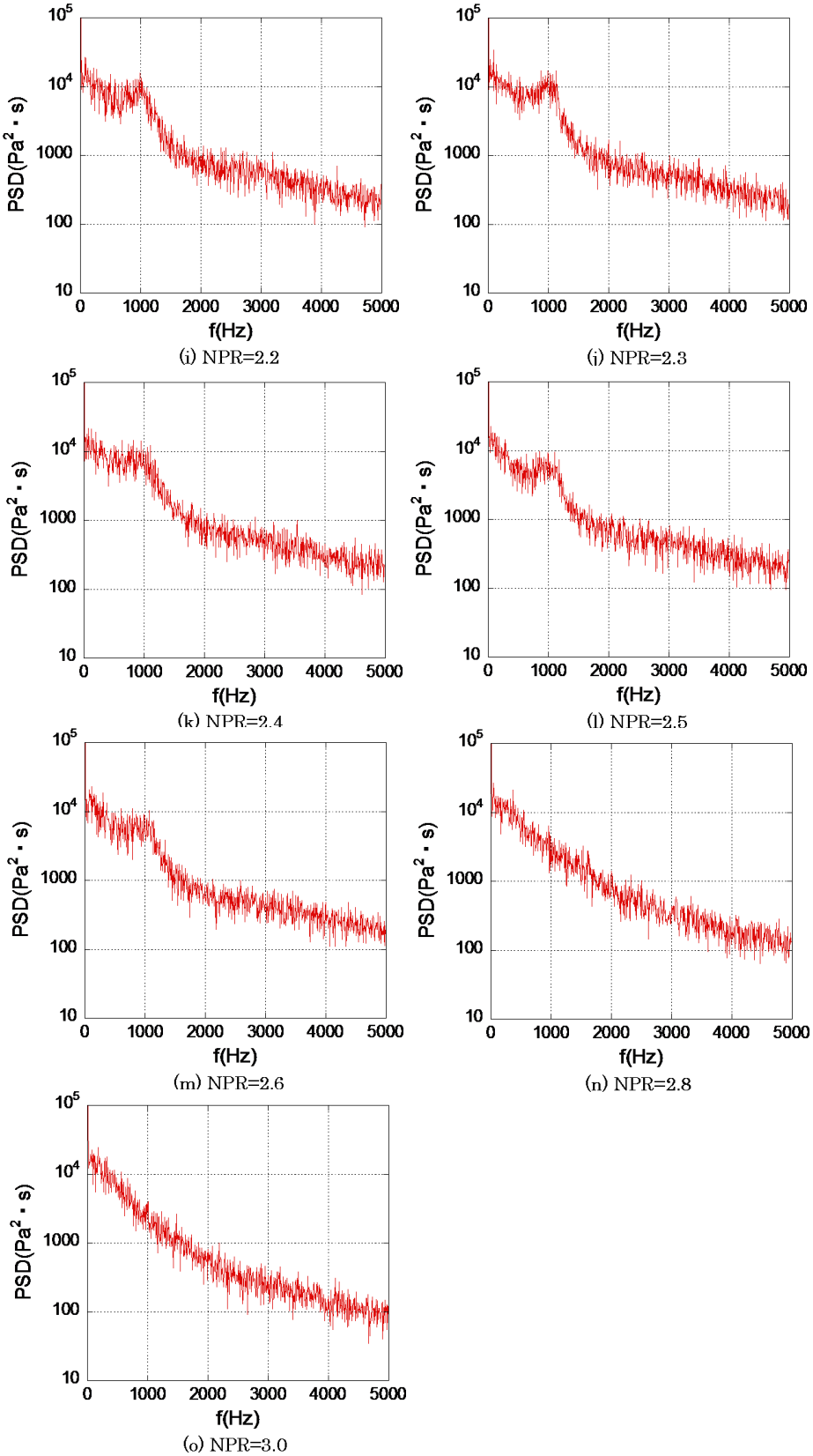

(i) NPR=2.2 (j) NPR=2.3

(k) NPR=2.4 (l) NPR=2.5

(m) NPR=2.6 (n) NPR=2.8

(o) NPR=3.0

Figure 5.8 Continued

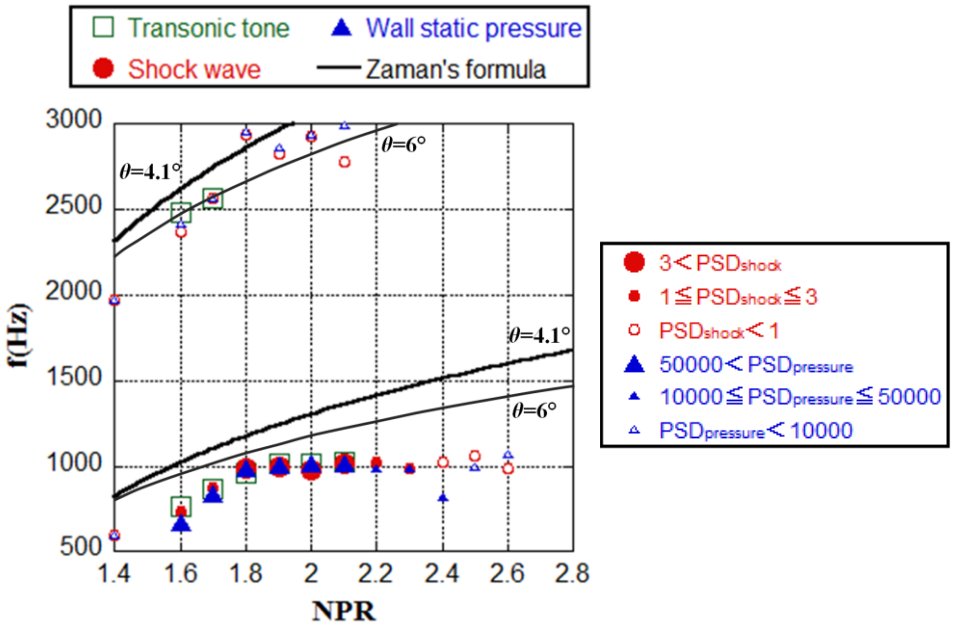

(a) Frequency variation vs NPR

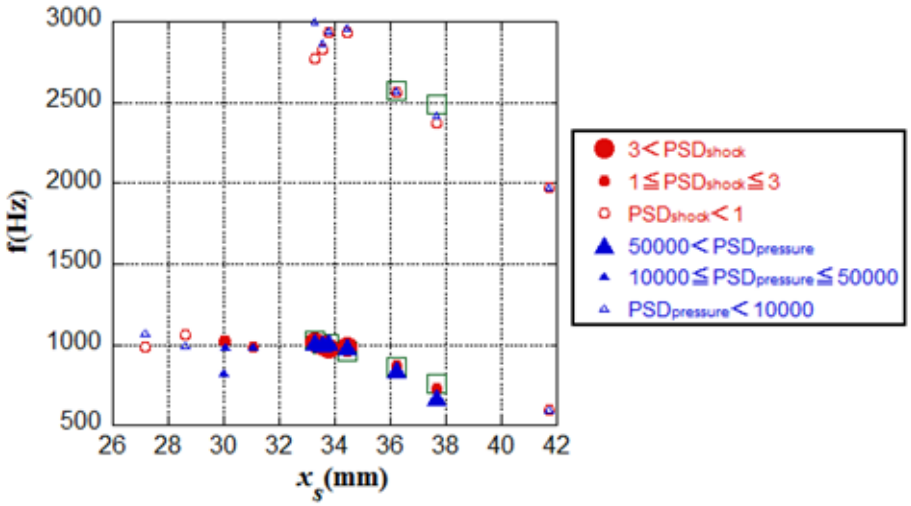

(b) Frequency variation vs x_s

Figure 5.9 Frequency comparison between transonic tone and first shock wave oscillation and wall static pressure fluctuation

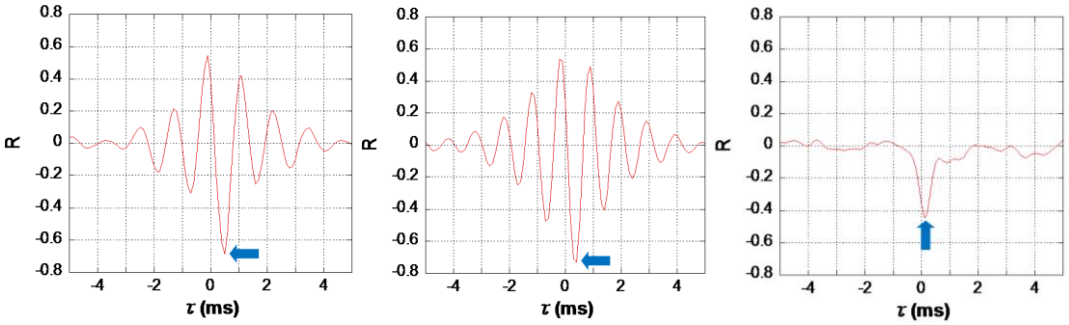

NPR 1.7 NPR 2.0 NPR 2.8

(a) Cross correlations (Shock wave vs wall static pressure)

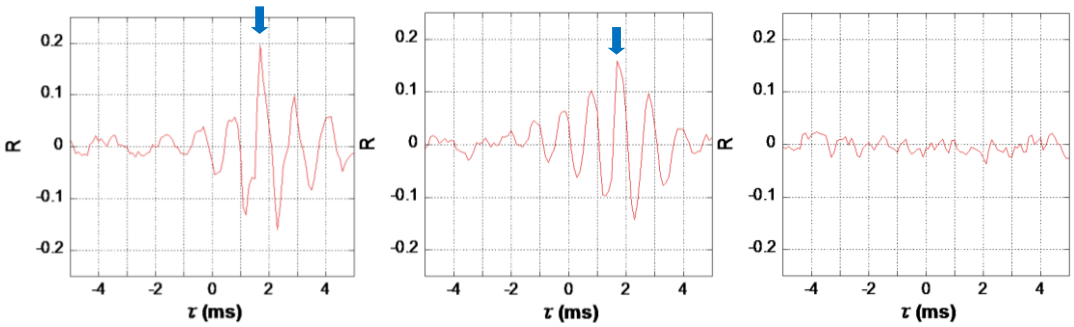

NPR 1.7 NPR 2.0 NPR 2.8

(b) Cross correlations (Wall static pressure vs sound pressure)

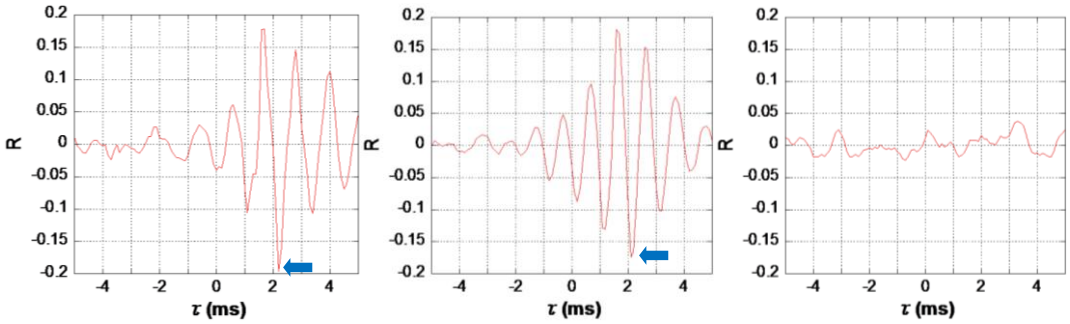

NPR 1.7 NPR 2.0 NPR 2.8

(c) Cross correlations (Shock wave vs sound pressure)

Figure 5.10 Cross-correlations at typical NPR

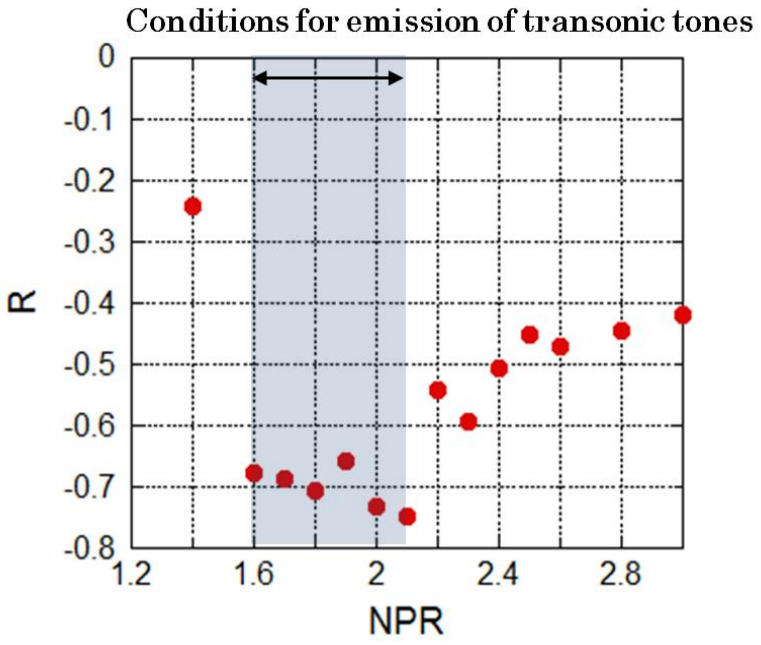

Figure 5.11 Plots of peak cross correlation coefficients
(Shock wave vs wall static pressure)

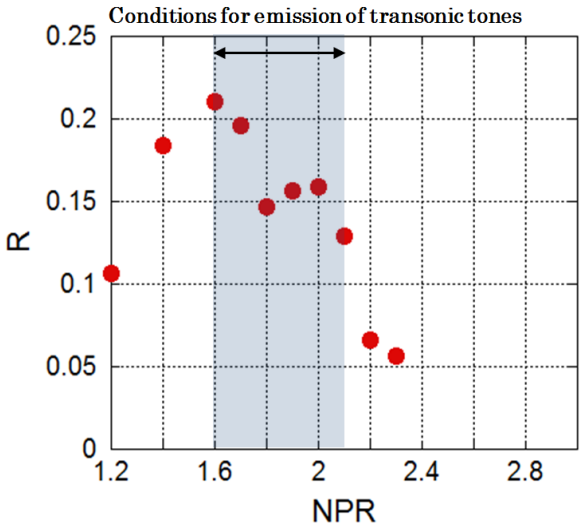

Figure 5.12 Plots of peak cross correlation coefficients
(Wall static pressure vs sound pressure)

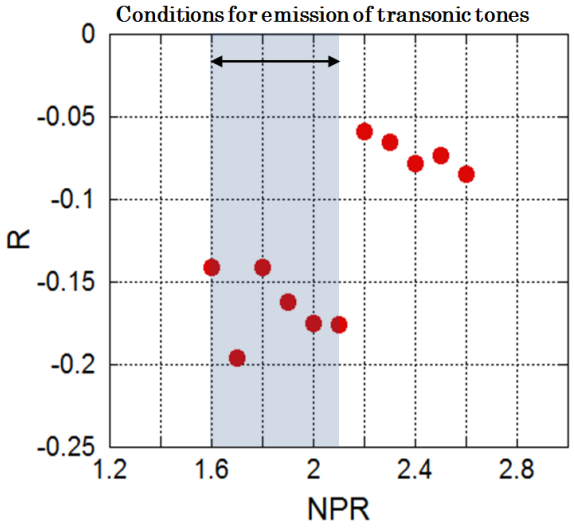

Figure 5.13 Plots of peak cross correlation coefficients
(Shock wave vs sound pressure)

Table 5.1 Delay time and velocity at peak cross correlation

NPR	$T_{s\text{-}p}$(ms)	$T_{p\text{-}m}$(ms)	$T_{s\text{-}m}$(ms)	$V_{s\text{-}p}$(m/s)	$V_{p\text{-}m}$(m/s)
1.6	0.5	1.7	2.2	63.3	304
1.7	0.5	1.7	2.2	60.4	304
1.8	0.4	1.7	2.2	71.1	304
1.9	0.4	1.7	2.2	68.9	304
2.0	0.4	1.9	2.2	69.4	304
2.1	0.3	1.7	2.1	90.9	272

Chapter 6

Effect of nozzle-Lip Length on Shock-Induced Separated Flow and Transonic Tone in 2-Dimensional Supersonic Nozzle

In the previous chapter, the acoustic characteristics of the transonic tone in 2-demnsional supersonic nozzle were investigated and the correlation between and the transonic tone and the first shock wave oscillation or wall static pressure fluctuation were discussed. In this chapter, the effect of nozzle-lip length on transonic tone in 2-demensional supersonic nozzle will be discussed. Especially, with considering the large separation location from which is expected the feedback loop developed, the effect of nozzle-lip length on the transonic tone, the first shock wave oscillation, wall static fluctuation and variation of the cross-correlations will be reported. Also, in this chapter, to analyze the shock wave frequency, a high speed video camera was employed for schlieren optical system and all measurements had been set up to capture output data simultaneously.

6.1 Experimental Conditions

Basically, all experimental system was configured same with the one explained at chapter 5 but some attachable metal cuboid tips were used for changing the nozzle-lip length. The cuboid tips has 3mm of length and 30mm of width as same width of the nozzle used and in this experimental work, the two cases of nozzle-

lip length were mainly considered as 6mm and 12mm.

Not only nozzle-lip length but the location of the large separation zone in the nozzle was also considered for experimental condition because there is another focus, actually, in this experimental work such as controlling the cross-correlation, which discussed previously, in the large separation zone. Because the 2-dimensional supersonic nozzle were used, two more experimental case could be added: the case that the large separation zone is held upwards of the 2-demensional nozzle(or the case of the jet plume extends downwards) and the other case that the large separation zone locates at bottom side of the nozzle(or the case of the jet plume extends upwards).

Acoustic measurements were made using a condenser microphone that has a diameter of 1/4 inch. The microphone was located over the nozzle at angles of 72° from the jet direction, and a radial distance of 520mm(r/D=32) from the nozzle exit.

In this experimental work, two of pressure transducers (Kulite XCS-190, XCQ-062) mounted on the nozzle pressure hole which stand at 6mm and 18mm distance from nozzle exit. And sampling frequency was set-up as 50kHz at external computer.

To measure a frequency of the shock wave oscillations in the divergent section of the nozzle, visualization was performed by schlieren method with high-speed digital video camera (Photron FASTCAM SA5). The movie was recorded at 10,000fps for 1.7 second, and the frame has 256x512 pixels.

In this experimental work, the NPR had been changed from 1.4 to 2.2 at an interval of 0.2, relatively narrow scope of NPR than previous work because of studying the nozzle-lip length effect, only when the transonic tone occurs from the nozzle.

6.2 Effects on The Transonic Tone Reduction

Fig. 6.1.1 shows the noise spectra form the two-dimensional supersonic nozzle

with comparing the two of flow direction. 'N', 'U', 'D' and 'UD' indicate, respectively, no-attached nozzle-lip (or normal nozzle condition), 'upper-side', 'Down-side', and 'both sides' and 6, 12 mean the extended nozzle-lip length in millimeter[mm]. At Fig. 6.1.1, the stage1 and stage2 of transonic tone are shown and there are some gaps of sound pressure level between two jet direction of flow but it is not so large amounts compared with the results of the attached cases which shown in next Figure. In Fig. 6.1.2 to 6.1.4 show the comparisons of transonic tone reduction according to the flow directions and nozzle-lip type. Overall, each amount of reduction is clearly shown with increase of nozzle-lip length and NPR until 2.0. In particularly, the transonic tone reduction is more distinct at stage 1 than stage2 and it is also found that an apparent tendency toward the tone reduction is shown at 'U-D' or 'D-U' case which indicates that the flow is extending to opposite side of attached nozzle-lip. In Fig. 6.2.1 and 6.2.2, the amount of the tone reduction is plotted by bar-type-plot at typical NPR. In this chart, it is obvious that the asymmetric extension of nozzle-lip is effective at stage1 even 'UD' case which is extended either side of nozzle-lip, but the reductions are smaller than 'U-D' or 'D-U' case. And one more the interesting trend is mostly found that the amounts of the tone reduction in 'U-D' and 'D-U' case of stage1 are approximated to 'UD-D' and 'UD-U', respectively. This means that the nozzle-lip-extension is valid when the large separation zone locates at same side of nozzle-lip attached only, even 'UD' case. In consideration of the feedback loop mechanism in large separation zone, it seems that the extended nozzle-lip affects the feedback loop mechanism or disturbs the periodic flow perturbations.

6.3 Flow Visualization

Schlieren photos of supersonic jets with a shock wave within the nozzle are shown in Fig. 6.3. In the same manner at described previous chapter, each pair of photos respectively show the shock wave location when the first shock wave locates at minimum and maximum distance from nozzle exit. Under this

experimental condition of NPR 1.4 to 2.2, the flow features are basically same, for example, λ-type pseudo-shock wave generation, the shock oscillating in a piston-like manner and the development of large separation zone, with the Figures shown in chapter 5. The jet plume direction(or the location of large separation zone) had been randomly controlled through a numerous experimental attempt.

6.4 Effects on The First Shock Wave

The traces of the first shock wave movements sampled for 80ms and the of histogram of shock displacement which define as '$Xs(i+1)$-$Xs(i)$' are plotted concerning a NPR of 1.8 in Fig. 6.4. The *Xs* means the first shock position from nozzle exit and '*i*' indicates a sampling step number of captured photo. Through the histogram, it can be found how much the shock wave movements activated. For instance, if the histogram of shock wave has sharp distribution which has high value around '0' of x-value, the shock wave movements is not active than the one that has flat distribution of histogram. In the Fig. 6.4, it is found that the amplitude of the first shock is lager at 'U-U' or 'D-D' case than the other cases, on the other hand, 'U-D' or 'D-U' case has noticeable amplitude decrease of shock wave oscillation. These trends also appears very similar to tone reduction at stage 1 in the Fig. 6.2.1 to 6.2.2. At the case of 'UD', there is no remarkable distinction according to flow direction but the amplitude of the first shock oscillation decreases gradually with increasing of the nozzle-lip length.

In addition to the consideration about the activity of the first shock movement, now, the trends of the position of the first shock wave and maximum displacement according to the flow condition, such as NPR, large separation location and nozzle-lip length will be discussed. Overall plotted charts with regard to the variation of the first shock wave positions which the shock wave stayed most frequently and maximum displacements are shown in Fig. 6.5. In the Fig. 6.5, of course, it is shown at the most case that the first shock wave moves to downstream in accordance with NPR increase but the position of the first shock

wave is alternatively changing with flow direction even at the same NPR. It is not clear where the differences result form, basically it seems that results from geometrical asymmetry, but the possibility of the transonic tone linked flow oscillation may not be excluded because at normal case, the difference of shock wave position is just found at 'NPR1.6U' and 'NPR1.8U' when the transonic tone emits intensively and the other cases that the differences of the first shock wave position are noticeable have remarkable tone level changes. In Fig. 6.6, the first shock wave positions were plotted totally. Interestingly, it is founded the shock position of 'U-U' and 'D-D' are similar to 'Normal' case, whereas the case of 'U-D' and 'D-U' are similar to 'UD' case. That is to say, only about the nozzle-lip which locates at same side of large separation zone is meaningful to the first shock position not only to the transonic tone reduction or shock wave activity. Overall, the first shock wave of 'UD' case locates at downstream according to the nozzle-lip length and the shock position of the other cases of 'U-U', 'D-D', 'U-D' and 'D-U' alternatively changed between the 'Normal' case and 'UD' case, mostly. At Fig. 6.7, the shock wave displacement also have similar tendencies mentioned above.

The PSD distributions of the first shock wave are shown in Fig. 6.8. It is clearly found that there are two corresponding peak frequencies to the transonic tone and the frequencies of the first shock wave distinctly decrease when the transonic tone decreases such as the case of 'D-U' or 'U-D' case and it can be said that the shock wave oscillation is directly linked to the transonic tone.(see Fig. 6.8.(c) and (d)) Furthermore, the amount of PSD reduction is proportional to the transonic tone reduction at the most case. The PSD distribution also has the tendency that the PSD distributions of 'U-D' and 'D-U' cases are very similar to the one of 'UD' case. And the PSD of shock wave were reduced at particular frequencies which correspond to the transonic tone frequency of stage1 and stage2. What's interesting is that the PSD frequencies about 1kHz are reduced in the case of 'U-D' or 'D-U' comparing with the case of 'U-U' or 'D-D' case, respectively and also, the PSD frequencies about 1kHz are reduced in 'UD' case

comparing with 'Normal' case according to nozzle-lip length. (see PSD distribution of 6mmD1.6U, 6mmU1.6D, 1.8D, 2.0D, 12mmD1.6D, 12mmU1.6D, and 2.0D in Fig. 6.8 and 'UD' case of Fig 6.8.(c) and (d)). It seems that the attached nozzle-lip length affects the peak frequency of the first shock wave oscillation through the large separation zone, that is to say, it is possible that the peak frequency of the first shock wave oscillation decrease because the period of feedback loop become longer due to the attached nozzle-lip length.

6.5 Effects on Wall Static Pressure Fluctuation

Fig. 6.9 shows comparisons of wall static pressure PSD measured at 12mm and 6mm distance of nozzle exit. The red line indicates the upstream wall static pressure(P1) and the blue line means downstream wall static pressure(P2). In Fig. 6.9, there are two of peak frequencies. And each peak frequency is corresponds to tone frequency of stage1 and the other one is corresponds to stage2 of the transonic tone. And also, the PSD of the peak frequency around 1kHz measured at upstream wall static pressure(P1) is larger than the other one measured at downstream(P2), and it can be said that the frequency corresponding to the tone's stage1 is predominant at upstream wall static pressure. On the other hand, at downstream of measurement has captured more densely of stage 2 frequency at NPR1.8 and NPR2.0. These facts imply that there is a possibility that the transonic tone generated by shock wave oscillation as stag1 of tone mode and the resonance of the tone generate in the large separation zone by feedback loop. In Fig. 6.10, the PSDs of wall static pressure measured at 6mm from the nozzle exit are shown, totally. Overall, the peak frequencies corresponding stage1 of the transonic tone decreased notable at 'U-D' or 'D-U' case as the transonic tone decrease. And also, the similar trend is shown that the PSD distributions at the case of 'U-D' and 'D-U' are similar to 'UD-D' or 'UD-U'.

6.6 Effects on Cross-correlations

To investigate the effect of the nozzle-lip length on correlation between the transonic tone and the first shock wave oscillation or wall static pressure fluctuation, the cross-correlation coefficient(*R*) was evaluated at typical case of experimental work at NPR1.8 as same manner shown in previous chapter. Fig. 6.11.(a) to 6.11.(b) shows the cross-correlation coefficient between the first shock oscillation, two of wall static pressure fluctuation in 2-dimensional supersonic nozzle. At 'Shock vs P1' charts in Fig. 6.11., the peak cross-correlation coefficient is large in all cases at positive time delay than negative delay time, even the case of transonic tone reduced because the pressure measurement point is close to the shock wave location and this means the first shock wave oscillation affects the wall static pressure fluctuations, dominantly. However, at the 'D-U' and 'U-D' case which is the case of the transonic tone reduced, the peak value of *R* is peculiarly decreased. The peak value of *R* is gradually decrease with nozzle-lip length changing(see 'Normal' and 'UD' case of 'Shock vs P1' charts). And the positive delay time means the wall static pressure fluctuates 'after' some delay time for the first shock wave movement. And the distributions of *R* at the case of 'UD-D' and 'UD-U' are very similar to the case of 'U-D' and 'D-U' at all cases. At 'Shock vs P2' charts in the Fig. 6.11., the value of *R* is significantly large comparing with 'Shock vs P1' charts. This fact also sustains the feedback loop mechanism between the shock wave and nozzle exit in large separation zone. And the value of *R* is changing periodic and this period is changed by changing the nozzle-lip length, for example, at the case of '6mmD1.8U' has long period of *R* comparing to '6mmD1.8D' and also this trend is shown in most cases. It is reasonable to suppose that the attached nozzle-lip length change the feedback loop period in large separation zone. At 'P1 vs P2' charts of Fig. 6.11., the flow oscillation can be understand easily at one view. As the measuring points of P1 and P2 are installed in upper nozzle wall, at the case of '6mmU1.8U', for example, the pressure measurements must be sampling the periodically changing pressure of the flow involved several pseudo shock waves oscillating like a piston. In this

case, the distribution of *R* is very similar between '6mm' and '12mm' case. From 'Normal1.8U', 6mmU1.8D(or12mmU1.8D) and 6mmD1.8U(or12mmD1.8U) of 'P1 vs P2' charts, it is found that the flow fluctuation are greatly influenced by nozzle-lip length. When the nozzle-lip is extended at the side of flow direction, the correlation between P1 and P2 become large of sinusoidal distribution. However, the nozzle-lip which extended at the side of the large separation zone, is more influential to 'P1 vs P2' correlation(see 'UD' case). It means there is a possibility that the piston-like oscillating shock waves are influenced dominantly by feedback loop of large separation zone. Overall, the peak value of *R* at the negative delay time, become small when the transonic tone decrease. It means the 'return loop' which indicates the perturbations propagate from the nozzle exit to upstream of flow wane due to extended nozzle-lip.

6.7 Summary

In this chapter, to understand the effect of nozzle-lip length on transonic tone, the correlation between the transonic tone and flow oscillation were investigated from a shock-containing flows in divergent part of 2-demensional supersonic nozzle. To measure the frequencies of the first shock wave oscillations, a high-speed video camera was employed for Schlieren system. And the range of NPR considered only 1.4~2.0 where the transonic tone occur.

In the 2-dimensional nozzle, attaching the nozzle-lip at same side of the large separation zone or the opposite side of the jet plume extending, was effective to reduce the stage 1 of transonic tone level about 5~10 dB. In these cases, the peak PSD of the first shock wave oscillation, wall static pressure fluctuation, according to tone frequencies, and the peak value of cross-correlations also decreased. The nozzle-lip which is extended at the opposite side of the large separation zone influences to the shock wave oscillation to excite. However, even 'UD' case which attached both of nozzle-lip, the nozzle-lip extended from a large separation zone, is meaningful to reduce the transonic tone. The nozzle-lip length affects the

transonic tone, the first shock wave movement and oscillation and the wall static pressure fluctuation. It seems that the changing of the nozzle-lip length directly affects to the first shock wave and feedback between shock wave and nozzle exit the large separation zone.

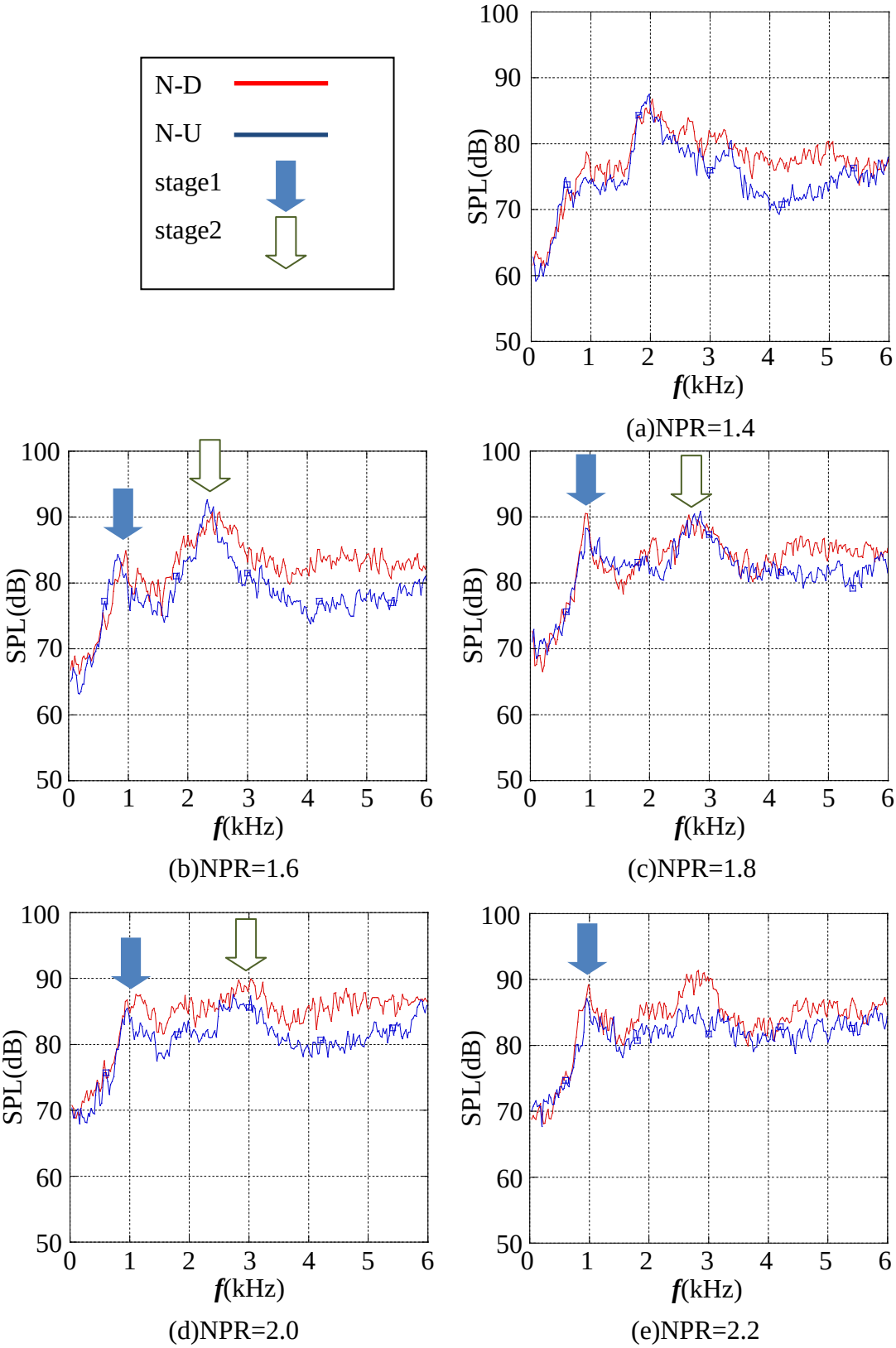

Figure 6.1.1 Comparisons of sound pressure level whit flow direction (Normal nozzle)

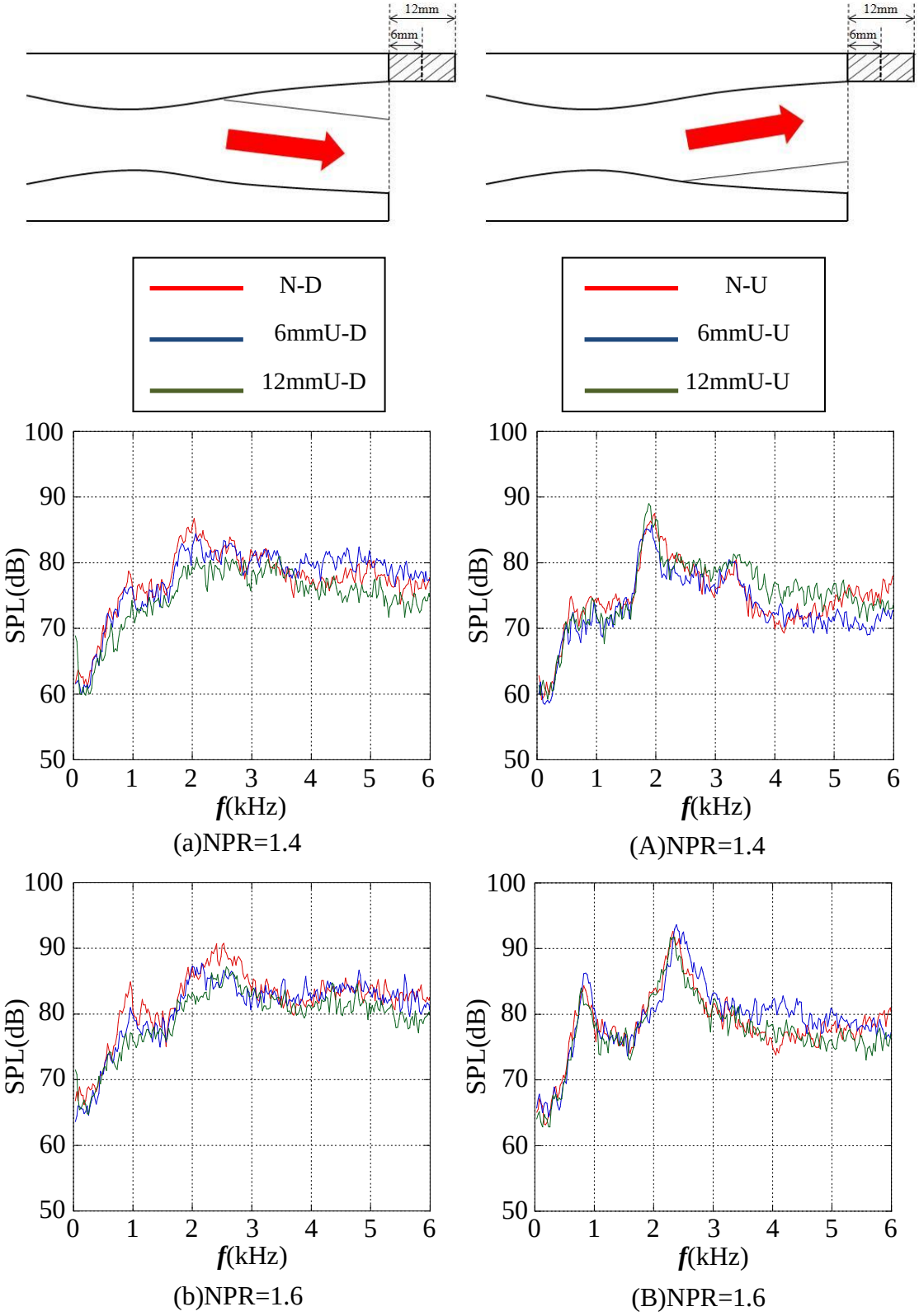

Figure 6.1.2 Comparisons of transonic tone reduction

(Case of the upper-side nozzle-lip extension)

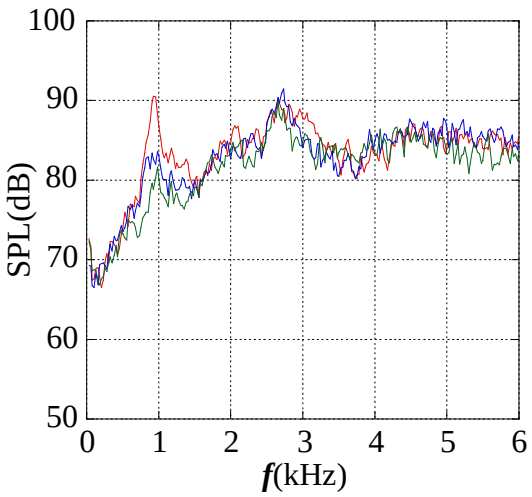

(c)NPR=1.8

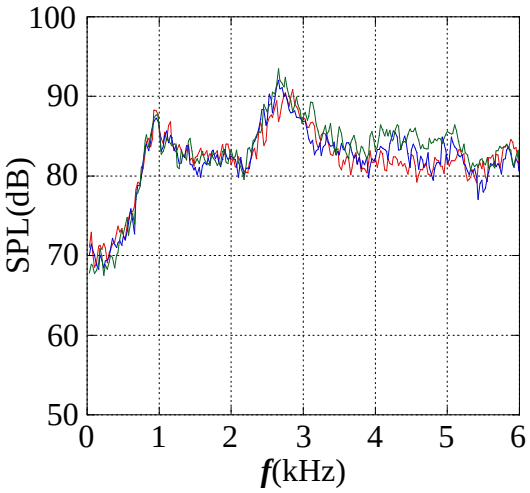

(C)NPR=1.8

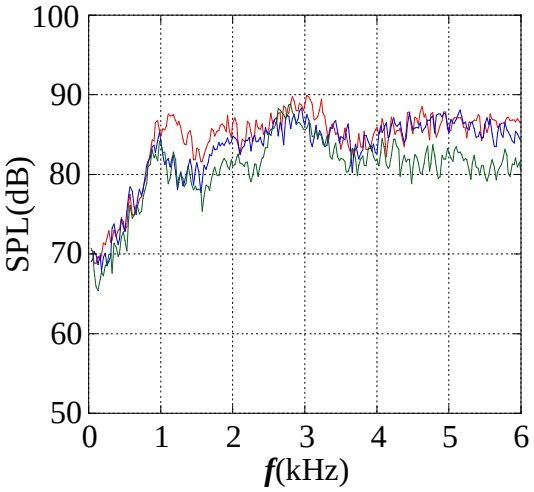

(d)NPR=2.0

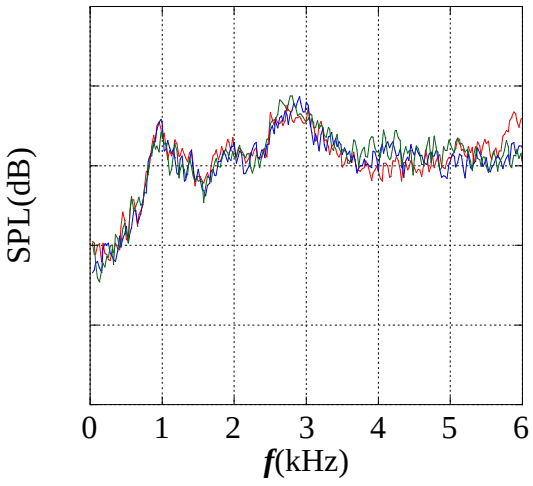

(D)NPR=2.0

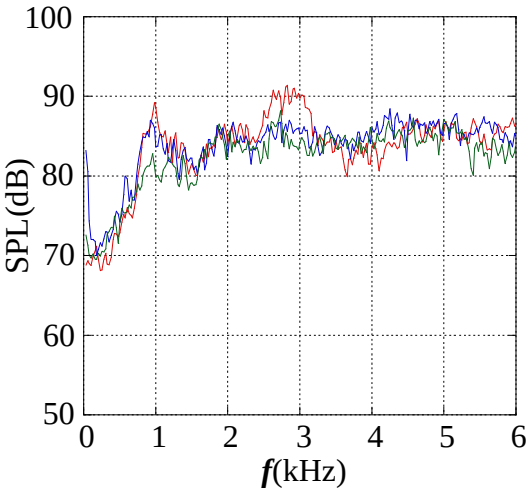

(e)NPR=2.2

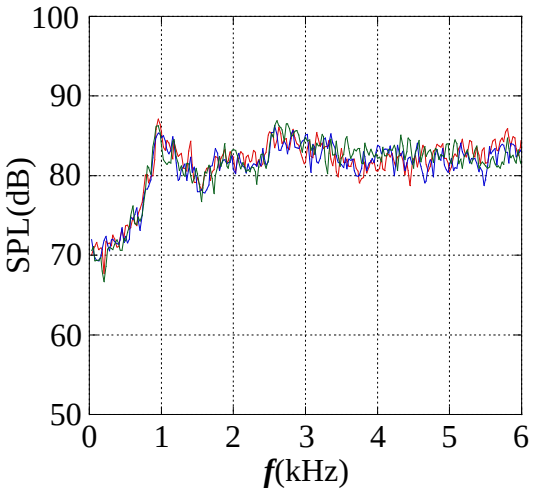

(E)NPR=2.2

Figure 6.1.2 Continued

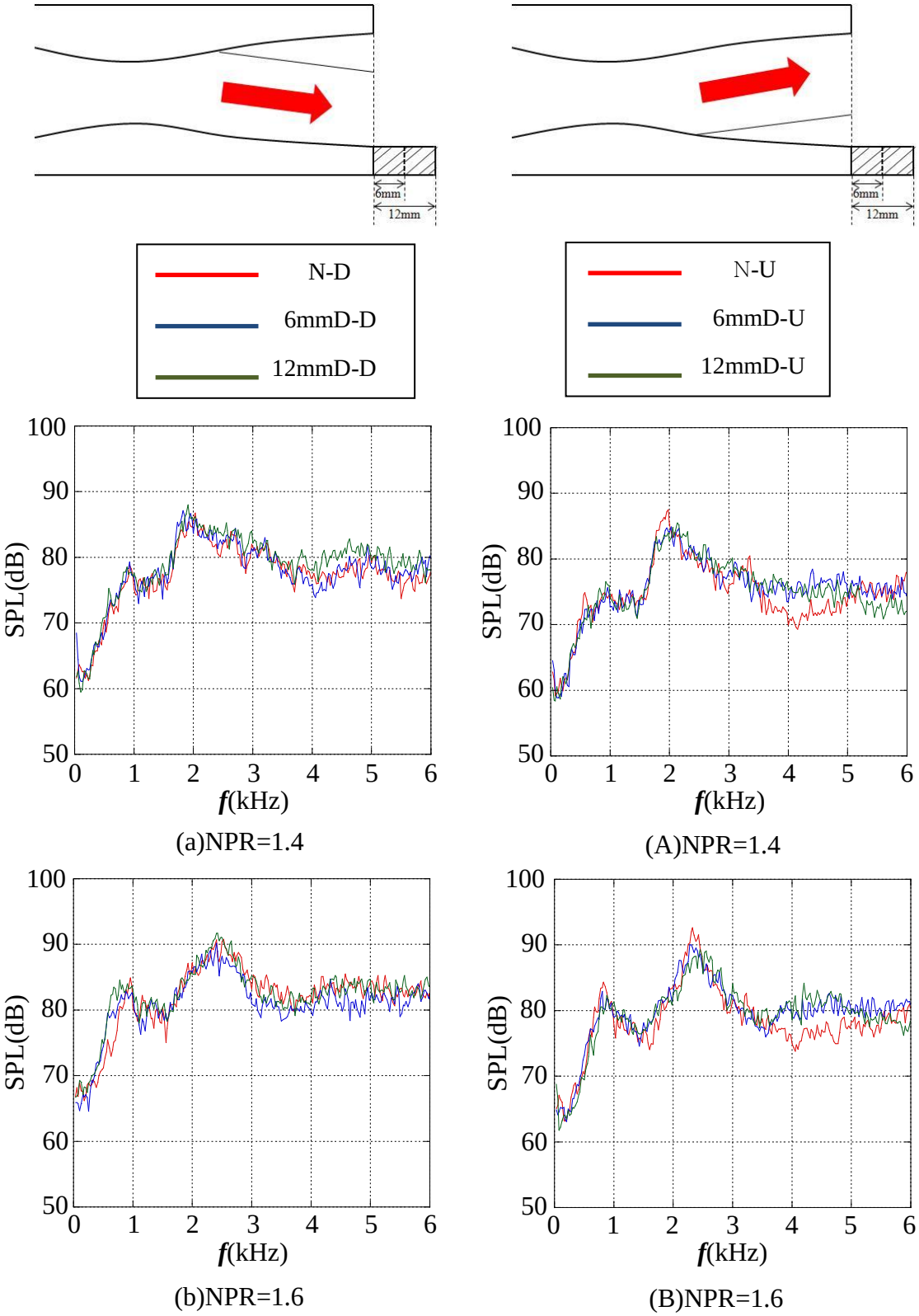

Figure 6.1.3 Comparisons of transonic tone reduction

(Case of the bottom-side nozzle-lip extension)

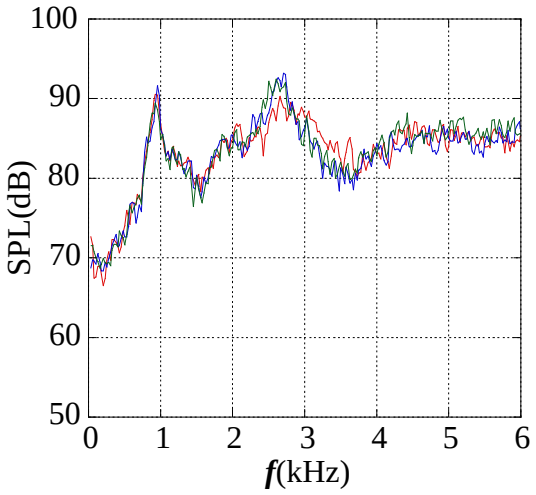

(c)NPR=1.8

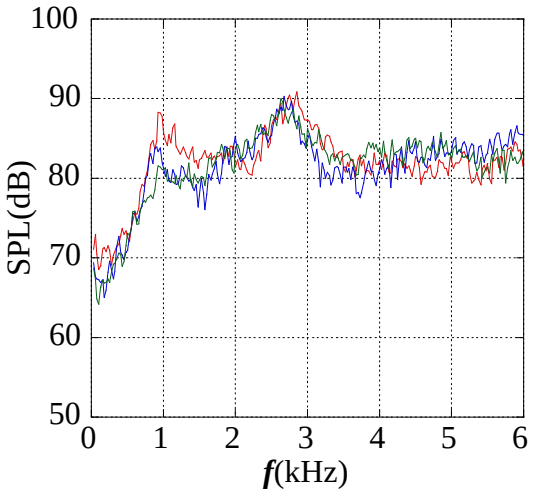

(C)NPR=1.8

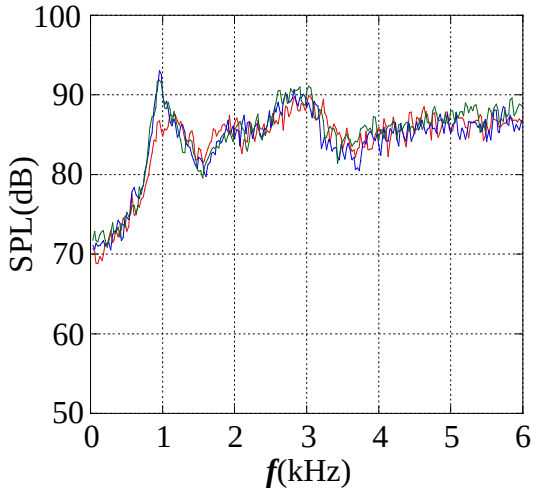

(d)NPR=2.0

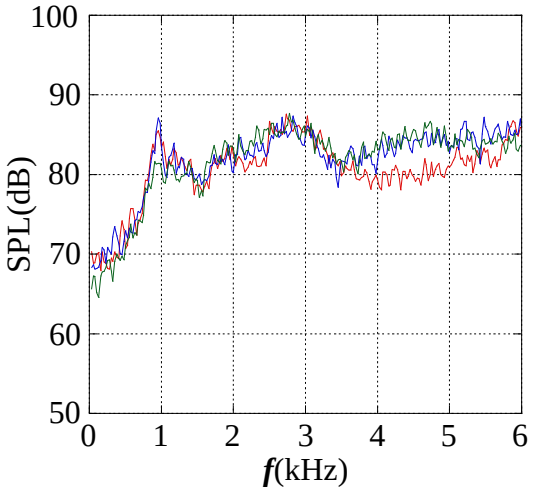

(D)NPR=2.0

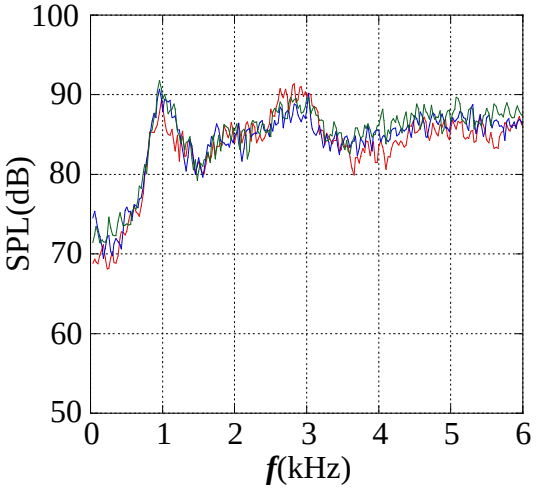

(e)NPR=2.2

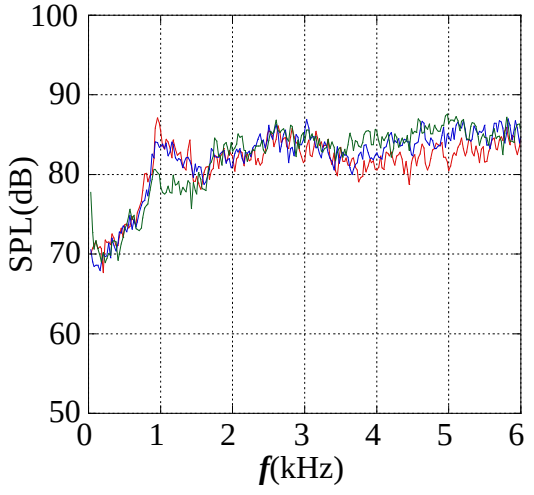

(E)NPR=2.2

Figure 6.1.3 Continued

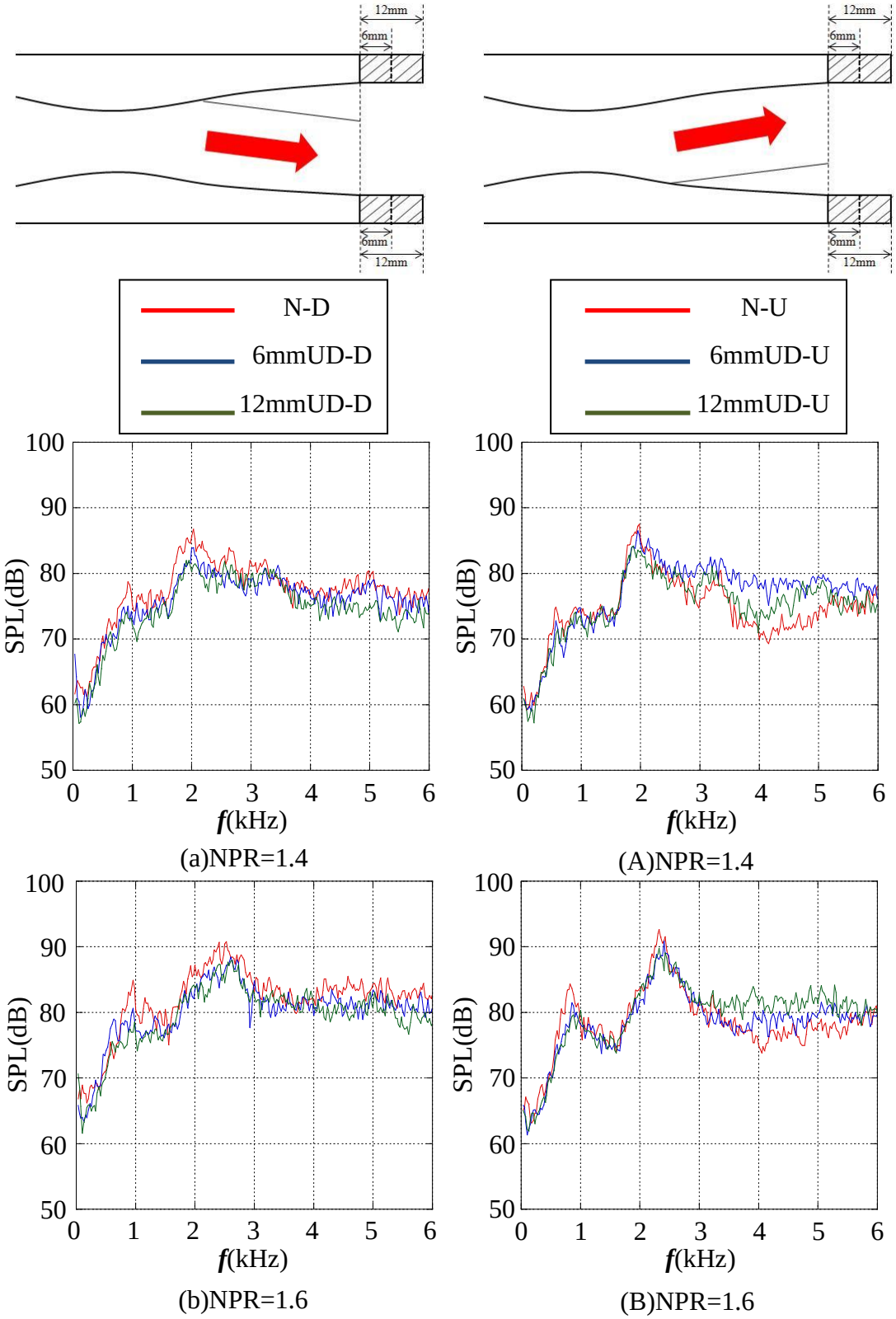

Figure 6.1.4 Comparisons of transonic tone reduction

(Case of the top and bottom-sides extension)

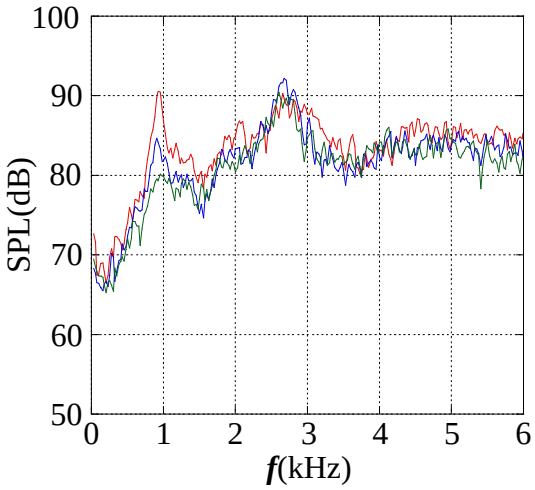

(c)NPR=1.8

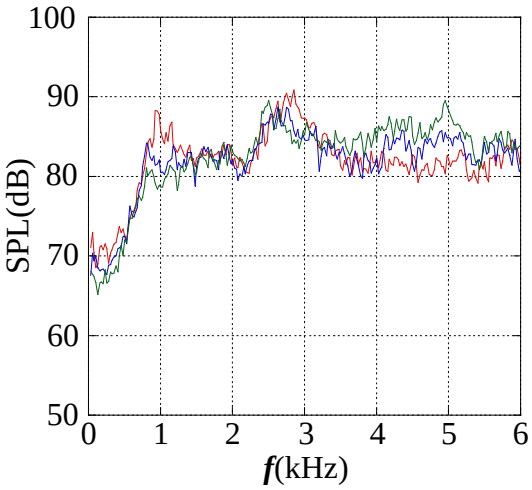

(C)NPR=1.8

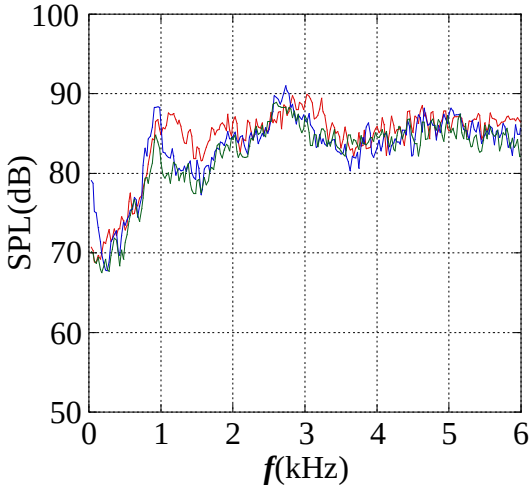

(d)NPR=2.0

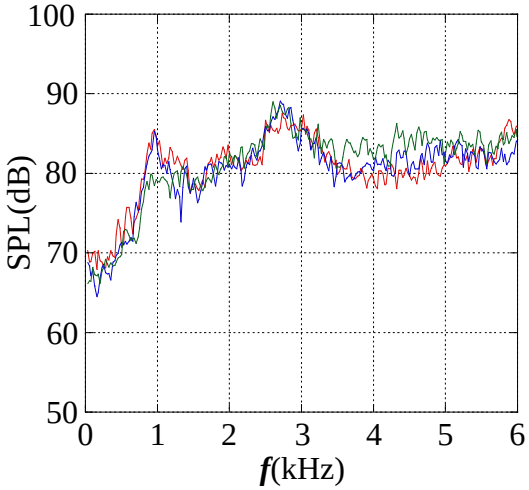

(D)NPR=2.0

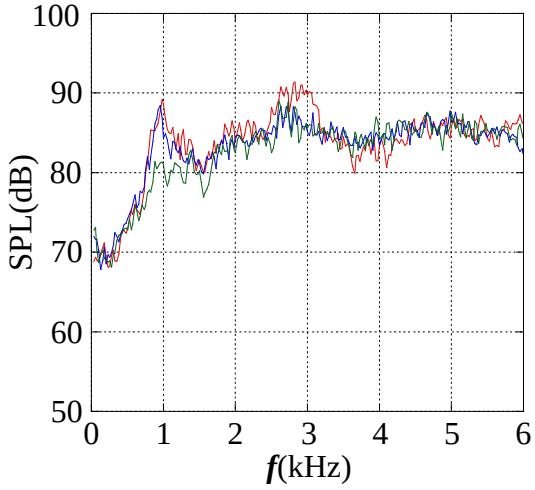

(e)NPR=2.2

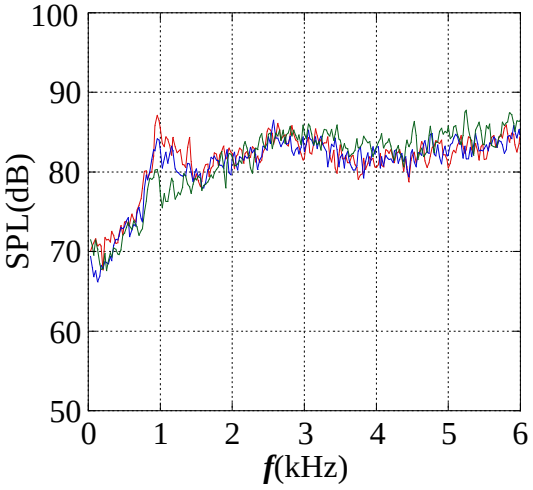

(E)NPR=2.2

Fig.6.1.4 Continued

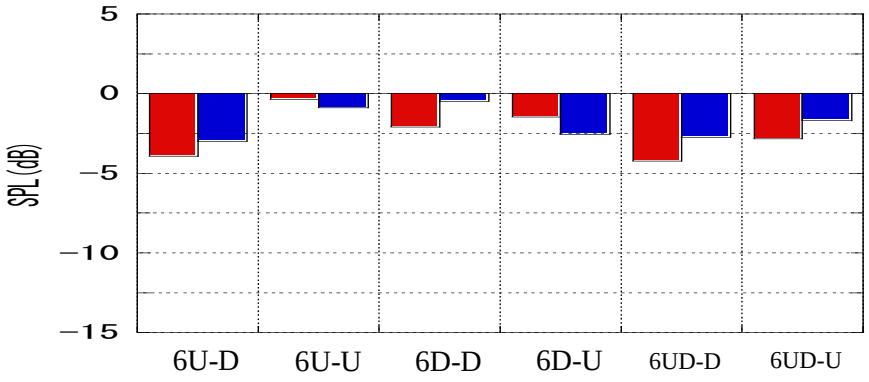

(a)NPR=1.6

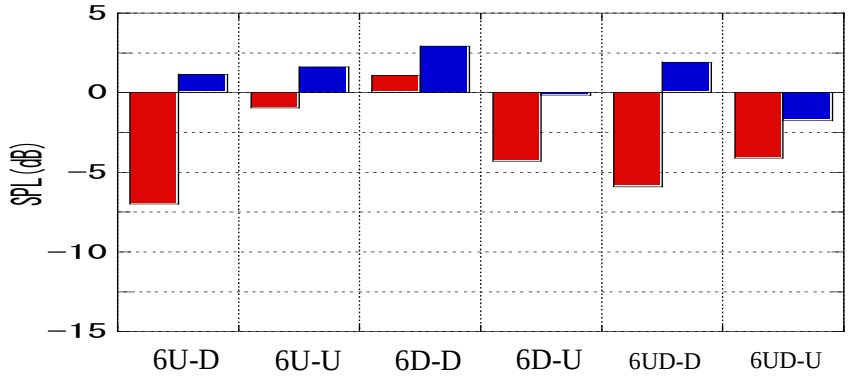

(b)NPR=1.8

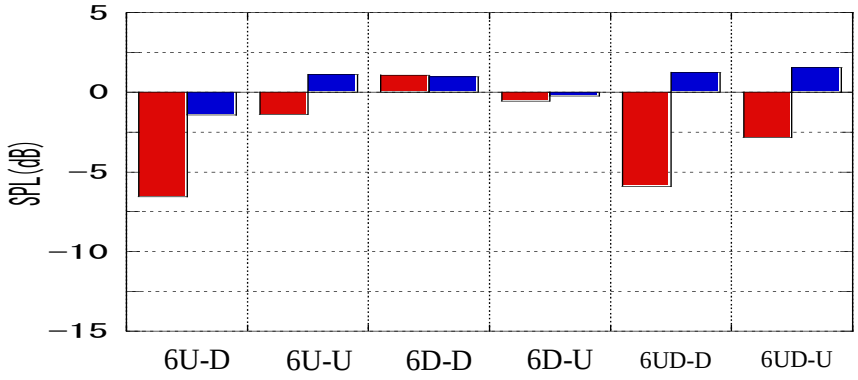

(c)NPR=2.0

Figure 6.2.1 Bar-plots of transonic tone reductions at typical NPR

(6mm-nozzle-lip attached)

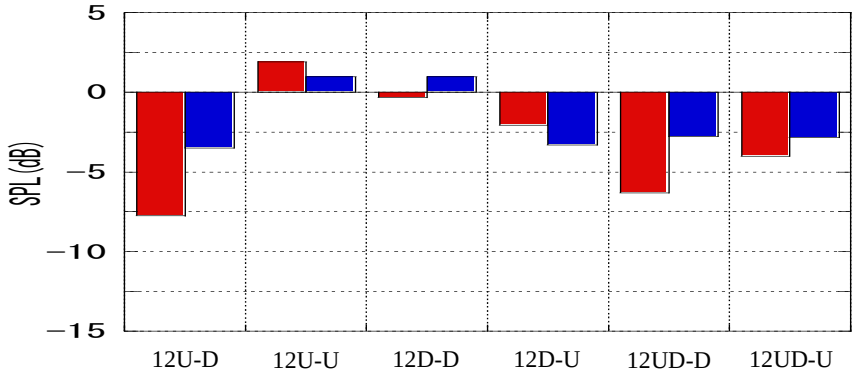

(A)NPR=1.6

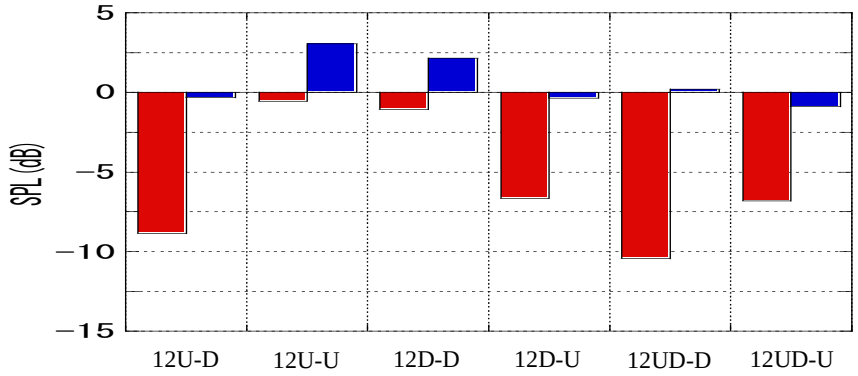

(B)NPR=1.8

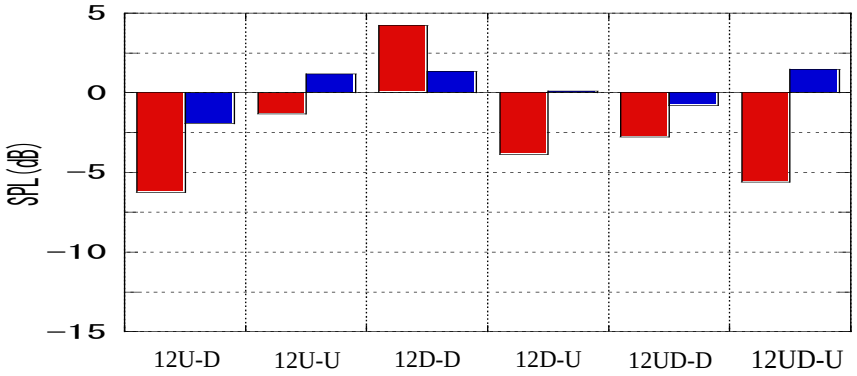

(C)NPR=2.0

Figure 6.2.2 Bar-plots of transonic tone reductions at typical NPR

(12mm-nozzle-lip attached)

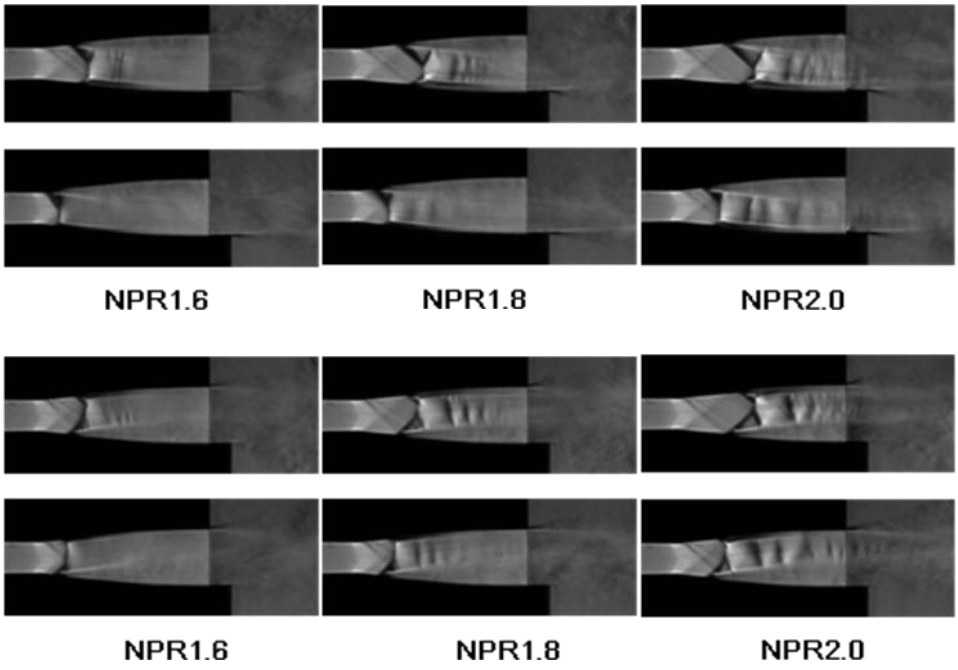

(a) 6mmD

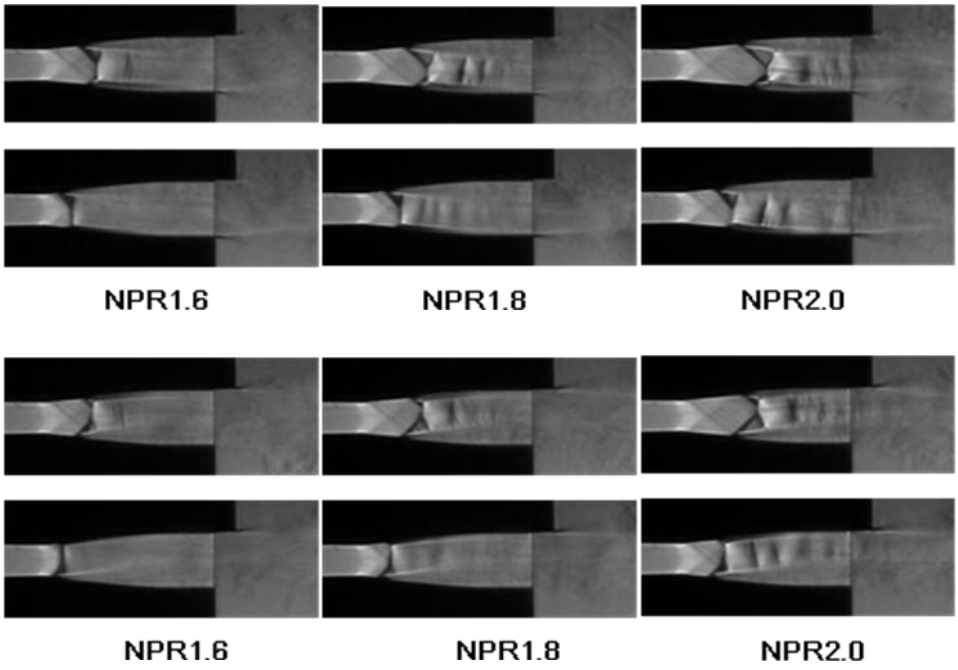

(b) 6mmU

Figure 6.3 Schlieren images showing limit position of shock wave

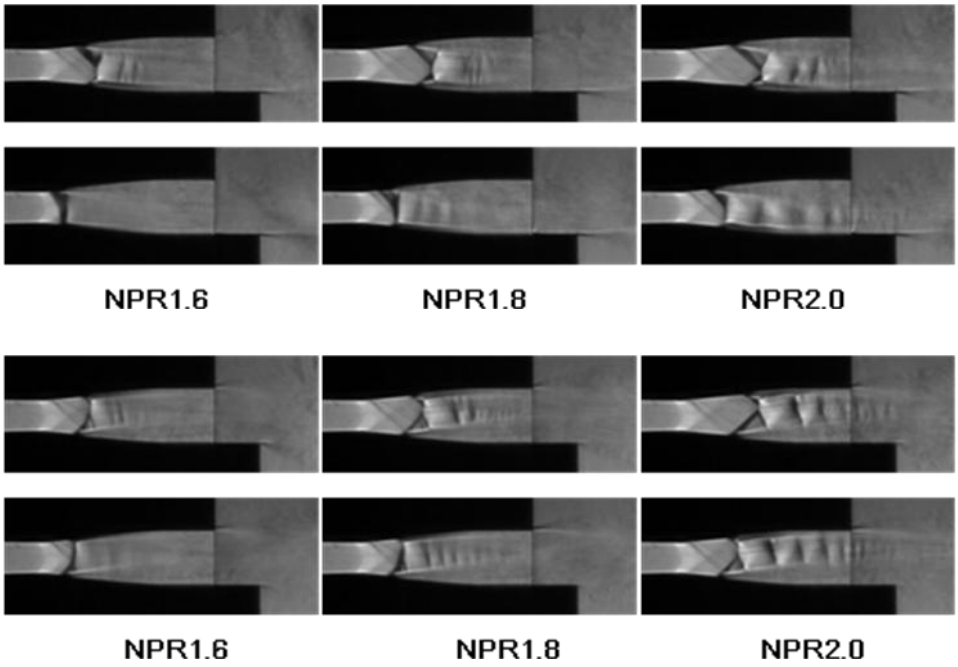

(c) 12mmD

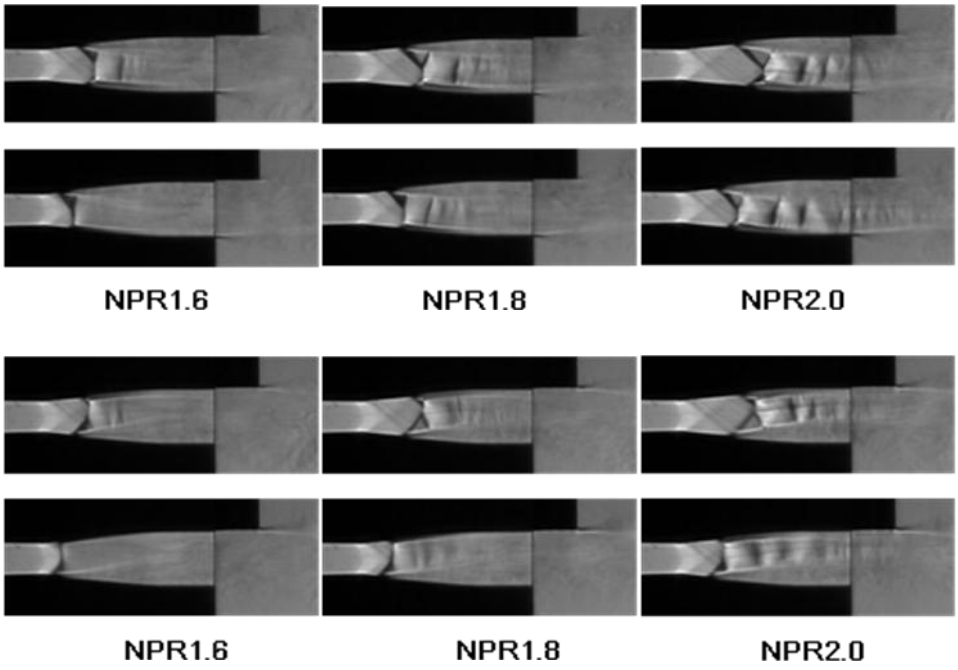

(D) 12mmU

Figure 6.3 Continue

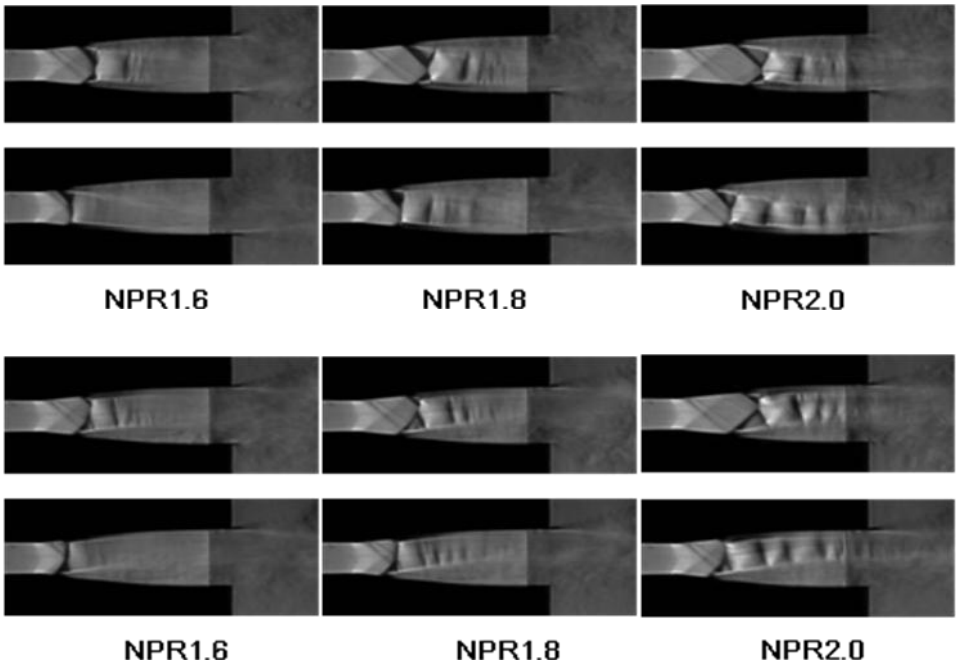

(e) 6mmUD

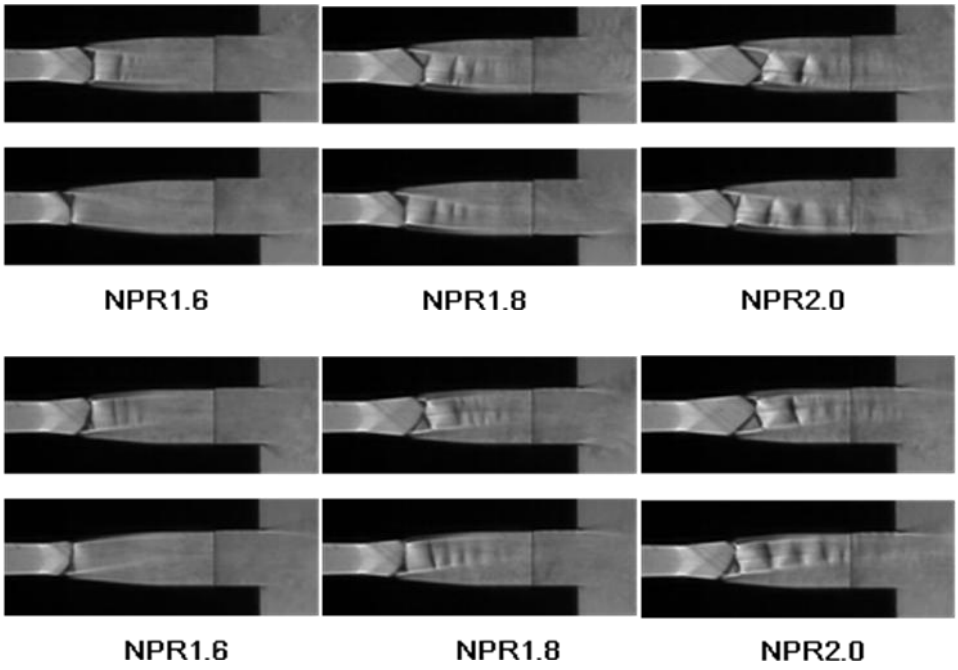

(f) 12mmUD

Figure 6.3 Continue

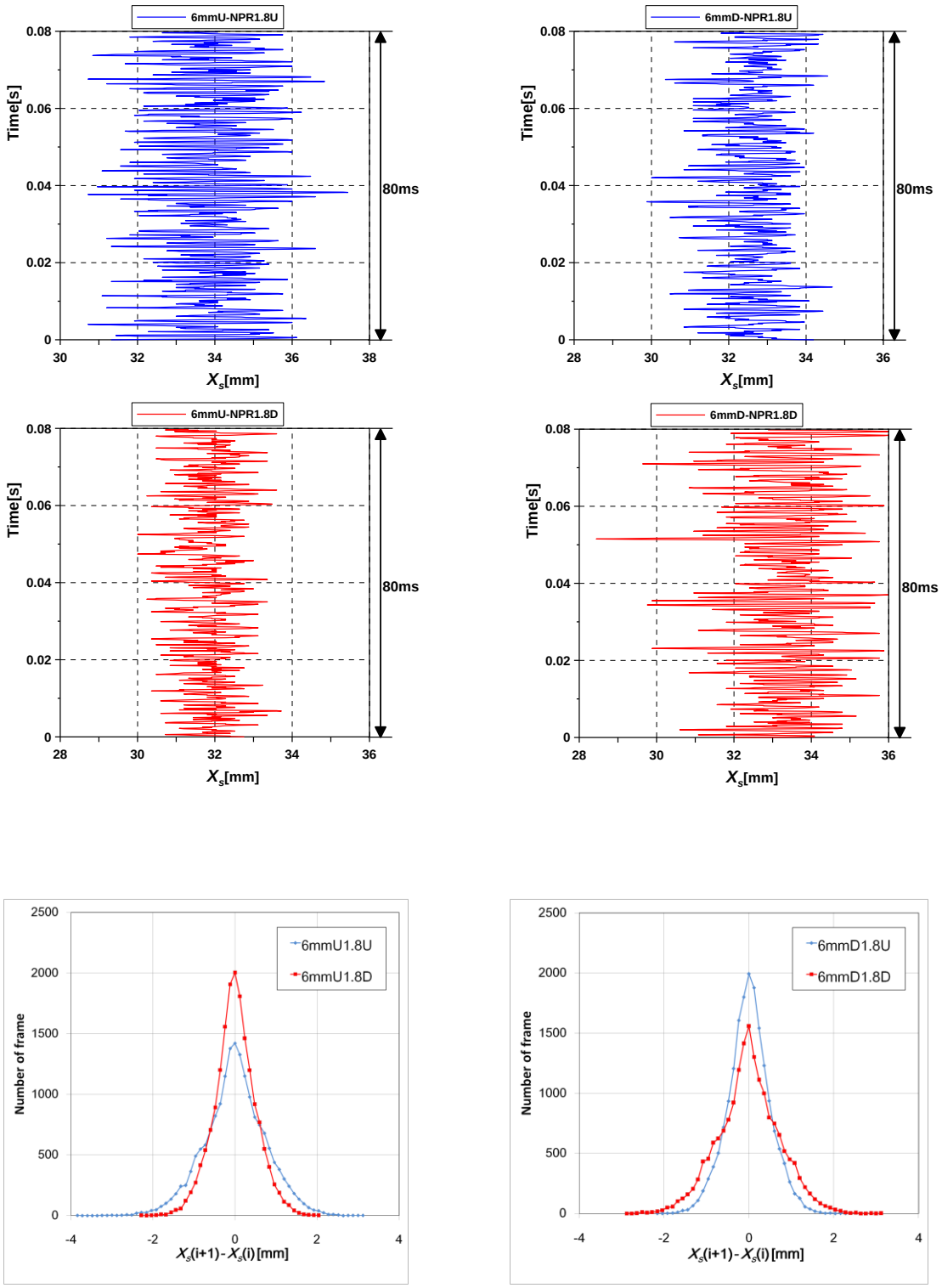

(a) 6mmU and 6mmD (NPR=1.8)

Figure 6.4 Traces and displacement histogram of the first shock wave

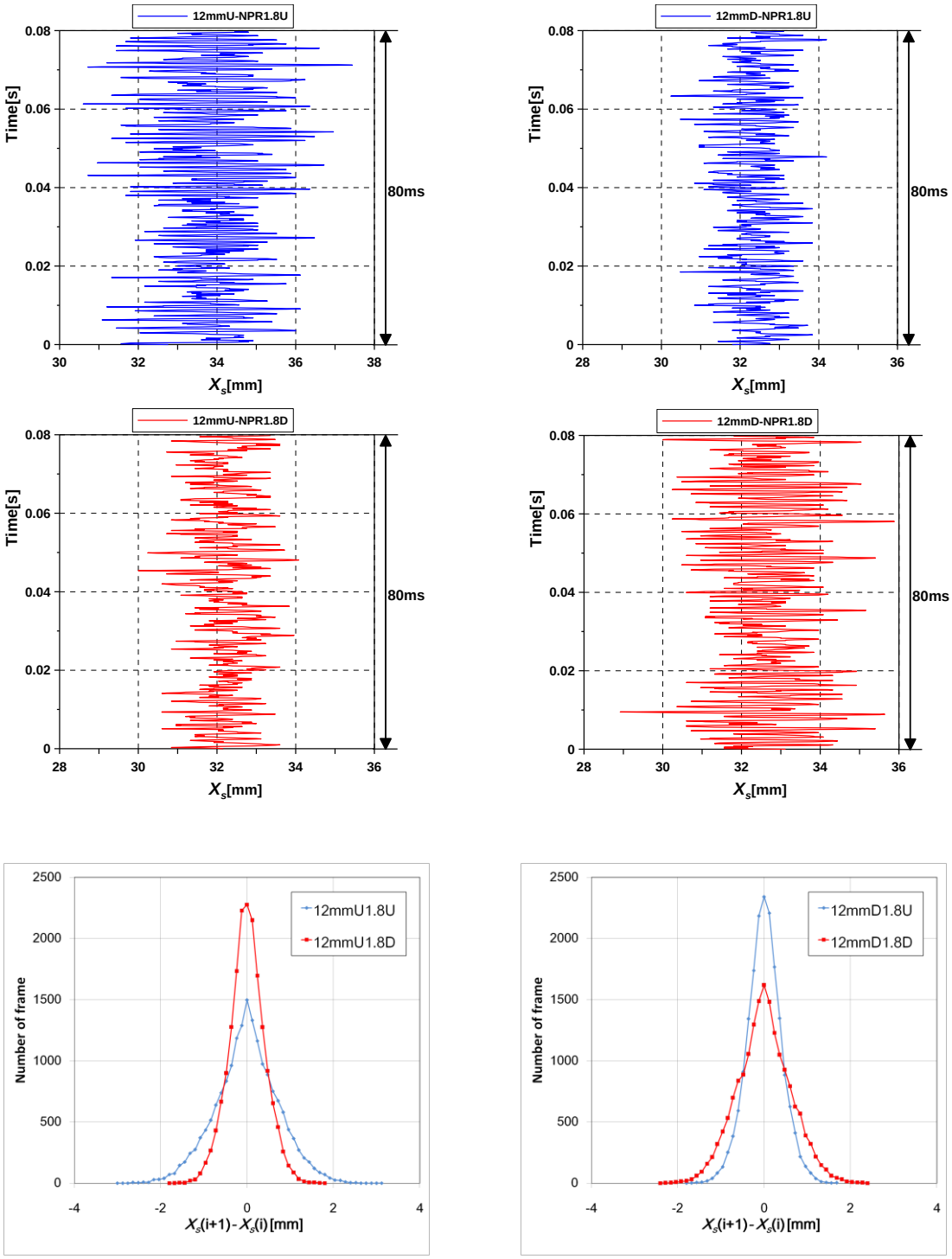

(b) 12mmU and 12mmD (NPR=1.8)

Figure 6.4 Continued

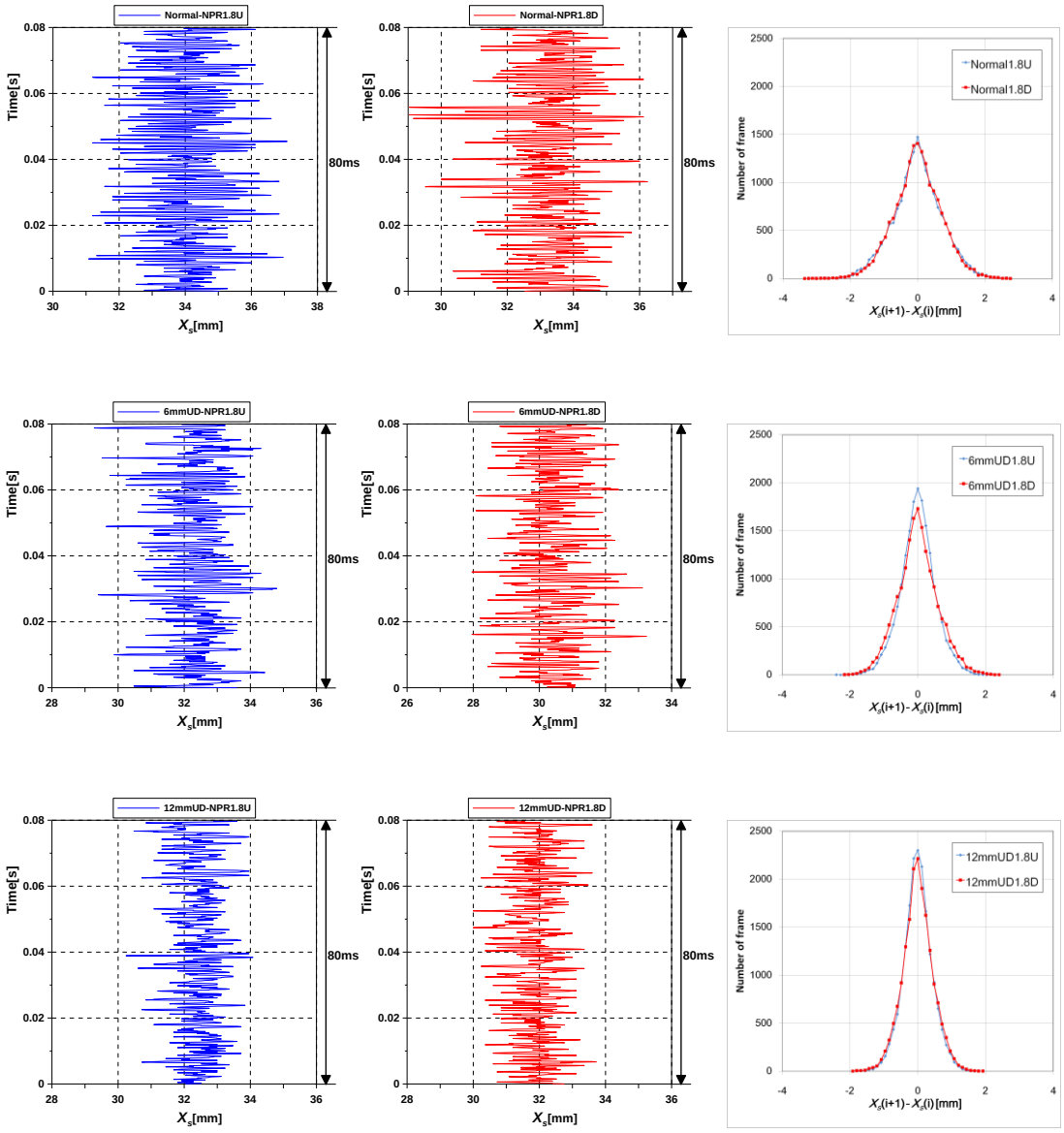

(c) Normal, 6mmUD and 12mmUD case (NPR=1.8)

Figure 6.4 Continued

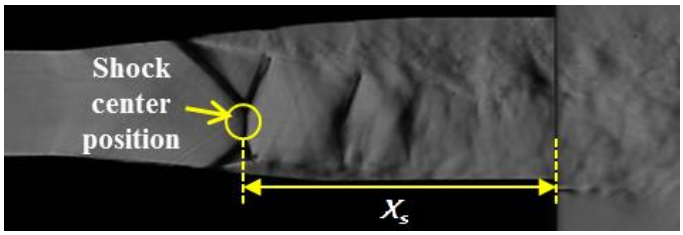

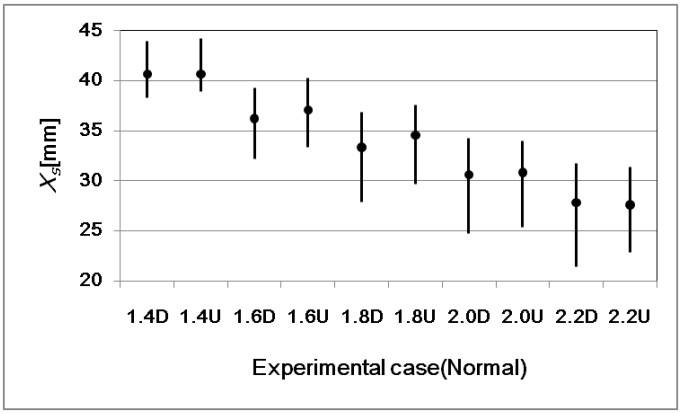

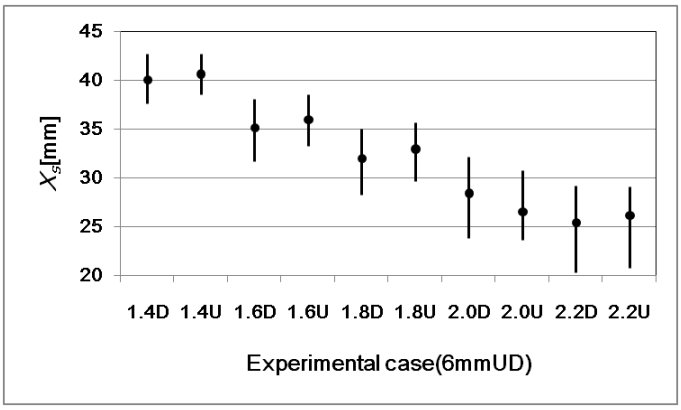

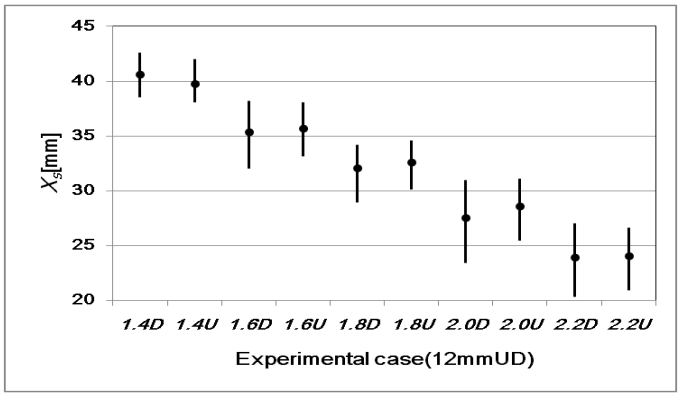

(a) Normal and 'UD' case

Figure 6.5 The variation of the first shock wave position from the nozzle exit

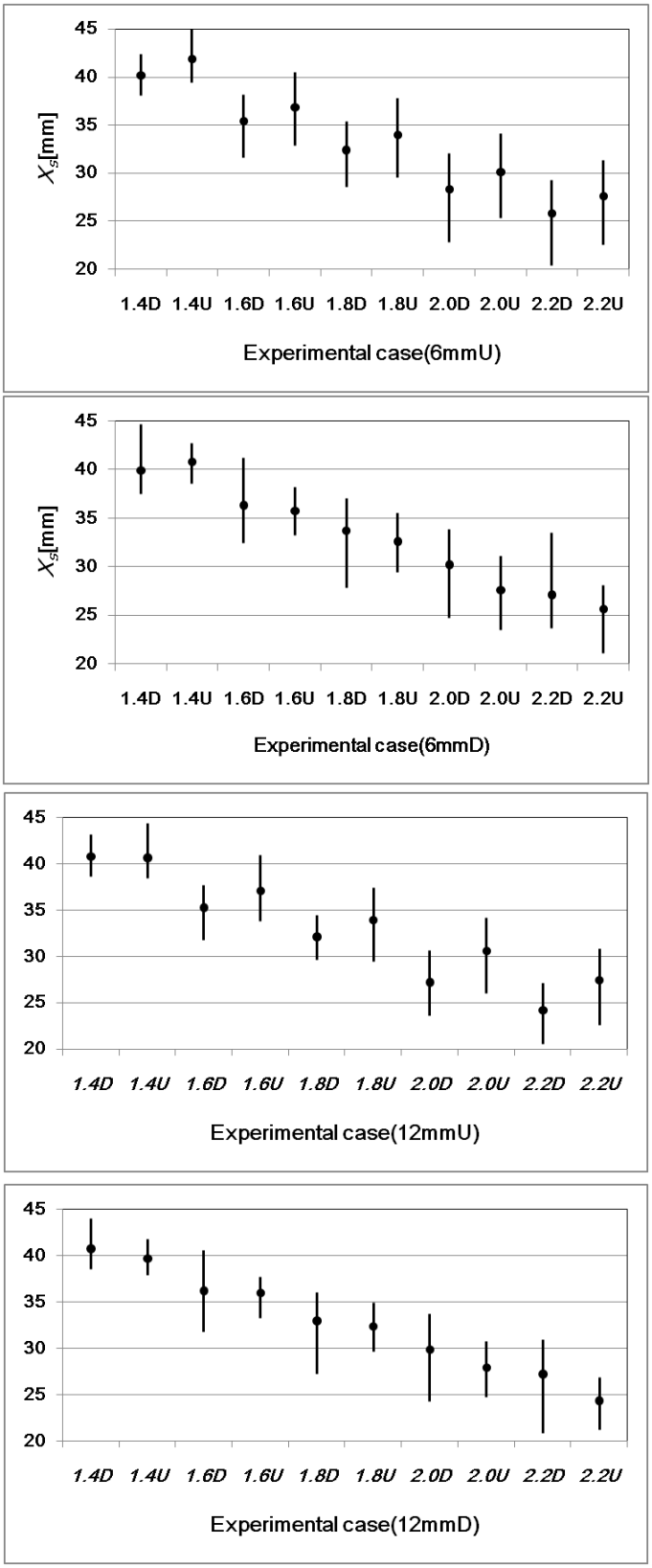

(b) 6mmU, 6mmD, 12mmU and 12mmD case

Figure 6.5 Continued

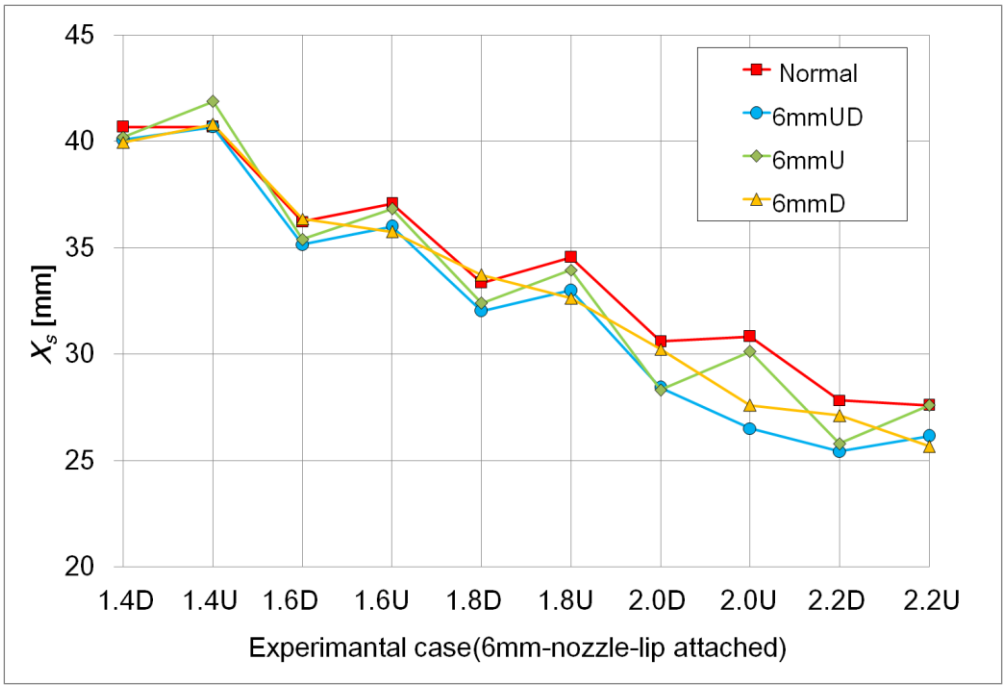

(a) 6mm-nozzle-lip attached

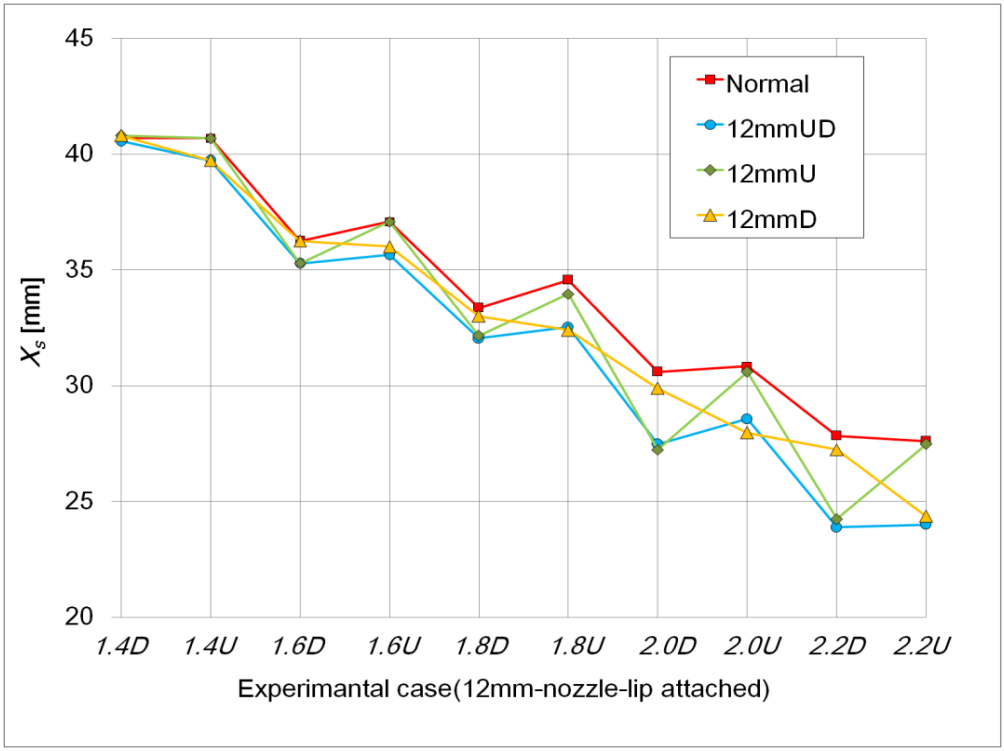

(b) 12mm-nozzle-lip attached

Figure 6.6 Long-stay position variations of the first shock wave

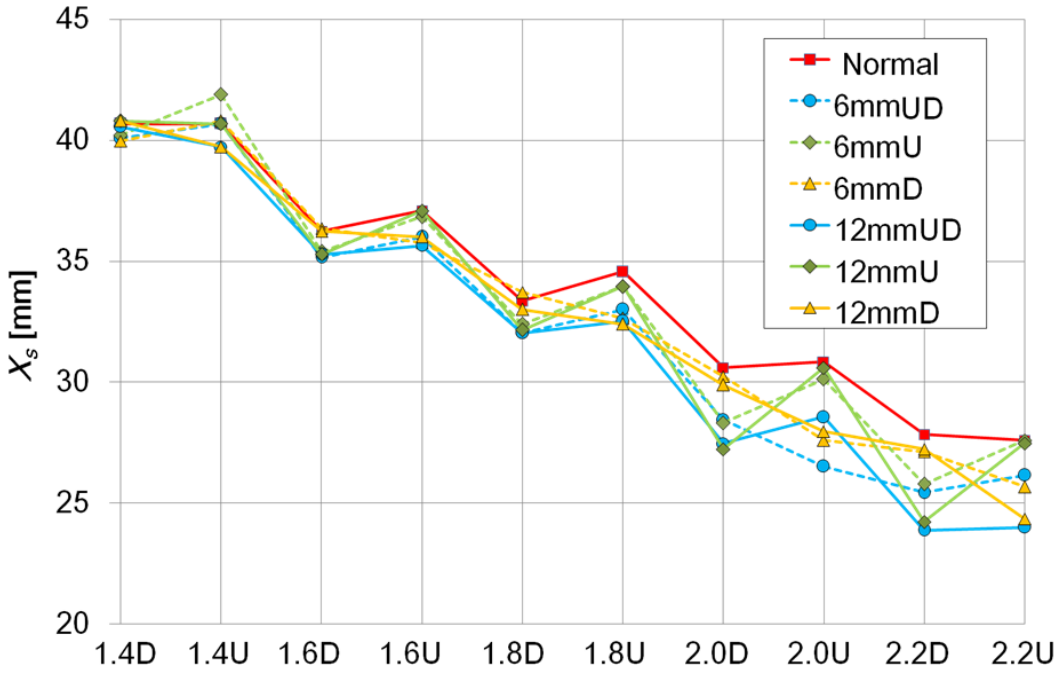

(c) overall plot

(dotted line:6mm-lip attached, solid line:12mm-lip attached)

Figure 6.6 Continued

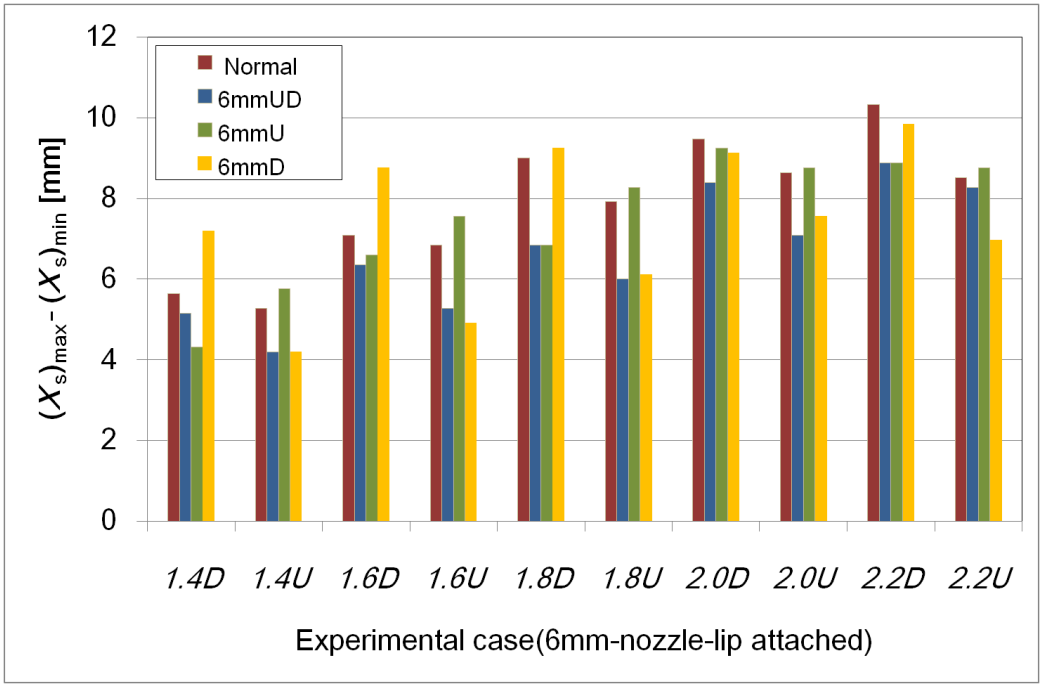

(a) 6mm-nozzle-lip attached case

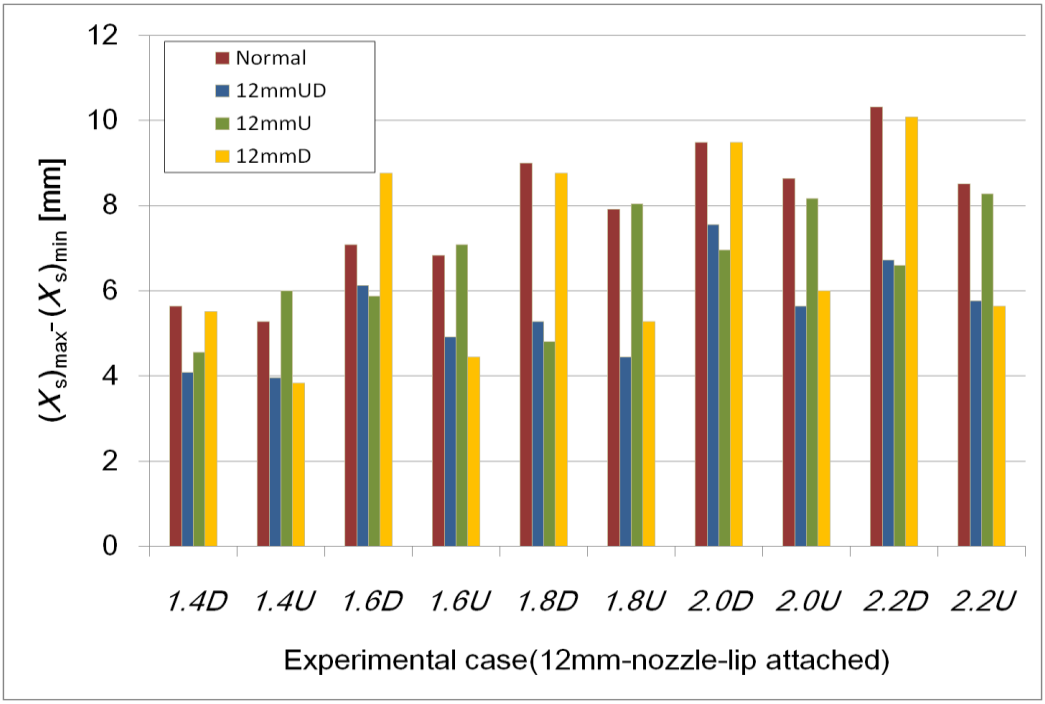

(b) 12mm-nozzle-lip attached case

Figure 6.7 Maximum displacement of the first shock wave

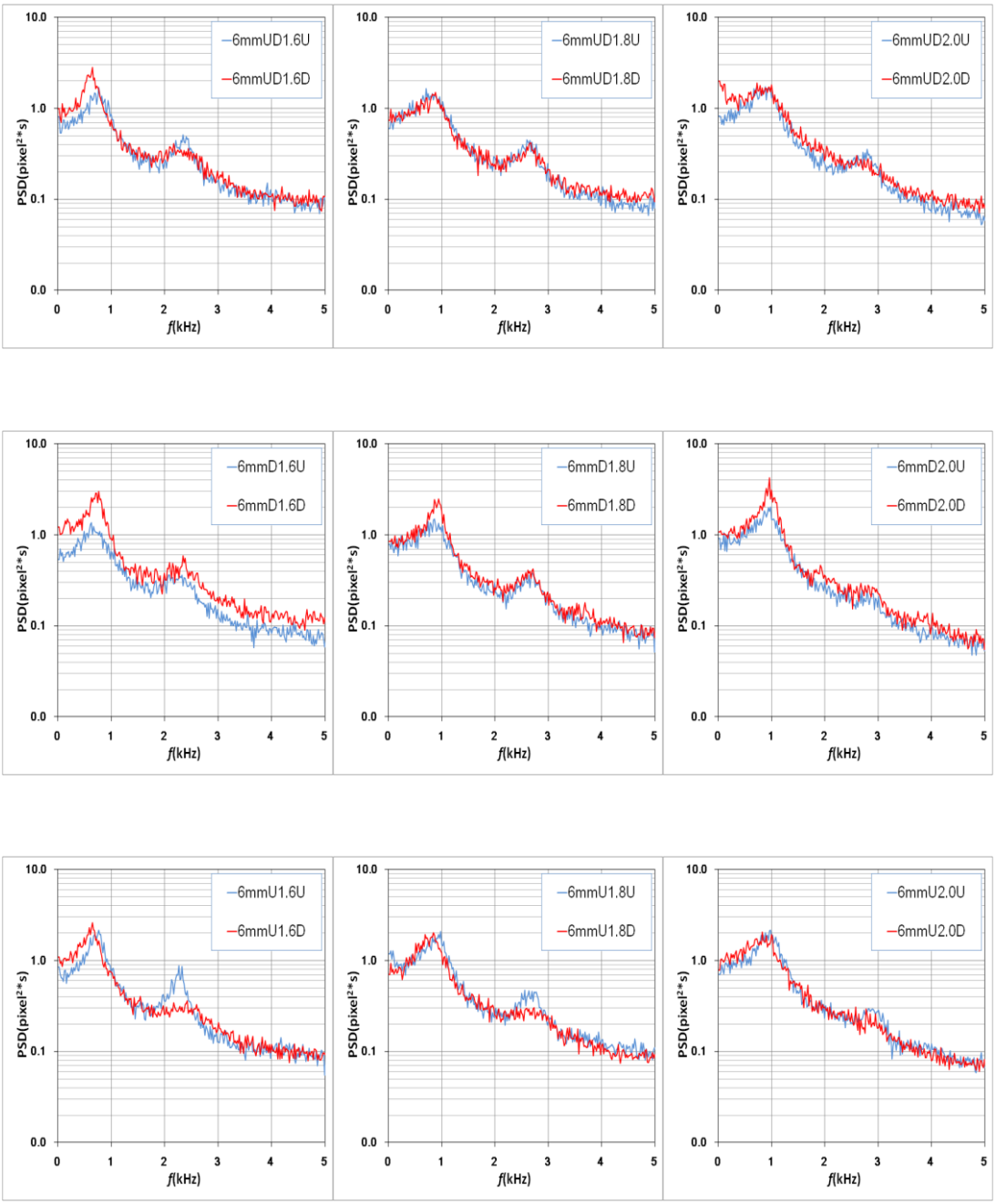

(a) for NPR=1.6, 1.8 and 2.0, 6mm nozzle-lip attached case

Figure 6.8 PSD distribution of the first shock wave oscillation

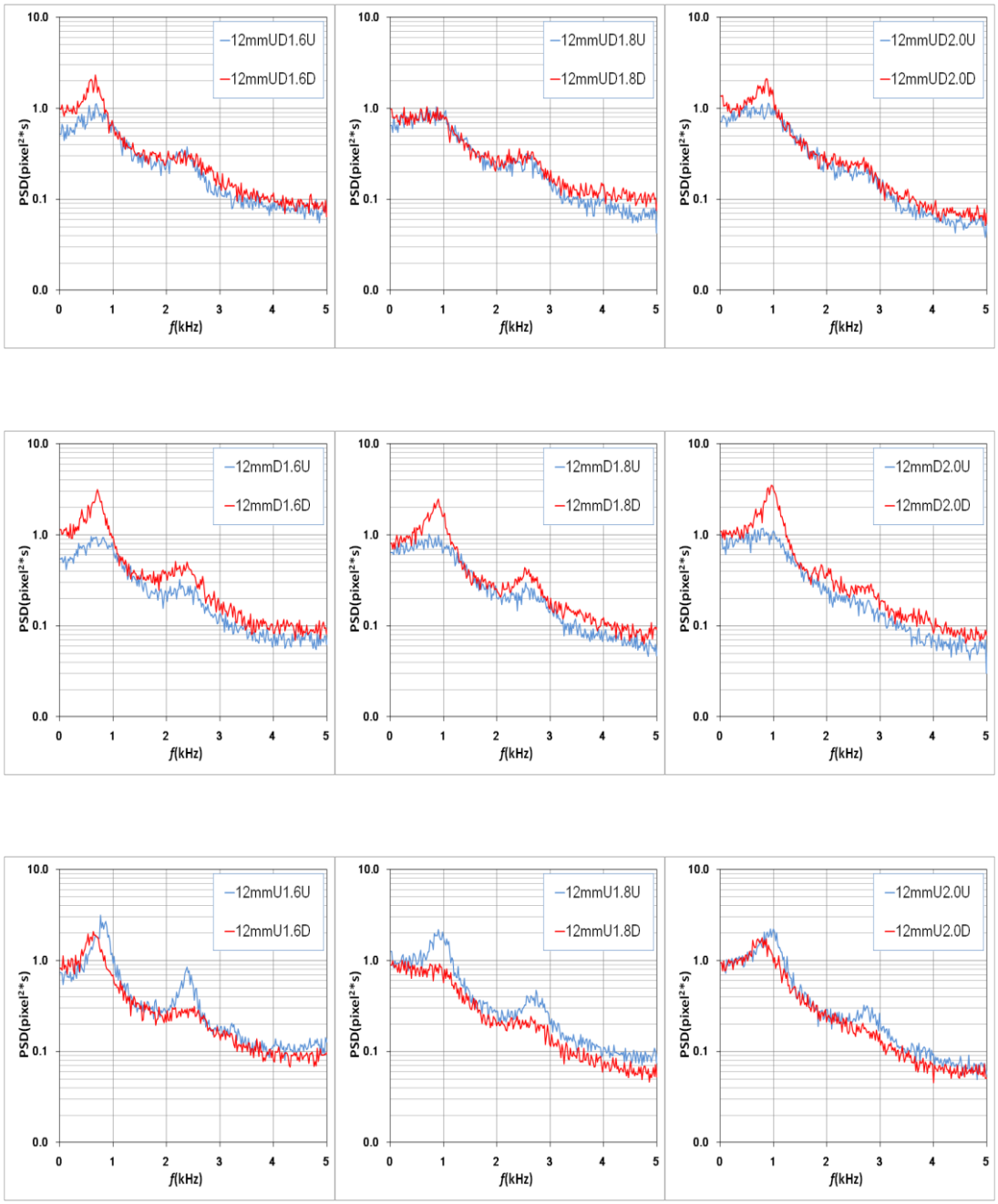

(b) for NPR=1.6, 1.8 and 2.0, 12mm nozzle-lip attached case

Figure 6.8 Continued

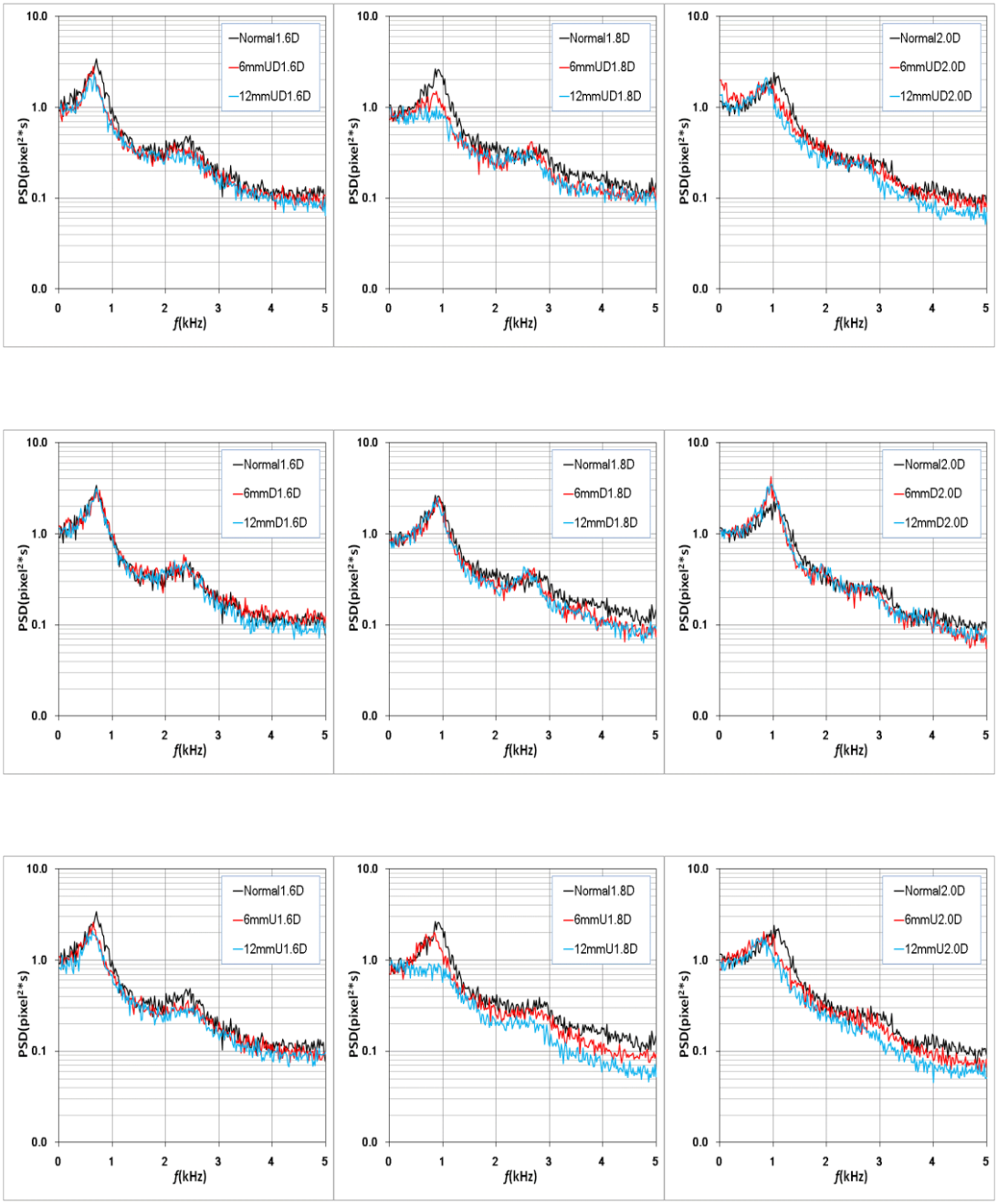

(c) for NPR=1.6, 1.8 and 2.0

Figure 6.8 Continued

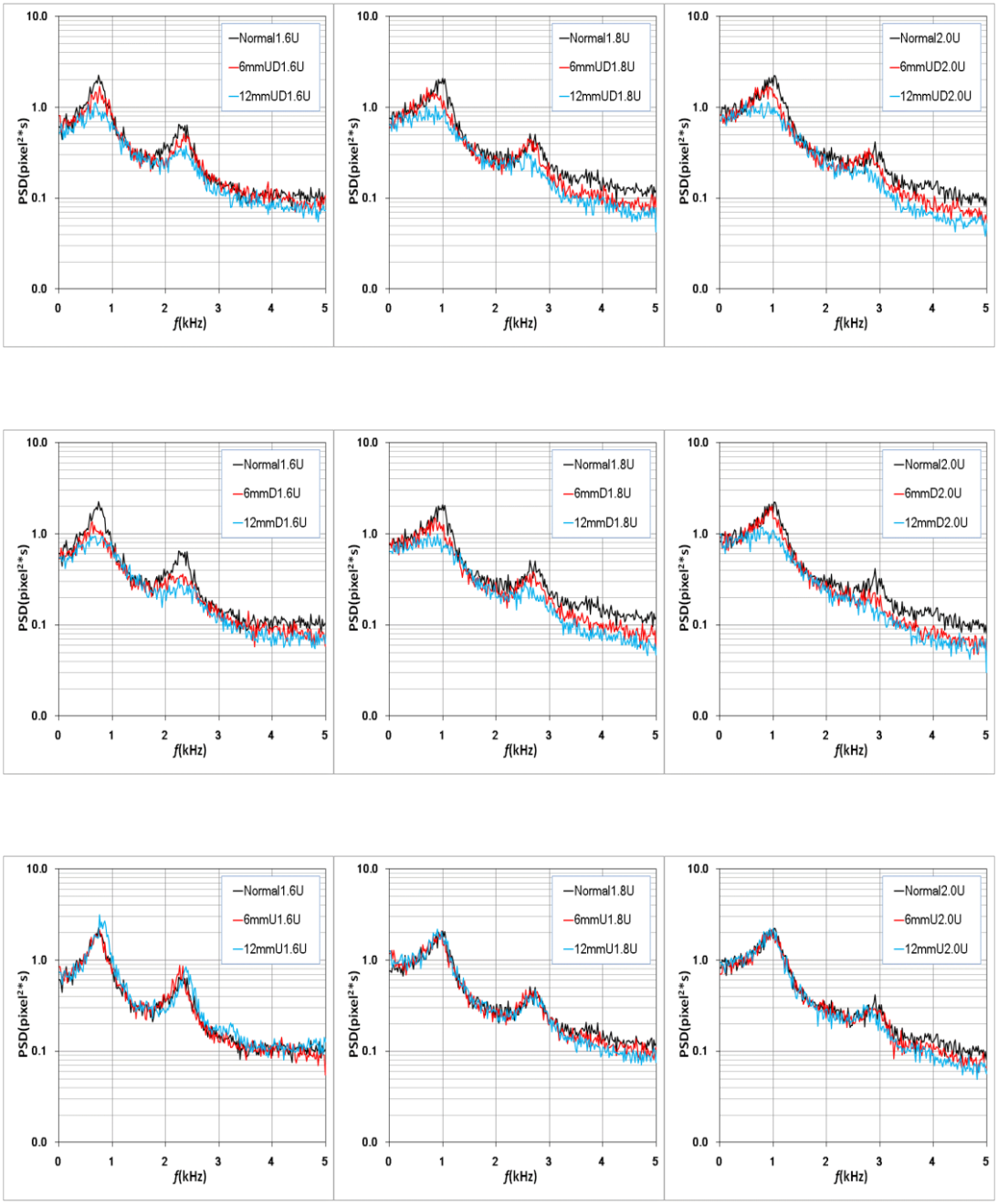

(d) for NPR=1.6, 1.8 and 2.0

Figure 6.8 Continued

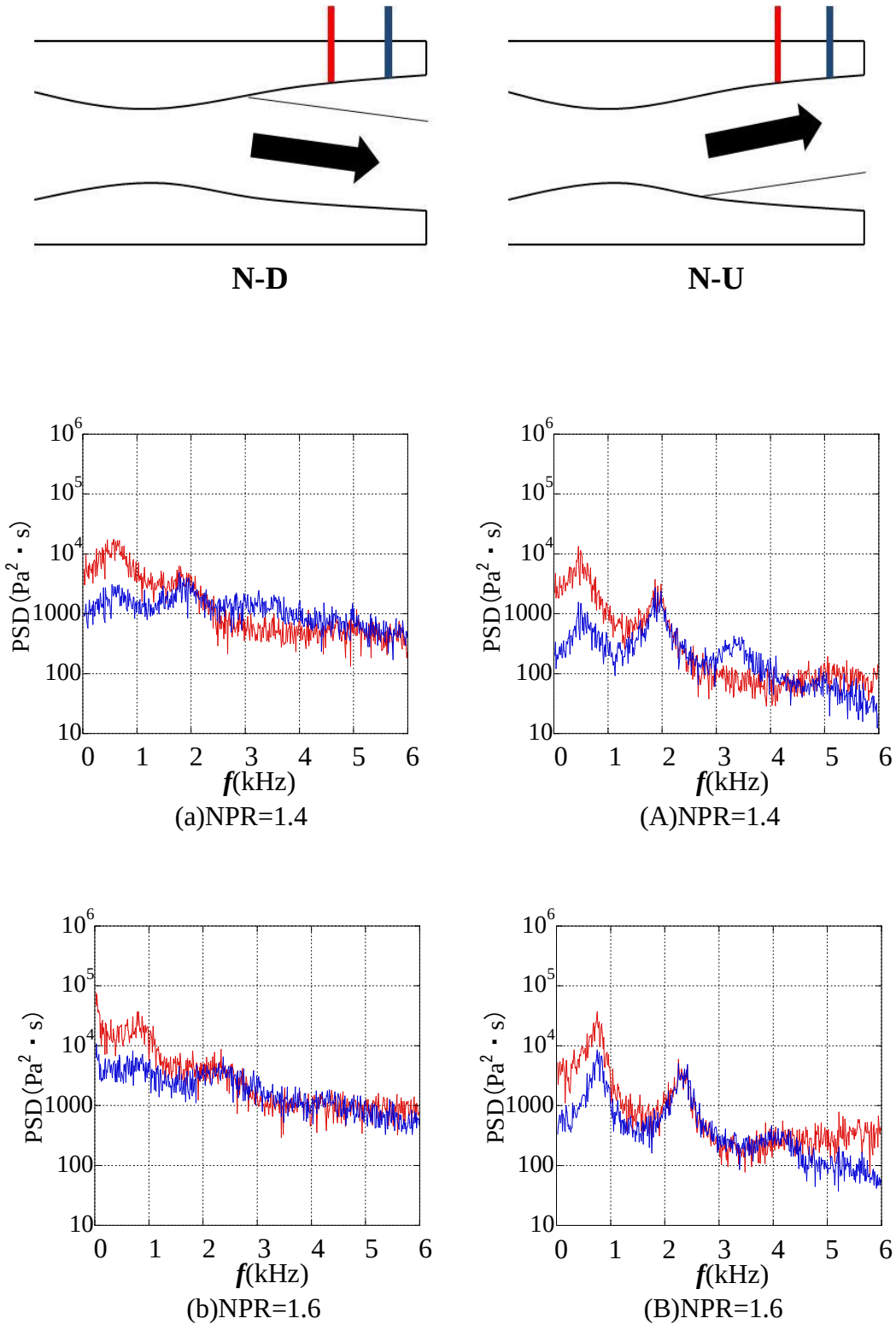

Figure 6.9 PSD comparison between wall static pressures

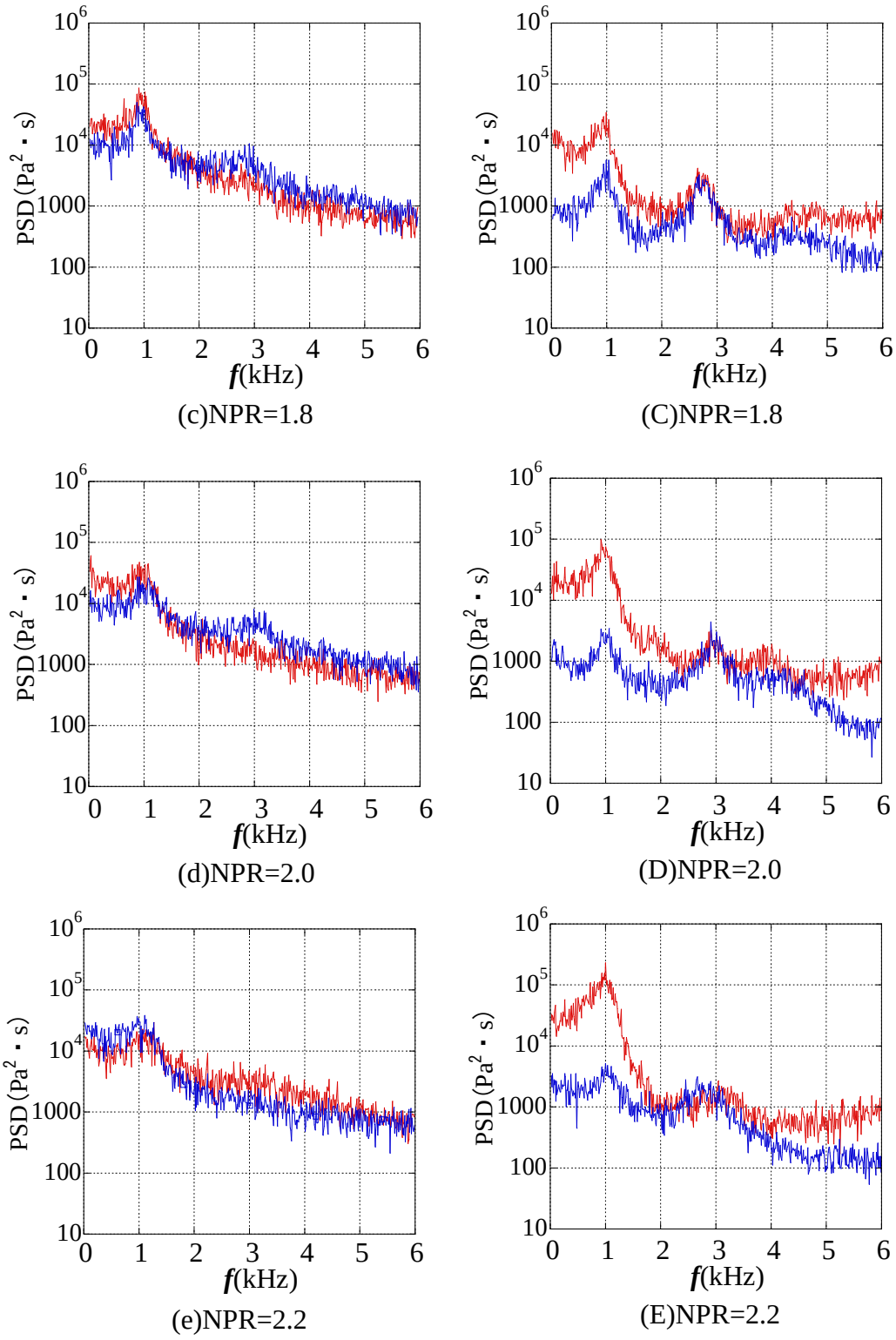

Figure 6.9 Continued

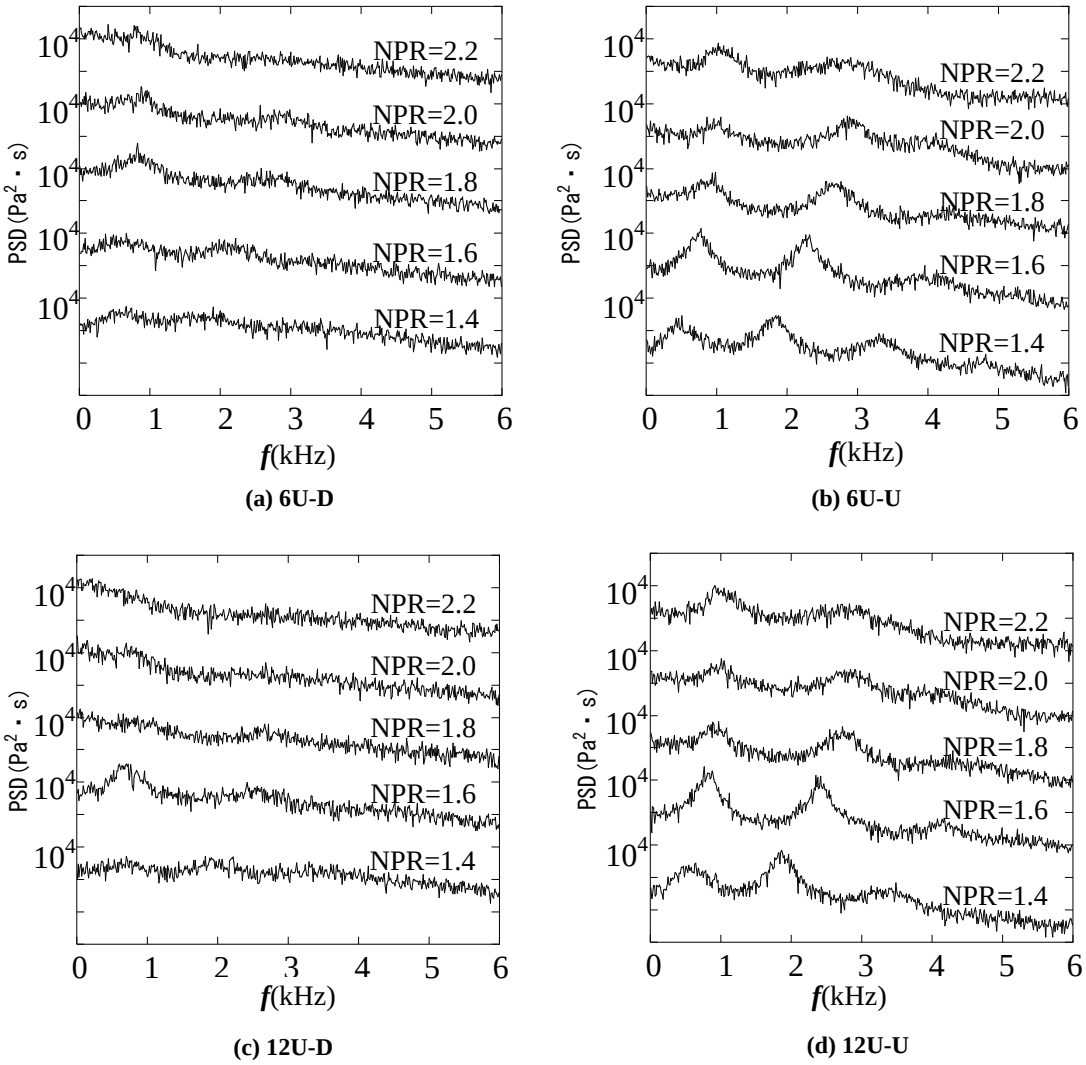

Figure 6.10 PSD distribution of wall static pressure(6mm from nozzle exit)

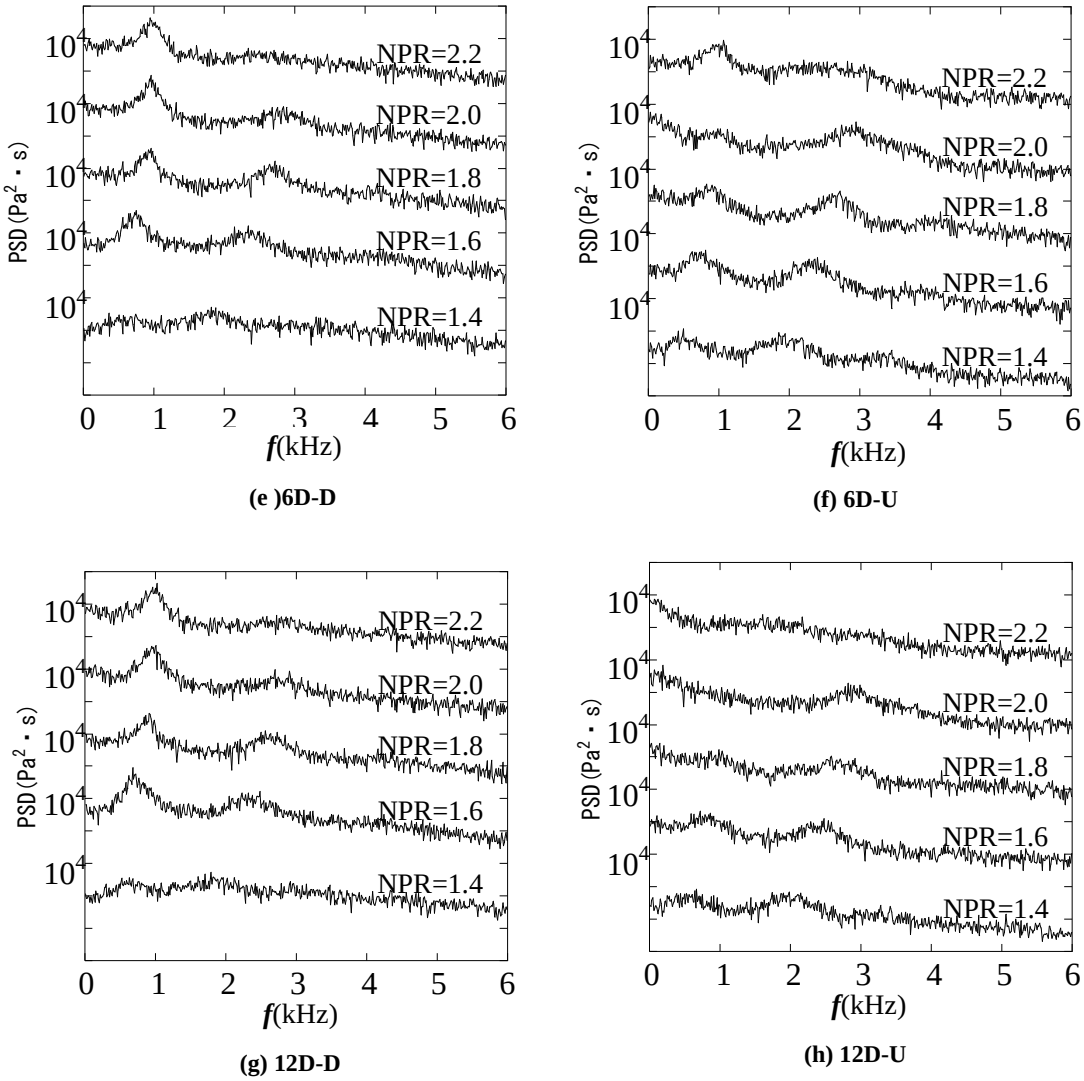

Figure 6.10 Continued(6mm from nozzle exit)

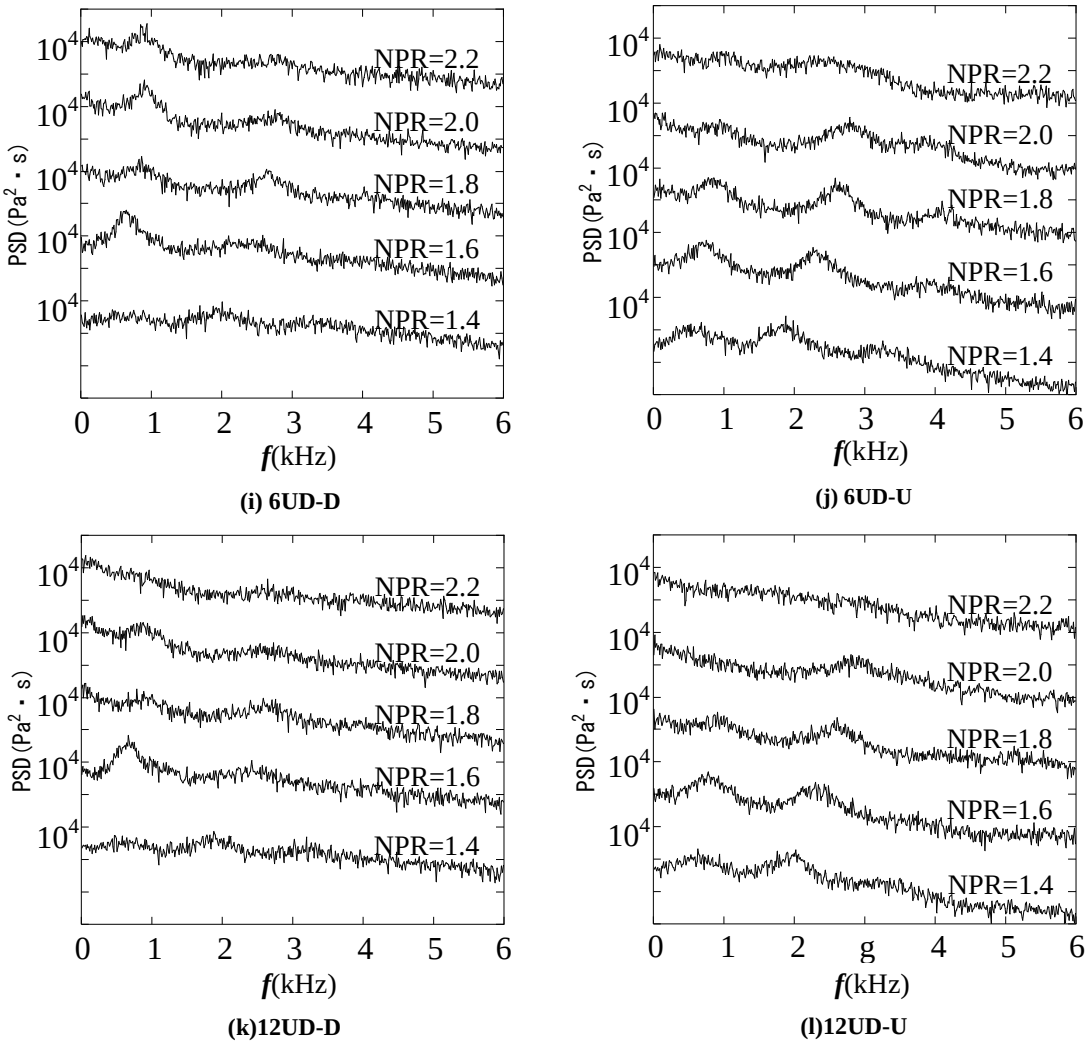

Figure 6.10 Continued(6mm from nozzle exit)

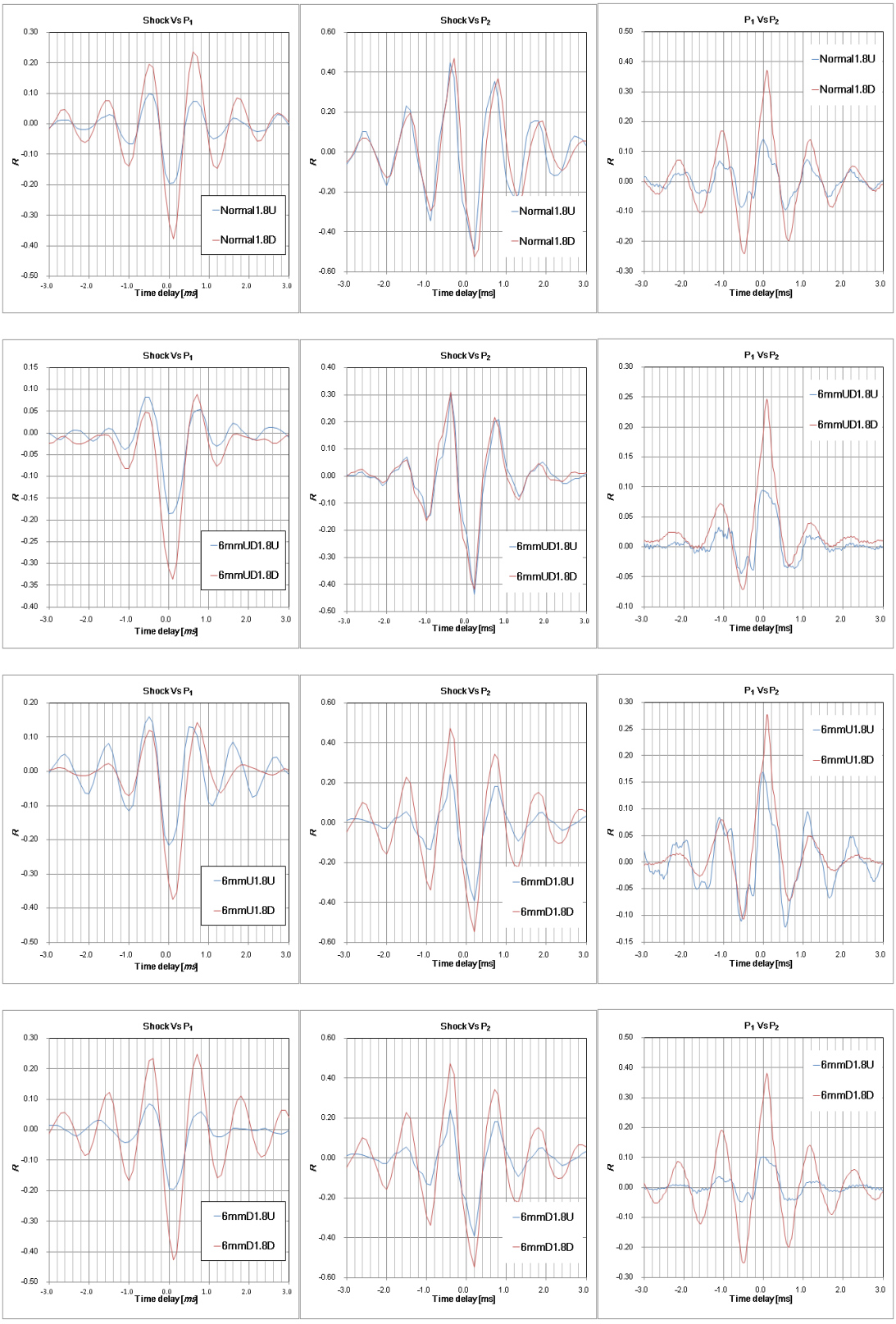

(a) Normal and 6mm-nozzle-lip attached case for NPR=1.8

Figure 6.11. Distributions of cross-correlation at typical case

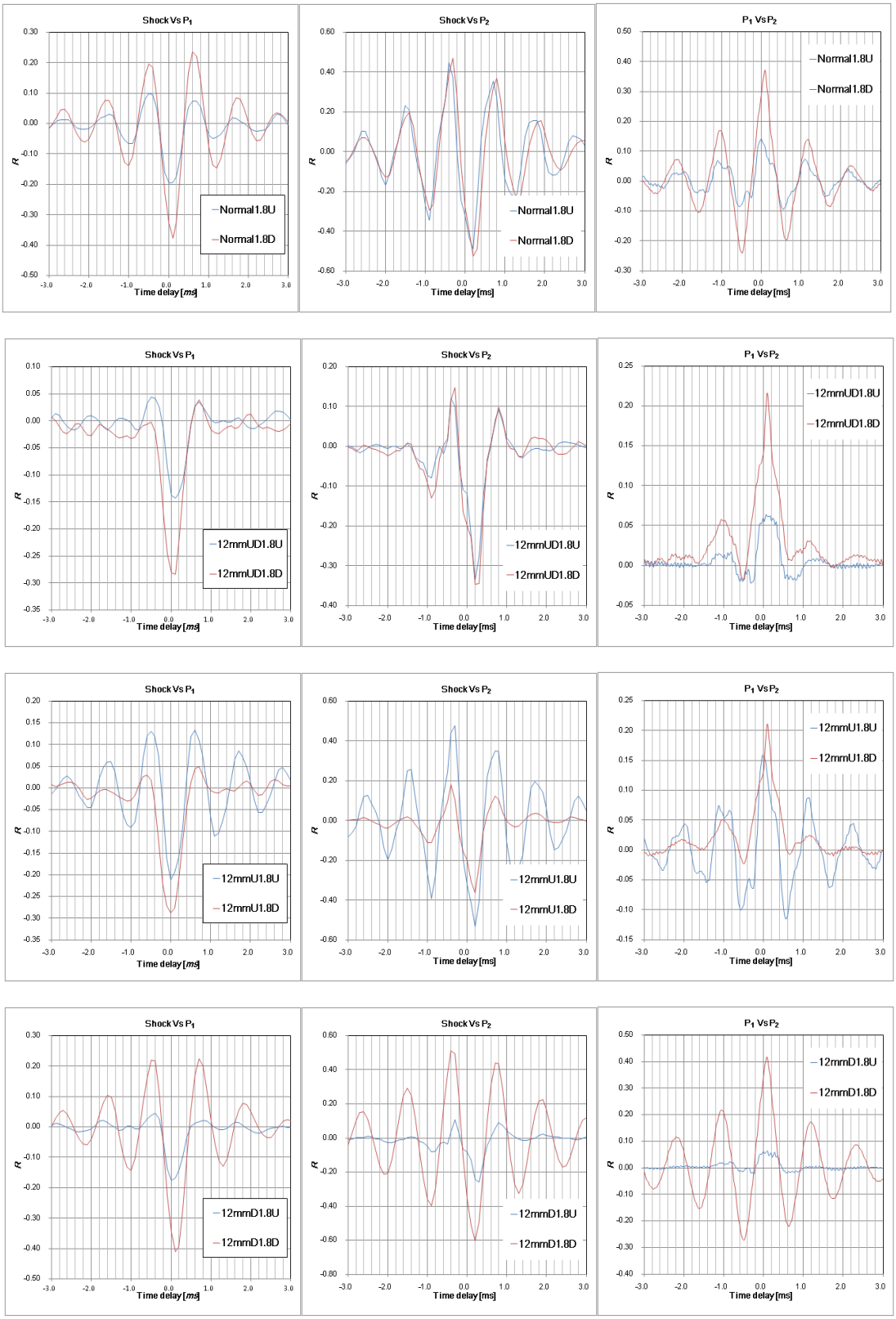

(b) Normal and 12mm-nozzle-lip attached case for NPR=1.8

Figure 6.11. Continued

Chapter 7

Conclusions

7.1 Conclusions

The main objectives of the present thesis is to understanding on characteristics of the transonic tone and investigate generation mechanism of transonic tone in convergent-divergent nozzle. At first, to understand the acoustic characteristics and the source of transonic tone, the effects of baffle plate on the tone had been examined by comparing with the screech tone in an axisymmetric convergent-divergent nozzle. And then, to fined the transonic tone generation mechanism, the relationships between the transonic tone and first shock wave oscillations or wall static pressure fluctuations had been investigated in 2-dimensional supersonic nozzle. As the transonic tone reduction method, the effect of the nozzle-lip length on the transonic tone had been carried out. To analyze the frequencies of the first shock oscillation, a high speed video camera had been used and for analyzing the relationships between the tone and flow oscillation, simultaneous measurements had been employed. The important results obtained from the present study are summarized as follows.

Acoustic Characteristics of Transonic Tone and effect of nozzle-lip thickness on Transonic Tone in Axisymmetric Nozzle

- The transonic tone occurred at the condition of non-isentropic shock-containing flow in one or two stages. And the stage1 and stage two corresponded to one-quarter and tree-quarter wave. With increasing of NPR, the transonic tone frequencies were increased contrasting with the screech tone.

- And distinctly with the screech tone, the transonic tone had changed little in the tone amplitude or frequency for variation of the nozzle-lip thickness. The fact results from the source location of the tone generation: the transonic tone had internal noise source.

Transonic tone in 2-Dimensional Supersonic Nozzle

- The generation of transonic resonance is closely related to the shock wave oscillations and wall static pressure fluctuations in the nozzle. In the 2-dimensional nozzle, the present results were similar to the acoustic characteristics of general transonic tones of the axisymmetric nozzle. When the transonic tone occur, the amplitude of the first shock wave oscillation become large. The dominant peaks of the first shock oscillations and wall static pressure fluctuations were occurred at nearly the same frequency of transonic tone (Mode A and Mode B). And there are considerable correlations between the tone and the first shock wave oscillation or wall static pressure fluctuation. And it is expected that a feedback loop is generated between the shock wave and nozzle exit when the transonic tone occur.

Effect of nozzle-lip length on transonic tone in 2-dimensional supersonic nozzle

- When the nozzle-lip extended at the side of the large separation zone located, the transonic tone was reduced at stage 1 about 5~10dB. It was more effective to reduce the transonic tone by attaching 12mm-nozzle-lip than 6mm. And the nozzle-lip which is extended at the opposite side of the large separation zone influenced to the shock wave oscillation to excite. Especially, the peak frequency of the shock wave is corresponding to the tone frequency of stage1. And even 'UD' case which attached both of nozzle-lip, the nozzle-lip extended from a large separation zone, is meaningful to reduce the transonic tone. The extended nozzle-lip affects the

transonic tone, the first shock wave movement and oscillation and the wall static pressure fluctuation. It seems that the changing of the nozzle-lip length directly affects to the first shock wave and feedback loop mechanism which is expected to develop in the large separation zone.

7.2 Future Work

The present thesis has reported several interesting conclusions concerning the transonic tone and its generation mechanism. Especially, It is expected that there is a feedback loop in the large separation zone between the shock wave and the nozzle exit but it is not clear yet because it is not found the upstream-propagating disturbance between the shock wave and pressure fluctuation in the flow. And it is also bounded to find the detail of the flow instability mechanism because the shock wave and wall static pressure fluctuation changed along with the transonic tone reduction or emission and it is difficult to control only one or more condition.

- It seems that to understand the flow instability mechanism or the shock wave unsteadiness phenomenon is an overriding concern to investigate the tone generation mechanism. In that sense, Papamoschou's result counts. (Papamoschou & Johnson 2006): according to Papamoschou, the instability mechanism is due to and interaction between the expansion fan reflected from the smaller lambda foot with the shear layer of the larger separation zone. However, even this result is not detail about 'the interaction'. And There are other possibilities of the shock unsteadiness : the downstream-propagating instability wave, upon interaction with the discontinuity at the nozzle exit, produces a feedback wave. (Zaman, Dahl, Bencic & Loh 2002) Or the shock becomes the upstream 'closed' end and also acts like a vibrating diaphragm similar to that involved in longitudinal acoustic resonance. (Zaman, Dahl, Bencic & Loh 2002) And It can be the one of the possibility that the growth and decline of the separation bubble make the pressure perturbation of the shock wave oscillations and produces a

feedback wave.

References

Addy, A. L. (1981), Effects of axisymmetric sonic nozzle geometry on Mach disk characteristics, *AIAA Journal*, Vol.**19**, No.1, pp.121-122.

Bartosiewicz, Y., Aidoun, Z., Desevaux, P. and **Mercadier, Y.** (2005), Numerical and experimental investigations on supersonic ejectors, *International Journal of Heat and Fluid Flow*, Vol.**26**, pp.56-70.

Bogar, T. J., Sajben, M. and **Kroutil, J. C.** (1983), Characteristic frequencies of transonic diffuser flow oscillations, *AIAA journal*, Vol.**21**, pp.1232-1240.

Brown, G. L. and **Roshko, A.** (1974), On density effects and large structure in turbulent mixing layers, *Journal of Fluid Mechanics*, Vol.**64**, pp.715-816.

Browand, F. K. and **Weidman, P. D.** (1976), Large-scales in the developing mixing layer, *Journal of Fluid Mechanics*, Vol.**76**, pp.127-144.

Chen, C. P., Sajben, M. and **Kroutil, J. C.** 1979 Shock-wave oscillations in a transonic diffuser flow, *AIAA jounal***,** Vol.**17,** pp.1076-1083

Crow, S. C. and **Champagne, F. H.** (1971), Orderly structure in jet turbulence, *Journal of Fluid Mechanics*, Vol.**48**, pp.547-591.

Eames, I. W. (2002), A new prescription for the design of supersonic jet-pumps : the constant rate of momentum change method, *Applied Thermal Engineering*, Vol.**22**, pp.121-131.

Ennix, K. A., Burcham Jr., F. W. and **Webb, L. D.** (1993), Flight-determined engine exhaust characteristics of an F404 engine in an F-18 airplane, NASA TM-4538.

Ffowcs Williams, J. E. (1963), The noise from turbulence convected at high speed, *Philosophical Transactions of the Royal Society*, Series A, Vol.**255**, pp.469-503.

Ffowcs Williams, J. E., **Simson, J.** and **Virchis, V. J.** (1975), Crackle : an annoy -ing component of jet noise, *Journal of Fluid Mechanics*, Vol.**71**, Part 2, pp.251-271.

Fisher, M. J., Lush, P. A. and **Harper Bourne, M.** (1973), Jet noise, *Journal of Sound and Vibration*, Vol.**28**, No.3, pp.563-585.

Harper Bourne, M. and **Fisher, M. J.** (1974), The noise from shock waves in supersonic jets, *Proceedings of the AGARD Conference on Noise Mechanisms, Brussels, Belgium*, No.**131**, pp.11:1-13.

Hill, W. G. and **Greene P. R.** (1977), Increased turbulent mixing rates obtained by self-excited acoustic oscillations, *Trans. ASME: J. Fluids Eng.*, Vol.**99**, pp.520–525.

Hsieh, T. and **Coakley, T. J.** (1987), Downstream boundary effects on frequency of self-excited oscillations in transonic diffuser flows, **AIAA 87-0161**.

Hunter. C. (2004), Experimental investigation of separation nozzle flows, *AIAA journal*, Vol.463, No.3, pp.527-532.

Hussain, A. K. M. F. and **Hasan, M. A. Z.** (1983) The `whistler-nozzle' phenomenon, *J. Fluid Mech.*Vol.134, pp.431-458.

Jameel, M. I., Cormack, D. E. and **Tran, H.** (1994), Sootblower optimization (part 1 : fundamental hydro-dynamics of a sootblower nozzle jet), *TAPPI Journal*, Vol.**77**, No.5, pp.135-142.

Krothapalli, A., Hsia, Y., Braganoff, D. and **Karamcheti, K.** (1986), The role of screech tones in mixing of an underexpanded rectangular jet, *Journal of Sound and Vibration*, Vol.**106**, No.1, pp.119-143.

Krothapalli, A. and **Hsia, Y. C**. (1996), Discrete tones generated by a supersonic jet ejector, *J. Acoust. Soc. Am.*, Vol.99, pp.777-784.

Krothapalli, A., Venkatakrishnan, L. and **Lourenco, L.** (2000a), Crackle : a dominant component of supersonic jet mixing noise, 6th *AIAA/CEAS Aero-acoustics Conference*, Lahaina, Hawaii, USA, **AIAA-2000-2024**.

Li, P. and **Halliwell, N. A.** (1985), Industrial jet noise : coanda nozzles, *Journal of Sound and Vibration*, Vol.**99**, No.4, pp.475-491.

Lighthill, M. J. (1952), On sound generated aerodynamically : I. general theory, *Proceedings of the Royal Society of London*, Series A, Vol.**211**, pp.564-581.

Lighthill, M. J. (1954), On sound generated aerodynamically : II. turbulence as a

source of sound, *Proceedings of the Royal Society of London*, Series A, Vol.**222**, pp.1-32.

Loh, C. Y. and **Zaman, K. B. M. Q.** (2002), Numerical investigation of `transonic resonance' with a convergent-divergent nozzle, *AIAA journal*, Vol.40, No.12, pp.2000-0077.

Love. E. S., Grigsby, C. E., Lee, L. P. and **Woodling, M. J.** (1959), Experimental and theoretical studies of axisymmetric free jets, NASA TR R-6.

Mabey, D. (1989), Phenomena associated with unsteady transonic flows, *Progress in Astronautics and aeronautics*, Vol.**120**, AIAA, Washington DC, pp.1-56.

Meier, G. E. A., Selerowicz, W. C. and **Szumowski, A. P.** (1990), A Nozzle Generating Low Jet Noise, *J. Sound and Vibration*, Vol.**136**, No.1, pp.65-73.

Miyazato, Y. Kweon, Y. H. Aoki, T. Setoguchi, T. Kim, H. D. (2004), Effect of Nozzle Lip Thickness on Supersonic Jet Noise from Laval Nozzle, JSME, Vol.2,pp29-30.

Norum, T. D. and **Seiner, J. M.** (1979), Experiments of shock associated noise on supersonic jets, *AIAA* 12th *Fluid and Plasma Dynamics Conference*, Williams-burg, Virginia, USA, **AIAA-79-1526**.

Norum, T. D. and **Seiner, J. M.** (1982a), Broadband shock noise from supersonic jets, *AIAA Journal*, Vol.**20**, No.1, pp.68-73.

Papamoschou, D. and Johnson, A. (2006), Unsteady phenomena in supersonic nozzle flow separation, **AIAA 2006-3360**.

Postel, O. and **Heberlein, J.** (1998), Deposition of boron carbide thin film by supersonic plasma jet CVD with secondary discharge, *Surface and Coatings Technology*, Vol.**108-109**, pp.247-252.

Powell, A. (1953a), On the mechanism of choked jet noise, *Proceedings of the Royal Society of London*, Vol.**66**, pp.1039-1056.

Powell, A. (1953b), The noise of choked jets, *Journal of Acoustical Society of America*, Vol.**25**, pp.385-389.

Puckett, A. E. (1946), Supersonic nozzle design, *Journal of Applied Mechanics*,

pp.A-265 – A-270.

Ramesh, R., Pradeep, S., Muraganadam, M. and **Sujith**, **R.** (2000), Studies on freejets from nozzles for high-speed mixing applications, *Experiments in Fluids*, Vol.**29**, pp.359-368.

Sajben, M., Bogar, T. J. and **Kroutil, J. C.** (1980), Unsteady transonic flow in a two-dimensional diffuser, *AFOSR Rep*. **TR-80-0628**.

Schwane, R., Wong, H. and **Torngren,** (2002), Vibration of unsteady turbulent flow predictions for over-expanded rocket Nozzles, *Proceedings of international conference in CFD2*, Spring-Verlag, Berlin, pp.707-712.

Seiner, J. M. (1998), NASA Langley Research Center, private communication.

Seiner, J. M. and **Yu, J. C.** (1984), Acoustic near-field properties associated with broadband shock noise, *AIAA Journal*, Vol.**22**, No.9, pp.1207-1215.

Strykowski, **P. J.** (1996) Counterflow thrust vectoring of supersonic jets, *AIAA Journal*, Vol.**34**, No.10, pp.2306-2314.

T. Handa, M. Masuda and **K.Matuo** (2002), Mechanism of shock wave oscillation in transonic diffusers, *AIAA journal*, Vol.41, No.1, pp.64-70.

Tam, C. K. W. and **Tanna, H. K.** (1982), Shock associated noise of supersonic jets from convergent-divergent nozzles, *Journal of Sound and Vibration*, Vol.**81**, No.3, pp.337-358.

Tam, C. K. W. (1995), Supersonic jet noise, *Annual Review of Fluid Mechanics*, Vol.**27**, pp.17-43.

Tanna, H. K. (1977a), An experimental study of jet noise : part I. turbulent mixing noise, *Journal of Sound and Vibration*, Vol.**50**, No.3, pp.405-428.

Tanna, H. K. (1977b), An experimental study of jet noise : part II. shock associated noise, *Journal of Sound and Vibration*, Vol.**50**, No.3, pp.429-444.

Thomas, R. H., Choudhari, M. M. and **Joslin, R. D.** (2002), Flow and noise control : review and assessment of future directions, NASA TM-2002-211631.

Winant, C. D. and **Browand, F. K.** (1974), Vortex pairing : the mechanism of turbulent mixing layer growth at moderate Reynolds number, *Journal of*

Fluid Mechanics, Vol.**63**, pp.237-255.

Witczak, K. J. (1977), Self-excited oscillations of gas flow in a duct, *Nonlinear Vibration Problems*, Vol.18, pp.147-207.

Zaman, K. B. M. Q. and **Dahl, M. D.** (1990), Some observations on transitory stall in conical diffusers, **AIAA Paper 90-0048.**

Zaman, K. B. M. Q., Dahl, M. D., Bencic, T. J. and **Loh, C. Y.** (2002), Investigation of a Transonic Resonance with Convergent-Divergent Nozzles, *J. Fluid Mechanics*, Vol.463, pp.313-343.